ALPHA-AMYLASE INHIBITORY COMPOUNDS FROM *LANNEA SCHWEINFURTHII* STEM BARK AND THEIR MODES OF INHIBITION

BY

OTIENO OOKO MICHAEL

A THESIS SUBMITTED IN PARTIAL FULFILMENT OF THE REQUIREMENTS FOR THE DEGREE OF MASTER OF SCIENCE IN CHEMISTRY

DEPARTMENT OF CHEMISTRY

MASENO UNIVERSITY

DECLARATION

This thesis is my original work and has not been submitted for examination for any degree in Maseno University or any other university or for any other award.

Michael Ooko Otieno Signature..... Date.....

MSC/SC/00126/2015

Department of Chemistry

SUPERVISORS

This thesis has been submitted for examination with our approval as the university supervisors

Dr. Charles Otieno Ochieng Signature.....Date.....

Department of Chemistry

Maseno University

Dr. Joab Otieno Onyango Signature.....Date.....

Department of Chemical Sciences and Technology

Technical University of Kenya

ACKNOWLEDGEMENT

I am grateful to God for giving me strength to carry out this study. My sincere gratitude goes to my able supervisors, Dr. Charles Otieno Ochieng and Dr. Joab Otieno Onyango for their immeasurable advice, remarkable commitment to supervise my work, limitless encouragement and patience throughout this research and writing of thesis.

I am grateful to Dr. Philip Onyango for identifying and depositing the specimen at Maseno University, Botanic Garden Herbarium in Kenya, voucher number, MOO/MSN/01/2017. Many thanks to Dr. Moses Lagat of University of Surrey, UK for spectroscopic analysis. Special thanks to Mr. Erick Omondi who assisted me access the UV-Vis spectrophotometer used in bioassay analysis alongside the entire Department of Chemistry Laboratory staff at Maseno University. I appreciate the chairman of Department of Chemistry, Professor Chrispin Kowenje for his encouragement and mentoring, and the entire teaching staff of Department of Chemistry for their helpful discussion during the study period. My appreciation to Prof. Phillip Okinda Owuor's Research Group members for the discussion, counsel and guidance.

Special thanks to my wife, parents, siblings, relatives and friends for their tolerance, emotional and material support they offered throughout the entire process, I will forever be grateful to you. May God bless you all.

DEDICATION

This thesis is dedicated to my wife, Florence, parents, Charles and Patricia, siblings, nieces and nephews for their continued love and support throughout the study period

TABLE OF CONTENTS

LIST OF ABREVIATIONS AND ACRONYMS

^{13}C NMR	Carbon-13 nuclear magnetic resonance
^{1}H NMR	Proton nuclear magnetic resonance
ANOVA	Analysis of variance
br	Broad
CC	Column chromatography
CD_3OD	Deuterated methanol
$CDCl_3$	Deuterated chloroform
COSY	Correlation Spectroscopy
d	Doublet
DCM	Dichloromethane
dd	Doublets of doublet
DEPT	Distortionless enhancement by polarization transfer
DNS	Dinitrosalicylic acid
E	Trans configuration/entgegen
EIMS	Electron ionization mass spectrum
ESIMS	Electrospray ionization mass spectrum
EtOAc	Ethyl acetate
HIV	Human immune virus
HMBC	Heteronuclear multiple bond correlation
HSQC	Heteronuclear single quantum correlation
Hz	Hertz
IC_{50}	Inhibitory concentration at 50% inhibition
J	Coupling constant
$[M]^+$	Molecular ion
m	Multiplet

MeOH	Methanol
mg	Milligram
MHz	Megahertz
mL	Millilitre
mM	Millmolar
m.p	melting point
MS	Mass spectrum
m/z	Mass to charge ratio
NMR	Nuclear magnetic resonance
NOESY	Nuclear overhauser enhancement spectroscopy
ppm	Parts per million
R_f	Retention factor
s	Singlet
t	Triplet
TLC	Thin layer chromatography
TMS	Tetramethylsilane
UV-Vis	Ultra violet visible
WHO	World health organization
δ	Chemical shift
µL	Microlitre
Z	Cis configuration/zusammen

LIST OF TABLES

LIST OF FIGURES

LIST OF APPENDICES

CHAPTER ONE
INTRODUCTION

1.1 Background of the study

Diabetes mellitus is a metabolic disorder characterized by chronic hyperglycemia or increased blood glucose levels with disturbance in carbohydrate, fat and protein metabolism resulting from absolute or relative lack of insulin secretion and/or defective insulin action (W.H.O, 2016). Following different ways of manifestation in different individuals, the disease is categorized as type 1, type 2 and gestational diabetes mellitus. Type-1 is characterized by autoimmune or idiopathic β-cells destruction leading to lack of insulin (Eckel, Grundy, & Zimmet, 2005; Schenk, Saberi, & Olefsky, 2008). Type-2 diabetes mellitus is multifaceted metabolic disorder consisting of hyperglycemia and defective insulin actions and/or insulin secretion (Lin & Sun, 2010). It ranges from predominantly insulin resistance to a total secretory defect with or without insulin resistance, a progressive diminishing pancreatic function over time (Eckel, Grundy, & Zimmet, 2005; Schenk, Saberi, & Olefsky, 2008). It is one of the primary threats to human health globally due to increasing prevalence, and disabling complications. Gestational diabetes mellitus a predisposing condition of high blood glucose (intolerance) occur among expectant mothers associated with persistent metabolic dysfunction in women (W.H.O, 2016; Whiting, Guariguata, Weil, & Shaw, 2011; Wild, Roglic, Green, Sicree, & King, 2004). Generally, increase in diabetes mellitus has been occasioned by life style changes including increased intake of processed food, food containing high sugar content and sedentary life style (W.H.O, 2016; Whiting, Guariguata, Weil, & Shaw, 2011; Wild, Roglic, Green, Sicree, & King, 2004). Efforts that promote the application and usage of indigenous natural food resources and life style management is thus being encouraged including consumption of indigenous food stuff and avoidance of sedentary lifestyles.

Diabetes mellitus manifest in different forms to different age groups despite several drug interventions (Akhilesh, 2012). Available anti-hyperglycemic drugs include those that stimulate endogenous insulin secretion, enhance action of insulin at the target tissues and inhibitors of digestion of dietary starch (Eichler, Korn, Gasic, Prison, & Businger, 1984). One of the management approaches proposed for hyperglycemia involves reduction of post-prandial hyperglycemia by delaying absorption of glucose (Akhilesh, 2012). Retardation of starch digestion and absorption by inhibition of enzymes play a key role in control of post-prandial hyperglycemia by lowering serum glucose levels (Shai, Masoko, Mokgotho, Magano, Mogale, Boaduo, et al., 2010; Tarling, Woods, Zhang, Brastianos, Brayer, Andersen, et al., 2008). An array of therapeutic options capable of managing post-prandial blood glucose levels are available (Tarling, et al., 2008). However, their modes of action are not clearly known while those with known modes of inhibition have side limitations that are associated with them.

Natural α-amylase inhibitors from medicinal plants offer an alternative option to control post-prandial hyperglycaemia (Shai, et al., 2010). Notably, several α-amylase inhibitors, such as acarbose (Schmidt, Frommer, Muller, Junge, Wingender, & Truscheit, 1977), valiolamine (Kameda, 1984), voglibose (Horii, 1986), nojirimycin (Eichler, Korn, Gasic, Prison, & Businger, 1984; Niwa, Inoue, Tsuruoka, Koaze, & Niida, 1970), miglitol (Bischoff, 1994) salacinol and kotalanol (Yoshikawa, Murakami, Shimada, Matsuda, Yamahara, Tanabe, et al., 1997) have their origins from plants. These plants isolates have been evaluated as potent inhibitors of α-amylases and α-glucosidases enzymes and confirmed in animal models as anti-hyperglycemic (Gulati, Serena, & Gupta, 2017), and most of them are prescribed for management of hyperglycemia (Yoshikawa, et al., 1997). This suggests that plant metabolites could be ethnomedicinally relevant as complementary and alternative for management of hyperglycemia as well as serving as lead sources for new anti-hyperglycemic drugs (Gulati, Serena, & Gupta, 2017). However, many of synthetic analogues have shown certain limitations

including non-specificity, displaying serious side effects and failure to manage hyperglycemia successfully. The scenario necessitates search for α-amylase inhibitors from natural materials, regarded as promising option for management of hyperglycemia. However, anti-hyperglycemic potential of *Lannea schweinfurthii* stem bark is not documented.

In recent times, medicinal plants have been noted to gain relevance in management of diabetes with less side effects and less expensive relative to synthetic anti-hyperglycemic agents (Mukherjee, Maiti, Mukherjee, & Houghton, 2006). Over 400 plant species elaborating different classes of compounds such as alkenyl cyclohexenone derivatives (Marles, 1995; Mukherjee, Pandey, & A.S., 2012), sterols, terpenoids, phenolic compounds and alkaloids (Yeo, Lee, & Popovich, 2011), have received scientific evaluation for their efficacy as anti-hyperglycemic agents (Marles, 1995; Mukherjee, Pandey, & A.S., 2012). A plant such as *Lannea schweinfurthii* is a good example that has been reported for use by communities in East Africa to manage hyperglycemia following case study reports from herbalists and traditional healers in many East African communities for use of its stem bark to treat hyperglycemia related ailments (Tshikalange, 2007). Some plants species from the genus *Lannea* have as well been cited for management of hyperglycemia and so far, been evaluated (Allenki, Vasantha, Chitturi, & K., 2014). For instance, the effect of ethanol leaf extract of *Lannea coromandelica* (Houtt) tested against alloxan-induced hyperglycemia in male Wister rats, showed significant hyperglycemic activity comparable to standard drug metformin (Allenki, Vasantha, Chitturi, & K., 2014). Such results were indicative of potential of *Lannea* species against post-prandial hyperglycemia (Deutschländer, Lall, & van de Venter, 2009; Rahmatullah, Azam, Khatun, Seraj, Islam, Rahman, et al., 2012) since plants of common genetic origin tend to have similar phytochemical components. This is not necessarily as plant species may exhibit variation in phytochemical constituents which ultimately may have influence on their biological properties.

However, phytochemical evaluation of *Lannea schweinfurthii* stem bark on post-prandial hyperglycemia is not documented.

Previously, compounds including 3,5,3',5'-tetrahydroxy-4'-methoxy-6,7-(2",2"-dimethylchromene)-flavonol (**1**) trivialized as lanneaflavanol, (*2R*,*3R*)-3,5,3',5'-tetrahydroxy-4'-methoxy-6,7-(2",2"-dimethylchromene)-dihydroflavonol (**2**) trivialized as lannea dihydroflavanol, sitosterol (**3**), lupenone (**4**), epicatechin (**5**), alcohols and hydrocarbons (Kihagi, 2016) were isolated from *Lannea schweinfurthii*, majority of which were established as good antioxidants. Antioxidants reduce oxidative stress induced as a result of excessive generation of free radicals when actions of insulin are impaired (Johansen, 2005; Van Wyk, Van Oudtshoom, & Gericke, 2005). Such results could link the plant to be helpful in managing impairment caused by diabetes mellitus. It is also possible that there could be unknown compounds from *Lannea schweinfurthii* stem bark responsible for α-amylase inhibitory effects on carbohydrate hydrolysis beyond managing free radicals. However, scientific facts to validate inhibition of α-amylase activities and modes of inhibition are not documented.

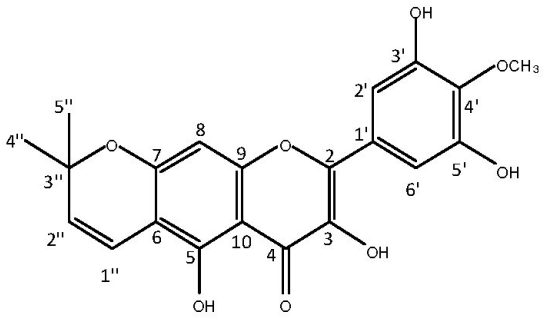

1

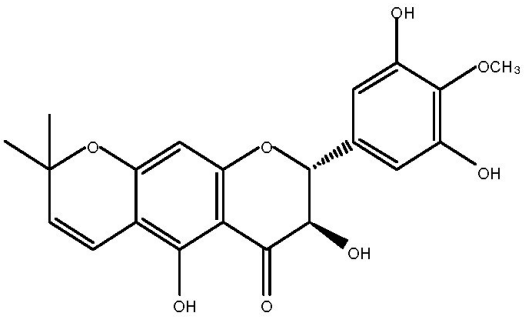

2

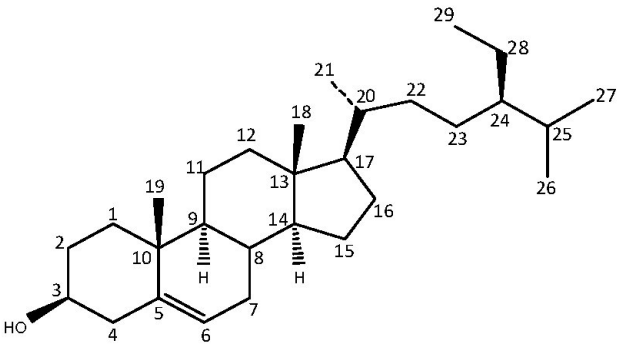

3

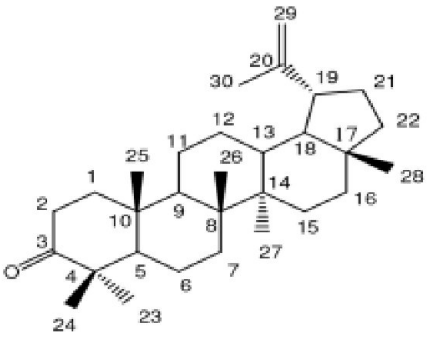

4

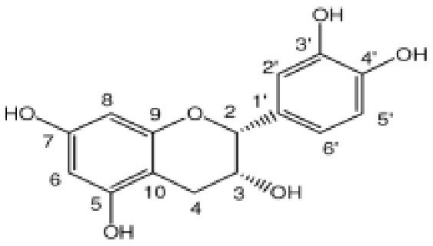

5

Different plants extracts and isolates have been reported to show inhibitory activities on α-amylase with different modes of inhibition such as mixed inhibition for majority of crude extracts while few extracts exhibit competitive, uncompetitive or non-competitive modes (Fatai, Anofi, & Ashafa, 2018; Priscilla, Roy, Suresh, & Kumar, 2014; Xu, 2010; Zhang, Wang, & Dong, 2014). The modes of inhibition against enzymatic activities is always established using Michaelis-Menten kinetic parameters based on double reciprocal plot of reaction velocity, 1/v $(mM/min)^{-1}$ against substrate concentration 1/[S] $(mM)^{-1}$ which then display dissociation constant (K_m) and maximum reaction velocity (V_{max}) values, and inhibition constants (K_i and $K_{i'}$) which would reveal mode of inhibition. Most plants with potent anti-hyperglycemic activities and active compounds identified, Michaelis-Menten kinetic parameters have been established to validate possible modes of action. *Lannea schweinfurthii* is an ethnomedicinal plant used against diabetic conditions. However, active phytochemicals and their modes of action have not been established, therefore efficacy of the plant remains undocumented.

1.2 Statement of the problem

Natural α-amylase inhibitors from food-grade plants or medicinal plants such as *Lannea schweinfurthii* may offer an alternative option to control post-prandial hyperglycaemia. However, the extent to which the plant extracts may inhibit α-amylase and control glucose absorption rate has not been established. Use of *Lannea schweinfurthii* has been reported in the

management of hyperglycemia widely by different communities in East Africa. This is without scientific evidence relating bioassay results against hyperglycaemia and chemical components. The inhibitory potential and mode of inhibition of compounds from *Lannea schweinfurthii* stem bark on α-amylase activities are not known.

1.3 Objectives

1.3.1 General objectives

To characterize and establish α-amylase inhibitory compounds and their modes of inhibition from *Lannea schweinfurthii* stem bark.

1.3.2 Specific objectives

i. To determine *in-vitro* inhibitory effects of crude extracts from *Lannea schweinfurthii* stem bark against α-amylase activities.

ii. To determine structures of isolates from *Lannea schweinfurthii* stem bark using chromatographic and spectroscopic techniques, respectively.

iii. To determine *in-vitro* inhibitory effects of isolates from *Lannea schweinfurthii* stem bark against α-amylase activities.

iv. To determine *in-vitro* modes of inhibition of active isolates from *Lannea schweinfurthii* stem bark against α-amylase activities based on Michaelis-Menten kinetic parameters.

1.4 Hypothesis

1.4.1 Null Hypothesis

i. Crude extract from *Lannea schweinfurthii* stem bark do not possess activities against α-amylase.

ii. Compounds from *Lannea schweinfurthii* stem bark do not have activities against α-amylase.

iii. Compounds from *Lannea schweinfurthii* stem bark do not have clear modes of inhibition on α-amylase.

1.5 Justification

The use of available anti-hyperglycemic drugs which have several drawbacks such as not safe and ineffective for management of hyperglycemia. The use of *Lannea schweinfurthii* stem bark by traditional practitioners may offer alternative and/or additional option, therefore its therapeutic potential needs to be authenticated.

CHAPTER TWO
LITERATURE REVIEW

2.1 Epidemiological aspects of diabetes mellitus

Prevalence of diabetes mellitus has been on an upward trend over the past few decades, ostensibly due to life style changes characterized by sedentary life style, certain dietary component, smoking, and psychological stress (Jeon, 2007). Over 350 million and 88 million people worldwide are estimated to suffer from type-2 and type-1 diabetes mellitus, respectively (Spiller & Sawyer, 2006; W.H.O, 2003, 2016). Type-1 is characterized by autoimmune or idiopathic β-cells destruction leading to insulin deficiency (Eckel, Grundy, & Zimmet, 2005; Schenk, Saberi, & Olefsky, 2008). Type-2 diabetes mellitus is multifaceted metabolic disorder consisting of hyperglycemia and defective insulin actions and/or insulin secretion (Lin & Sun, 2010). It ranges from predominantly insulin resistance to a total secretory defect with or without insulin resistance, a progressive diminishing pancreatic function over time (Eckel, Grundy, & Zimmet, 2005; Schenk, Saberi, & Olefsky, 2008). It is one of the primary threats to human health globally due to increasing prevalence, and disabling complications. Insulin is the principle hormone that regulates the uptake of glucose from the blood (Gardner & Shoback, 2011) and its deficiency or the insensitivity of its receptors play a crucial role in all forms of diabetes mellitus. Gestational diabetes mellitus, a predisposing condition of high blood glucose (intolerance) occur among expectant mothers associated with persistent metabolic dysfunction in women (Schenk, Saberi, & Olefsky, 2008). Following such variations in manifestation of diabetic ailments, its management requires multifaceted approach of both chemotherapeutic and non-chemotherapeutic interventions. However, it remains undocumented the best option in management of diabetic conditions.

Impairment of insulin actions (insulin resistance), failure of which can induce oxidative stress through excessive generation of free radical that may impair endogenous antioxidant

defense and in turn cause various secondary complications (Johansen, 2005). Diabetes mellitus complications cause damage to organs like kidneys, liver, eyes, nerves, heart and blood vessels, resulting in increased disability, reduced life expectancy and enormous health cost (Nathan, Genuth, Lachin, Cleary, Crofford, Davis, et al., 2003) and can lead to death (Pari, Latha, & Rao, 2004). Chronic occurrence of insulin resistance leads to hyperglycemia (Fernandez-Mej, 2013) of which post-prandial hyperglycemia is prominent and early defects of diabetes mellitus (Johansen, 2005). Therefore, a prominent therapeutic approach is to manage post-prandial hyperglycemia by delaying absorption of glucose.

A safe and more effective paradigm is yet to be achieved in management of hyperglycemia despite numerous available synthetic and indigenous anti-hyperglycemic agents (Spiller & Sawyer, 2006). Available anti-hyperglycemic management options include; stimulation of endogenous insulin secretion, enhancements of action of insulin at the target tissues, use of oral hypoglycemic agents such as biguanids and sulfonylureas and inhibition of degradation of dietary starch by α-amylase (Eichler, Korn, Gasic, Prison, & Businger, 1984). However, such management options have several limitations such as non-specificity, failure to manage other diabetes mellitus complications and produce serious side effects (Cheng & Fantus, 2005). For instance, α-amylase inhibitors and thiazolidines based drugs have been reported to pose a significant risk of morbidity, mortality and secondary permanent damages to organs as liver, kidney after prolonged period of administration (Scheen & Paquot, 2013; Singh, Bhat, & Wang, 2013). Generally, several drugs present inadequate efficacy and adverse side effects such as flatulence, digestive and liver function disorders (Nasri, Shirzad, Baradaran, & Rafieian-kopaei, 2015). Due to these risks of synthetic anti-hyperglycemic therapy, indigenous medicinal plant remedies may offer alternative and/or complimentary management strategy. However, there are non-established efficacies across the broad spectrum of plant-based remedies such as *Lannea schweinfurthii*.

One of the strategies adopted to treat hyperglycemia is inhibition of carbohydrate hydrolytic enzymes such as α-amylase in the epithelial mucosa of small intestine which thus retard intestinal glucose absorption and decrease post-prandial blood glucose levels (Shai, et al., 2010). Pancreatic amylase is a key enzyme in the digestive system and catalyzes the initial step in hydrolysis of starch to a mixture of smaller oligosaccharides consisting of maltose, maltotriose and a number of a (1-6) and a (1-4) oligoglucans. These are then acted on by α-glucosidases and further degraded to glucose which on absorption enters the blood-stream. Inhibition of α-amylase would result in reduced levels of post-prandial hyperglycemia (Eichler, Korn, Gasic, Prison, & Businger, 1984). However, the challenge is finding suitable medicinal plant-based remedies i.e anti-hyperglycemic metabolites which would reduce degradation levels of carbohydrates through α-amylase inhibition with less severe side effects.

Based on these facts, the search for effective, unique and safe inhibitors for carbohydrate hydrolytic enzymes such as α-amylase from natural sources as plants has been given priority, on the premise that nature has diverse chemical and biological entities. Therefore, discovery of α-amylase inhibitors from natural materials such as plant and establish their mode of enzymatic inhibition can be regarded as promising direction towards management of diabetes mellitus. However, much is not documented about many of the natural sources of ethnomedicinal plants such as *Lannea schweinfurthii* known for treatment of diabetes mellitus.

2.2 Ethnobotanical management of diabetes mellitus

Over 1000 plant species have been reported for management of type-2 diabetes mellitus worldwide (Trojan-Rodrigues, Alves, Soares, & M., 2012). W.H.O recommendations on the use of plant products as anti-hyperglycemic agents is based on their ability to restore functions of pancreatic tissues by causing an increase in insulin output or inhibit intestinal absorption of glucose or facilitation of metabolites in insulin dependent process (W.H.O, 2016). However,

the major hindrance in integration of herbal medicine into modern medical practice is lack of scientific and clinical data giving efficacy thus, before any clinical research there is need for metabolite identification and appropriate biological tests for standardization (W.H.O, 2016). The current scientific evidence demonstrates that preventing onset of hyperglycemia using dietary supplement and herbal medicines have attracted increasing attention (Gulati, Serena, & Gupta, 2017). Consequently, many other plants have been reported in traditional system of medicine of many cultures to have beneficial anti-hyperglycemic effects and herbal treatments have been used in patients with insulin-dependent and non-insulin-dependent diabetes mellitus, diabetic retinopathy and diabetic peripheral neuropathy (Gulati, Serena, & Gupta, 2017; Marles, 1995; Mukherjee, Pandey, & A.S., 2012).

Plant isolates have been evaluated as potent inhibitors of α-amylase and α-glucosidases enzymes and confirmed in animal models as anti-hyperglycemic (Gulati, Serena, & Gupta, 2017) and most of them are prescribed for management of hyperglycemia (Yoshikawa, et al., 1997). This suggests that plant metabolites could be ethnomedicinally relevant as complementary and alternative options for management as well as used as templates for drug development (Gulati, Serena, & Gupta, 2017). For instance, the discovery of salacinol (**12**) and kotalanol (**13**) from the Sri Lanka and Indian plant *Salacia reticula* (Yoshikawa, et al., 1997; Yoshikawa, Murakami, Yashiro, & Matsuda, 1998) which have proved to be in the rank of most potent inhibitors. Salacinol (**12**) exhibited inhibitory activities towards maltase and sucrase nearly equal to those of acarbose (**6**) and towards isomaltase was much more potent than acarbose (**6**) (Yoshikawa, et al., 1997; Yoshikawa, Murakami, Yashiro, & Matsuda, 1998). Kotalanol (**13**) showed a more potent inhibitory activity than salacinol (**12**) and acarbose (**6**) towards sucrase (Yoshikawa, et al., 1997; Yoshikawa, Murakami, Yashiro, & Matsuda, 1998). Furthermore, salacinol (**12**) strongly inhibited increase of serum glucose levels in sucrose-loaded rats than acarbose (**6**) (Yoshikawa, Murakami, Yashiro, & Matsuda, 1998).

Plant and plant products have proved to have least associated side effects and more effective in management of hyperglycemia compared to synthetic anti-hyperglycemic drugs available in the market. Ethnomedicinal remedy thus provides an alternative research options, since a lot remain unestablished regarding their underlying principle active compounds in plants and their inhibitory kinetics. Traditional herbal medicines constitute a good basis for new anti-hyperglycemic discovery and development of synthetic medicinal remedies. However, α-amylase inhibitory compounds from traditional medicinal plants such as *Lannea schweinfurthii* and their modes of inhibition remains undocumented as there is no study relating metabolites with α-amylase inhibitory activities and modes of inhibition.

2.3 Common natural inhibitors of human intestinal glucosidases

Inhibition of all or some of the intestinal disaccharides and pancreatic amylase as a way of regulating absorption of carbohydrates and using inhibitors as therapeutic option in oral management of non-insulin-dependent diabetes mellitus was realized in 1970s (Asano, 2003). The first and still a relevant inhibitor, acarbose (**6**) was discovered from actiniplanes strain of bacteria as a potent inhibitor of pig intestinal sucrase with an IC_{50} of 0.5 mM (Schmidt, Frommer, Muller, Junge, Wingender, & Truscheit, 1977). Acarbose (**6**) was also effective in carbohydrate loading tests in rats and healthy volunteers, where it reduced post-prandial blood glucose and increasing insulin secretion (Puls, Keup, Krause, Thomas, & Hoffmeister, 1977). Thus, it became the drug of choice for management of diabetes mellitus for nearly 40 years (Asano, 2003). In 1984, *N*-substituted glucose-like compound valiolamine (**7**) isolated from *Streptomyces hygroscopicus* var. *limoneus* was established to inhibit pig intestinal maltase and sucrase with IC_{50} of 2.2 and 0.049 mM, respectively (Kameda, 1984). Following such potent activities, several other *N*-substituted valiolamine derivatives were synthesized, and one of the derivatives, voglibose (**8**) was discovered as an oral anti-hyperglycemic agent with IC_{50} values of 0.015 and 0.0046 mM towards maltase and sucrase, respectively (Horii, 1986). The

successful application of these natural compounds in management of post-prandial hyperglycemia indicates that discovery of alternative options would help bridge the gap as less toxic, readily available or effective.

In 1966, (Inoue, 1966) discovered a glucose analog with nitrogen atom in place of the ring oxygen, nojirimycin (**9**) from *Streptomyces roseochromogenes* and *S. lavendulae* as antibiotic but later was realized to inhibit α-amylase (Niwa, Inoue, Tsuruoka, Koaze, & Niida, 1970). However, this iminosugar with hydroxyl group at C-1 was quite unstable, so it was reduced to 1-deoxynojirimycin (**10**). The compound was later isolated from roots of mulberry trees and named as Molanoline (Yagi, Kouno, Aoyagi, & Murai, 1976) and many genera of *Bacillus* and *Streptomyces* bacteria (Ezure, Murao, Miyazaki, & Kawamata, 1985; Murao & Miyata, 1980; Schmidt, Frommer, Muller, & Truscheit, 1979). In all the natural sources, the compound showed good α-glucosidase inhibitory activities *in-vitro* but failed *in-vivo* (Junge, 1996), an observation that led to synthesis of several other derivatives to enhance *in-vivo* activities. The synthetic effort led to discovery of miglitol (**11**), which showed better inhibitory potential and absorption ability across the intestinal walls than acarbose (**6**) (Joubert, 1990). Following successful clinical trials, miglitol (**11**) was granted market clearance by U.S Food and drug Administration (FDA) in 1999 as a second-generation α-glucosidase inhibitor (Asano, 2003).

Generally, Acarbose (**6**) was noted to inhibit primarily α-amylase activity and selected inhibitory activity on glucoamylase (90%), sucrase (65%), maltase (60%) and isomaltase (10%). In comparison, miglitol (**11**) and voglibose (**8**) preferentially inhibited intestinal glucosidase activity rather than α-amylase activity (Bischoff, 1994). Despite their differential targets, clinical effects of miglitol (**11**) and voglibose (**8**) were still comparable to those of acarbose (**6**) (Chehade & Mooradian, 2000).

Overall, the main side effects of this class of inhibitors were gastrointestinal discomfort such as gas, bloating and loose stool although acarbose (**6**) was worse (A. J. Krentz, & Bailey, C.J, 2005). This was thought to be due to higher starch loads that were processed and fermented in colon (A. J. Krentz, Ferner, R.E., & Bailey, C.J, 1994). However, tolerance usually occurred after continued administration for 3 months suggesting an adaptive response within intestinal tract (Rabasa-Lhoret & Chiasson, 1998). These common inhibitors isolated from plants and later synthesized as anti-hyperglycemic drugs have several side effects such as gastrointestinal discomfort (gas), bloating and loose stool and also showed low inhibitory effects on α-amylase, based on their low IC_{50} (mM) values obtained. This prompted search for new plant-based α-amylase inhibitors from *Lannea schweinfurthii* that could form anti-hyperglycemic drug templates that have least side effects but more effective.

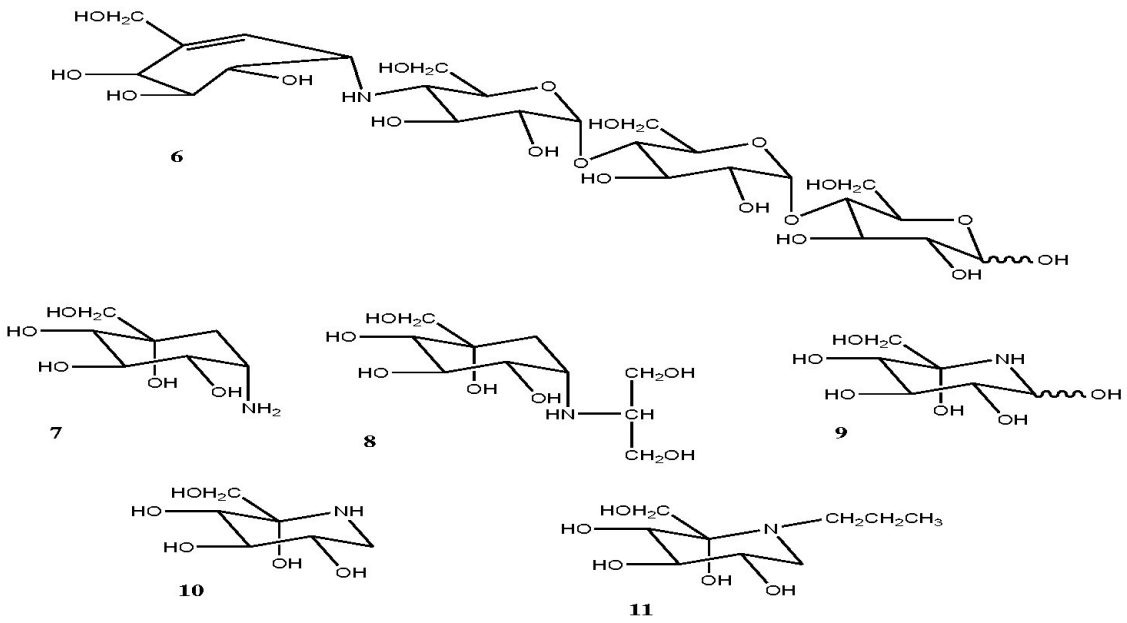

2.4 Modes of enzymatic inhibition for human intestinal glucosidases

Different plants are reported to show α-amylase inhibition and varied modes of inhibition with majority of crude extracts showing mixed mode of inhibition while few either competitive, uncompetitive or non-competitive modes (Fatai, Anofi, & Ashafa, 2018; Priscilla, Roy, Suresh, & Kumar, 2014; Xu, 2010; Zhang, Wang, & Dong, 2014). The specific modes of inhibition of

some plant metabolites have been studied and established through double reciprocal plots of reaction velocity, 1/v $(mM/min)^{-1}$ against substrate concentration, 1/[S] $(mM)^{-1}$ as either mixed, competitive, non-competitive or uncompetitive modes (Table 1). Furthermore, inhibition constants (K_i and $K_{i'}$) can be established which would reveal either mixed, competitive, non-competitive or uncompetitive modes of inhibition (Poongunran, Perera, Fernando, Jayasinghe, & Sivakanesan, 2015).

Table 1: Summary different equations and graphs used for determination of modes of enzymatic inhibition

Type of inhibition	Graph of inhibition modes	$K_{m\,app}$	$V_{max\,app}$
None	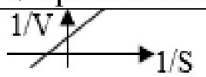	K_m	V_{max}
Competitive (Inhibitor only binds to free enzyme)	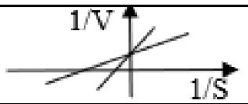	$Km(1+\frac{[I]}{Ki})$	V_{max}
Mixed (Inhibitor binds E and ES)	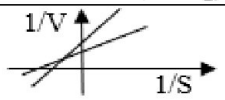	$Km\frac{(1+\frac{[I]}{Ki})}{(1+\frac{[I]}{Ki'})}$	$\frac{Vmax}{1+\frac{[I]}{Ki'}}$
Non-competitive (Inhibitor binds E and ES with equal affinity)	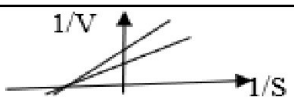	K_m	$\frac{Vmax}{1+\frac{[I]}{Ki'}}$
Uncompetitive (Inhibitor only binds to ES complex)	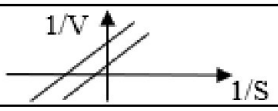	$\frac{Km}{1+\frac{[I]}{Ki'}}$	$\frac{Vmax}{1+\frac{[I]}{Ki'}}$

KEY: K_m = concentration of substrate at 1/2 V_{max}, V_{max} = maximum reaction velocity, K_i = free enzyme binding inhibition constant/competitive inhibition constant, $K_{i'}$ = enzyme-substrate binding inhibition constant/uncompetitive inhibition constant, V = initial velocity in absence and presence of inhibitor, S = concentration of substrate, I = concentration of inhibitor.

Normally, a decrease in apparent affinity of enzymes for substrate (K_m (apparent)>K_m), would be indicated by a higher value of K_m apparent when inhibitor favors binding to free enzyme, whereas an increase in apparent affinity (K_m (apparent) <K_m), would be indicated by a lower value of K_m apparent when inhibitor binds favorably to enzyme-substrate complex (Zhang, Wang, & Dong, 2014). Following this principle, the ability of plant extracts to exhibit different compounds with different binding characteristics to enzymes other than the active site enables most plants crude extracts to act as mixed inhibitors compared to pure compounds like

acarbose (**6**) (Zhang, Wang, & Dong, 2014). However, the pattern can never be assumed to be same in all compounds. For instance, ethanol extract of *Gazania krebsiana* (Less) showed uncompetitive inhibition of α-amylase characterized by reduction in V_{max} and K_m values whereas flavonoid rich leaf extract showed competitive inhibition of α-glucosidase activity characterized by increase in K_m and constant V_{max} values (Fatai, Anofi, & Ashafa, 2018). This demonstrated that crude extracts bound at other sites aside the active site of the enzyme with likelihood of adhering to either free enzyme or enzyme-substrate complex, thus modifying the activity of substrate or enzyme or both (Fatai, Anofi, & Ashafa, 2018).

It is generally believed that carbohydrate analogs containing nitrogen such as acarbose (**6**) and miglitol (**11**) are protonated in the active site and act as glycosidase inhibitors because of their ability to mimic the shape and/or charge of the presumed transition state for enzymatic glycoside hydrolysis (Stuttz, 1999).The mechanism of inhibition of acarbose (**6**) and 1-deoxynojirimycin (**10**) have been studied in human pancreatic α-amylase and on intact maltase-glucoamylase through structural and kinetic analysis indicated both as competitive inhibitors (Breitmeier, Günther, & Heymann, 1997).

The active compounds of *Salacia reticulata*, salacinol (**12**), kotalanol (**13**) and de-*O*-sulfonated kotalanol (Muraoka, Xie, Tanabe, Amer, Minematsu, & Yoshikawa, 2008; Yoshikawa, et al., 1997; Yoshikawa, Murakami, Yashiro, & Matsuda, 1998), whose structures consist of 1, 4-anhydro-4-thio-*D*-arabinitol core and polyhydroxylated acyclic chain displayed zwitterionic characteristics and positive charge was postulated to mimic the transition state intermediate and bound in the same way as a protonated amine inhibitor in the active sites of glucosidases thus showed competitive modes of inhibition (L Sim, 2010a).

Following combined kinetic and molecular docking studies revealed that acarbose (**6**), miglitol (**11**) and salacinol (**12**) all formed hydrogen bonds with two active-site water molecules which were tightly bound *via* hydrogen bonding to enzymes maltase-glucoamylase

sites. However, the three inhibitors showed marked difference in their abilities to inhibit enzymes, acarbose (**6**) was realized as relatively poor inhibitor of α-glucosidase with a K_i of 62 ± 13 μM, followed by miglitol (**11**) and salacinol (**12**) which displayed K_i of 1.0 ± 0.1 μM, and K_i of 0.19 ± 0.02 μM, respectively (L Sim, 2010a). These inhibition profiles were attributed to differences in their chemical properties such as size, charge, and ring structure (L Sim, 2010a). Acarbose (**6**) which is larger in size had the poorest inhibition potentials whereas Miglitol (**11**), a selective inhibitor of intestinal α-glucosidases and considered a poor inhibitor of α-amylases (Bischoff, 1994) and much smaller inhibitor compared to acarbose (**6**) was stronger inhibitor. Although the two had similar hydrogen bonding interactions, miglitol (**11**) exhibit additional side chain interactions (L. Sim, 2010). However, Salacinol (**12**) which is slightly larger inhibitor than miglitol (**11**), appeared to have additional interaction due to ring hydroxyl groups and additional electrostatic charge interaction between the sulfonium ion center and the catalytic nucleophilic sites of the enzymes (L. Sim, 2010).

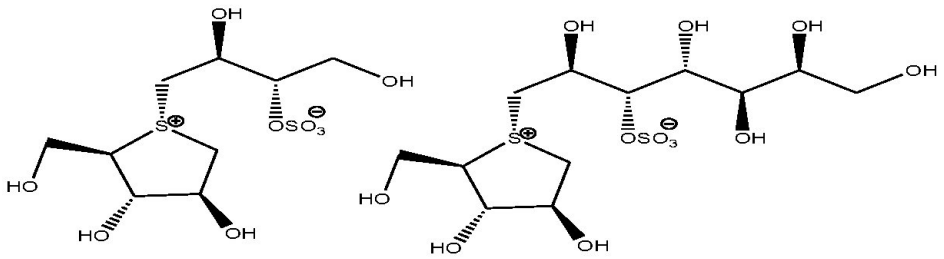

There is limited biophysical knowledge on specific modes of action for most of other plants metabolites used in management of hyperglycemia, although, several plants used have been found to contain varied secondary metabolites like glycosides, sterols, flavonoids, alkenyl cyclohexenone derivatives, terpenoids, phenolic compounds, alkaloids etc., that are frequently implicated as inhibitors of α-amylase (Osadebe, Omeje, Uzor, David, & Obiorah, 2013; Poongunran, Perera, Fernando, Jayasinghe, & Sivakanesan, 2015). Previously, it had been reported in other plants that polar fractions with high levels of glycosides displayed potent inhibitory effects against α-amylase due to structural similarities to carbohydrates thus

competing with carbohydrates substrates (Elya, Basah, Munim, Yuliastuti, Bangung, & Septriana, 2012). However, α-amylase inhibitory effects have not been done with different forms of glycosidic compounds such as flavonoids and steroid glycosides expected in *Lannea schweinfurthii* stem bark.

2.5 Ethnomedicinal uses of *Lannea* species

Several species of this genus have been noted with wide economic importance including being source of edible fruits, medicine, dyes for clothes, and general-purpose timber used for making doors (Okoth, Chenia, & Koorbandly, 2013). Moreover, many species of *Lannea* genus have been reported for management of many diseases in humans and animals as listed in Table 2.

The plant parts used in management of hyperglycemia among *Lannea* species include roots, stem bark and leaves, as outlined by a study designed to evaluate effect of ethanol leaf extract of *Lannea coromandelica* (Houtt) on alloxan-induced hyperglycemic male Wister rats, that showed significant hyperglycemic activity at oral doses of 100 mg/kg and 200 mg/kg b.w ($p<0.001$) comparable to standard drug metformin (Allenki, Vasantha, Chitturi, & K., 2014).

Herbalists and traditional healers in Venda also use *Lannea edulis* and *Lannea schweinfurthii* stem barks to treat diabetes mellitus (Tshikalange, 2007). The plants *Lannea edulis* and *Lannea schweinfurthii* are reported to contain sterols, alkenyl cyclohexenone derivatives, flavonoids, terpenoids, phenolic compounds, saponins and tannins (Van Wyk, Van Oudtshoom, & Gericke, 2005). These secondary metabolites like glycosides, sterols, flavonoids, alkenyl cyclohexenone derivatives, terpenoids, phenolic compounds, alkaloids etc., are frequently implicated as inhibitors of α-amylases (Osadebe, Omeje, Uzor, David, & Obiorah, 2013; Poongunran, Perera, Fernando, Jayasinghe, & Sivakanesan, 2015). However, no study has been conducted to relate the secondary metabolites with α-amylase inhibition and determine their modes of inhibition that would confirm the α-amylase inhibition potency.

Table 2: List of ethnobotanical and biological uses of *Lannea* species

Species	Plant part	Ethnobotanical uses	Biological activity	Reference
L. schweinfurthii Engl.	Stem and root bark, leaves	Stomachache, diarrhea, swelling of abdomen, skin rashes, oral infection, boils, febrifuge, malaria, syphilis, cellulitis, abscesses, oral candidiasis, gingivitis, nasal ulcers, asthma, neurological disorders, anaemia, coughs, diabetes mellitus	Antibacterial, antifungal, antiviral (Semliki forest virus, HIV type I and II), antiplasmodial, antimalarial, toxicity, antigiardial, inhibition of acetylcholinesterase, antioxidant	(Adewusi, 2011; Gathirwa, Rukunga, Njagi, Omar, Mwitari, Guantai, et al., 2008; Geissler, Harris, Prince, Olsen, Achieng', Oketch, et al., 2002; Johns, 1995)
L. humilis Oliv	Roots	Anaemia, stomach pains, nausea, general body weakness	Cytotoxicity, Anti-trypanosomal	(Maregesi, 2007; Nibret, Ashour, Rubanza, & Wink, 2010)
L. rivae	Bark	colds, chewed for its sweet taste and as a source of water	Antibacterial, antioxidant, anti-plasmodial, cytotoxicity	(Kokwaro, 2009; Okoth, Chenia, & Koorbandly, 2013)
L.alata	Bark, roots	fever, malaria, snake bites, fractures and injuries	Antibacterial and antioxidant	(Maundu, 2005; Okoth, Chenia, & Koorbandly, 2013)
L.triphylla	Bark	Coughs, constipation, colds	None	(Kokwaro, 2009),
L. stuhlmanii Engl	Root	Tonic, antifungal, pain relief, herpes zoster, herpes simplex, skin infections, oral candidiasis, anaemia	Cytotoxicity, Anti-trypanosomal, antifungal	(Chinsembu & Hedimbi, 2010; Nibret, Ashour, Rubanza, & Wink, 2010; Runyoro, Matee, Ngassapa, Joseph, & Mbwambo, 2006)
L. microcarpa	Leaves, bark, Root	Conjunctivitis, stomatitis, gingivitis, dressing wounds, skin eruptions, stomachache, beriberi, schistosomiasis and haemorroids; mouth blisters, rheumatism, sore throat, dysentery, as a cathartic and as a dressing on boils	Anti-inflammatory effect, antidiarrheoic activity, antioxidant	(Bationo, Hilou, Savadogo, & Nacoulma, 2012; Lamien-Meda, 2008; Marquet, 2005; L. Ouattara, Koudou, Karou, Giaco, Capelli, Simpore, et al., 2011a; Picerno, Mencherini, Della Loggia, Meloni, Sanogo, & Aquino, 2006; Tapsoba & Deschamps, 2006)

Table 2 contd': List of ethnobotanical and biological uses of *Lannea* species

L. schimperi (A. Rich) Engl	Bark	Chronic diarrhea, pain, stomach and chest problems, tuberculosis, skin problems, herpes zoster, herpes simplex	Antiulcer, antibacterial, cytotoxicity, antifungal	(Chinsembu & Hedimbi, 2010; Haule, 2012; Jeruto, 2008; D. P. Kisangau, Hosea, K.M., Lyaruu, H.V.M., Joseph, C.C., Mbwambo, Z.H., Masimba, P.J., … Sewald, N, 2009; D. P. Kisangau, Lyaruu, H.V.M., Hosea, K.M., & Joseph, C.C, 2007)
L. velutina	roots and bark	diarrhoea, rachitic children, wounds and strained muscles, respiratory diseases, oedema, paralysis, epilepsy and insanity	Antioxidant and radical scavenging activities, larvicidal, molluscicidal, lipoxygenase inhibition	(Diallo, Eklu-hachegkeku, Agbonon, Aklikokou, Creppy, & Gbeasser, 2010; Maiga, 2007; L. Ouattara, Koudou, J., Karou, D.S., Giaco, L., Capelli, G., Simpore, J., … Traore, A. S, 2011a)
L. acida	Stem bark, Root	Diarrhea, stomach ache, gonorrhea, rheumatism, oral diseases, malaria	Antibacterial, antioxidant, vibriocidal, cytotoxicity	(Akinsinde & Olukoya, 1995; Etuk, Ugwah, Jagbonna, & Onyeyili, 2009; W. M. Kone, Atindehou, K.K., Terreaux, C., Hostettmann, K., Traore, D., & Dosso, M, 2004 ; L. Ouattara, et al., 2011a; Sowemimo, van de Venter, Baatjies, & Koekemoer, 2009; Tapsoba & Deschamps, 2006)
L.edulis	Root bark	Diarrhea, sore eyes, boils, abscesses, diabetes, schistosomiasis (bilhazia), gonorrhea, pre-hepatic jaundice	Mutagenic effects, antioxidant	(Deutschländer, Lall, & van de Venter, 2009; Maroyi, 2011; Segawa & Kasenene, 2007; Sohni, Davis, Deschamps, & Kale, 1995; Van Wyk, van Oudtshoorn, & Gericke, 1997)

Table 2 contd': List of ethnobotanical and biological uses of *Lannea* species

L. discolor		Malaria, fever, constipation, menorrhagia, infertility	Antimalarial	(Clarkson, Maharaj, Crouch, Grace, Pillay, Matsabisa, et al., 2010; Kazembe, 2012; Maroyi, 2011)
L. welwitschii	Bark, seeds	Diarrhea, haemorroids, menstrual problems, abdominal pains, pain after birth, epilepsy, oedema, gout, swelling, palpitation, skin infections and ulcers, snake bites, wounds, diabetes	Cytotoxicity, antibacterial, anti-diarrheal, antidiabetic, anti-sickling activity	(Groweiss, Cardellina, Pannell, Uyakul, Kashman, & Boyd, 1997; A. K. Nyarko, Okine, Wedzi, Addo, & Ofosuhene, 2005; A. K. Nyarko, Okine, L.K.N., Wedzi, R.K., Addo, P.A., & Ofosuhene, M, 2005; Olatokunboh, Mofomosara, & Ekene, 2010; Olukoya, Idika, & Odugbemi, 1993)
L. coromandelica (Houtt) Merril	Bark, leaves	Bark used for treatment of diabetes, diarrhea, toothache, astringent, lotion for leprous and ulcers, impetigenious eruptions from contagious disease. Leaves are used for pain relief	Antioxidant, analgesic, cytotoxicity, hypotensive activity, hyperglycemic, anti-atherothrombosis, antibacterial, antifungal, anti-inflammatory	(Abdul, Hirak, Mohibur, Jerin, Aziza, Mahabuba, et al., 2010; Akter, Uddin, Grice, & Tiralongo, 2013; Alam, A.B., Moniruzzaman, A., R.U.H., M.R., et al., 2012; Rahmatullah, et al., 2012; Reddy, Joy, & Kumar, 2011; Saravanam, Dhasarathan, Indira, & Venkataraman, 2010; Sathish, 2010)
L. barteri	Bark	Wounds, rheumatic, diarrhea, gastritis, sterility, intestinal helminthes, oedema, scurvy, epilepsy, malaria, anaemia	Antibacterial, acetylcholinesterase inhibitor, antioxidant	(Adoum, 2009; Allabi, Busia, Ekanmian, & Bakiono, 2011; W. M. Kone, Koffi, A.G., Bomisso, E.L., & Bi, F.H.T, 2012)
L. transuta	Bark, flowers, leaves	Haemostatic for wounds, abrasion and sores	Anticancer, antioxidant, Antimicrobial	(Mothana, Lindequist, Gruenert, & Bednarski, 2009) (Adoum, 2009; Allabi, Busia, Ekanmian, & Bakiono, 2011; W. M. Kone, Koffi, A.G., Bomisso, E.L., & Bi, F.H.T, 2012)
L. nigritana	Stem, root, leaves	diarrhea, dysentery; pain-killers, pulmonary troubles; skin, mucosae, paralysis, epilepsy, convulsions,	Cytotoxic, anticancer	(Burkill, 1985; Fadeyi, Fadeyi, Adejumo, Okoro, & Myles, 2013; Kapche, 2007; Magassouba)

2.6 Phytochemistry of *Lannea* species

Phytochemical analysis of genus *Lannea* indicated presence of alkenyl cyclohexenone derivatives, flavonoids, sterols, triterpenoids, coumarins, saponins and carotenoids (Van Wyk, Van Oudtshoom, & Gericke, 2005). Specifically, triterpenoids from *Lannea* species included sitosterol (**3**), lupenone (**4**), lupeol (**14**), sitosterol-glycoside (**15**), taraxerol (**16**), taraxerone (**17**), and lutein (**18**), which were attributed to antibacterial, immune-stimulant, antioxidant, anti-trypanosidal, anti-arthritic, antimalarial and anti-inflammatory activities (Okoth, Chenia, & Koorbandly, 2013). Other compounds *Lannea* species are known for prenylated flavonoids; 3,5,3',5'-tetrahydroxy-4'-methoxy-6,7-(2",2"-dimethylchromene)-flavonol (**1**) trivialized as lanneaflavanol and (*2R*,*3R*)-3,5,3',5'-tetrahydroxy-4'-methoxy-6,7-(2",2"-dimethylchromene)-dihydroflavonol (**2**) trivialized as lanneadihydroflavanol (Okoth, Akala, Jonson, & Koorbanally, 2016), together with epicatechin (**5**), epicatechin gallate (**19**), myricetin (**20**), myricetin-3-*O*-α-rhamnopyranoside (**21**), myricetin-3-*O*-α-arabinofuranoside (**22**), myricetin-3-*O*-β-galactopyranoside (**23**), catechin (**24**) and rutin (**25**), which are associated with antibacterial, antioxidant, radical scavenging activity, anti-plasmodial, lipoxygenase, anti-inflammatory, analgesic, antiviral, antifungal and anti-HIV, have been isolated (Okoth, Chenia, & Koorbandly, 2013). However, efficacy of such compounds from *Lannea* species on α-amylase inhibition is not established and remains undocumented.

Mixtures of phenolic lipids (cardanols), alkenyl cyclohexanols and alkenyl cyclohexenone derivatives have similarly been isolated from *Lannea schimperi*, *Lannea rivae* and *Lannea schweinfurthii* (Okoth, Akala, Jonson, & Koorbanally, 2016). For instance, furanocyclohex-2-enone (**26**), and 2,4,5-trihydroxycyclohexanone (**27**) were the latest compounds established from *Lannea schweinfurthii* (Okoth, Akala, Jonson, & Koorbanally, 2016). The non-isoprenyl aliphatic side chains of these compounds varied in length with odd carbon chains of between 13 to 23

carbons and either fully saturated or contained one or two double bonds (Okoth, Chenia, & Koorbandly, 2013; Yaouba, Andreas, Erick, Solomon, Beatrice, Matthias, et al., 2017). The specific compounds isolated from *Lannea* species included (**3**, **4**, **5**, **15**, **24**, **26** and **27**) from *Lannea Schweinfurthii*, (**1**, **2**, **3**, **14**, **18**, **22** and **25**) from *Lannea alata*, (**3**, **15**, **16**, **17**, **19**, **20** and **23**) from *Lannea rivae* and (**3**, **16** and **17**) from *Lannea schimperi*.

These secondary metabolites like glycosides, terpenoids, flavonoids, alkenyl cyclohexenone derivatives are frequently implicated as inhibitors of α-amylases (Osadebe, Omeje, Uzor, David, & Obiorah, 2013; Poongunran, Perera, Fernando, Jayasinghe, & Sivakanesan, 2015). Despite the isolation of a number of compounds with molecular diversities, there has been no any attempt to evaluate these molecules towards α-amylase inhibition and determine the modes of inhibition of compounds isolated against α-amylase that would confirm α-amylase inhibition potency. There could be unknown compounds from stem bark of *Lannea schweinfurthii* responsible for α-amylase inhibitory effects.

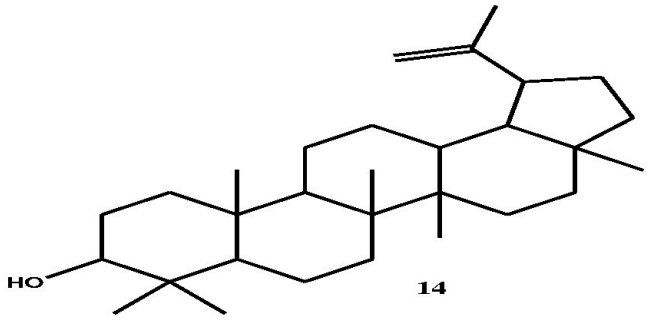

14

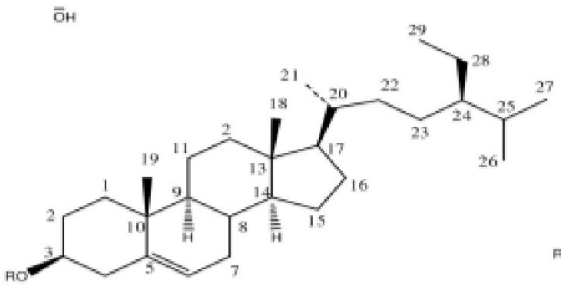

15: R=glucose

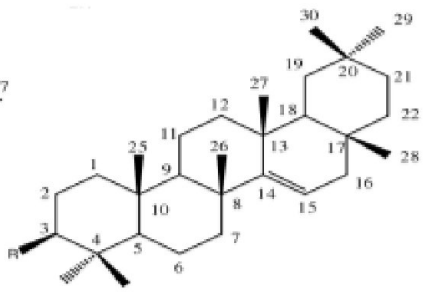

16: R=OH
17: R=O

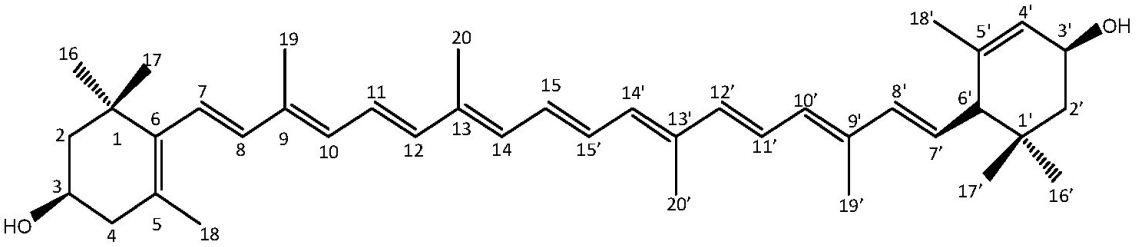

18

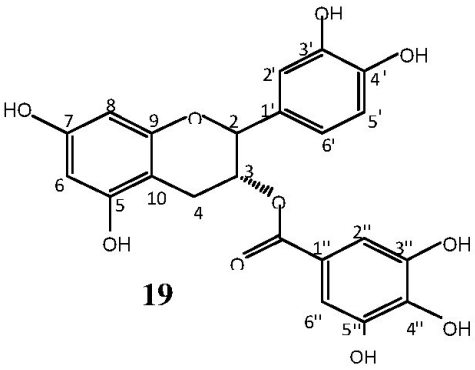

19

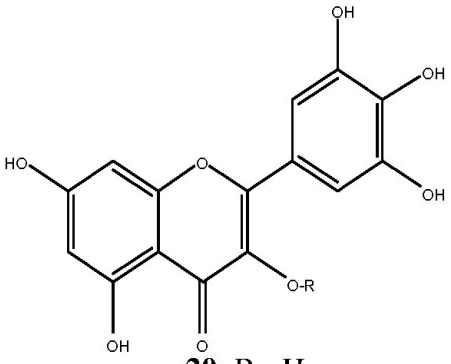

20: R= H
21: R= rhamnose
22: R= arabinofuranose
23: R= galactose

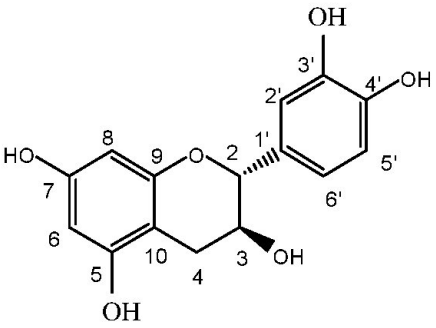

24

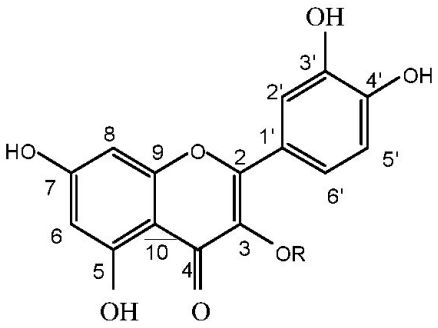

25: R = rutinose

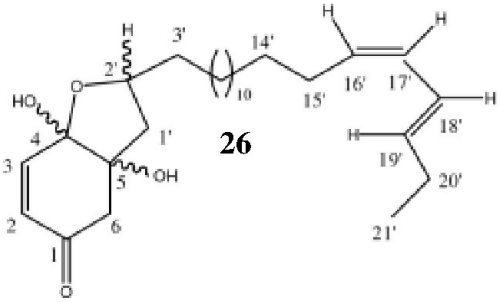

26

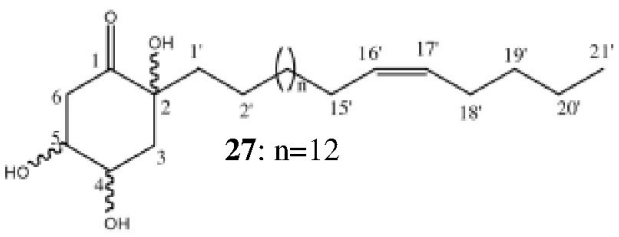

27: n=12

CHAPTER THREE

MATERIALS AND METHODS

3.1 General experimental procedures, instrumentation, solvents and fine consumables

Grinding was done using kika, M-20 electric pulverizer, weighed using a Shimadzu UX, top-loading analytical balance. Organic solvents; *n*-hexane, dichloromethane, ethyl acetate and methanol, reagents; glacial acetic acid, *p*-anisaldehyde, concentrated sulphuric acid and ammonia and fine chemicals; silica gel (Merck 60 G, 70-230 mesh) and sephadex LH-20 were sourced from Kobian, Kenya and Sigma Chemical Company, St. Louis, USA. The α-amylase, starch, DNS and standard drug metformin were purchased from Sigma-Aldrich. The 1D (^{1}H, ^{13}C and DEPT) and 2D (COSY, NOESY, HSQC and HMBC) NMR spectroscopy were recorded using $CDCl_3$, CD_2Cl_2 or CD_3OD on a Bruker Avance III 500 MHz spectrometer for ^{1}H and 125 MHz for ^{13}C. The ^{1}H and ^{13}C NMR chemical shifts (δ) were measured in ppm and coupling constants (*J*) in Hz relative to chemical shifts of the deuterated solvent and TMS. EIMS spectra were recorded on a direct inlet, 70 eV, on SSq 710, Finnigan MAT mass spectrometer. The melting points were determined on an Ernst Leitz Wetziar micro-hot stage melting point apparatus and were uncorrected. EYELA, N-100 rotary evaporator was used to concentrate the samples under reduced pressure. Merck 60 G, 70-230 mesh silica gel was used for column chromatography and pre-coated Merck 60, Kieselgel F_{254} aluminum silica gel plates were used for thin layer chromatography. The spots were visualized using *p*-anisaldehyde: concentrated sulphuric acid: methanol: glacial acetic acid spray reagent [1:2:96:1] (Krishnaswamy, 2003), followed by heating at 100°C using heat gun for two minutes. The standards for α-amylase inhibitory assay tests and kinetic analysis were incubated in the oven, gallenkamp INC 200, and the absorbances were measured using the SpectraMax 190,

UV-Visible light spectrophotometer (molecular device, Sunnyvale, USA) at the instrument room, Department of Chemistry, Maseno University.

3.2 Collection of plant material

The stem bark of *Lannea schweinfurthii* was collected in October 2017, from Kisumu County, Kisumu Karateng (34°45'0'', 0°6'0''), Kenya and the specimen identified and authenticated by Dr. Philip Onyango, Maseno University, Botany Department and deposited at Maseno University, Botanic Garden Herbarium in Kenya, voucher number MOO/MSN/01/2017.

3.3 Extraction of plant material

The 4 kg stem bark of *Lannea schweinfurthii* was chopped into small pieces, air dried under a shade at room temperature, then ground into fine powder using electric pulverizer. The 4 kg powdered plant material was sequentially extracted at room temperature in 5 litres of each solvents of increasing polarity in the order *n*-hexane, dichloromethane, ethyl acetate and methanol. The respective solvent was added to the material, vigorously shaken on an orbital shaker, then set aside for 24 hours after which it was filtered with Whatman No. 1 filter paper using Buchner filter funnel. Filtrate was concentrated *in vacuo*, using rotary evaporator, under reduced pressure at 45°C. The procedure was repeated thrice to ensure maximum yield of extracts. The extracts were split into two portions, 2 g for bioassay tests and the remaining for isolation and elucidation. Before isolation of the compounds, TLC analysis was carried out using part of the isolation portion to establish the composition of each crude extracts. The extract was spotted on silica gel pre-coated TLC plates with *p*-anisaldehyde as visualizing agent. The concentrated crude *n*-hexane (12.0 g), dichloromethane (15.0 g), ethyl acetate (57.0 g) and methanol (150.7 g) extracts were then carefully sealed, labeled and stored in sample bottles at -20 ^{0}C in a deep freezer. The 2 g portion of each crude extracts were then set aside for α-amylase inhibition assays.

3.4 Isolation of compounds from *Lannea schweinfurthii* stem bark

The *n*-hexane, dichloromethane, ethyl acetate and methanol extracts were spotted on silica gel pre-coated aluminium TLC plates and sprayed with *p*-anisaldehyde: sulphuric acid: methanol: glacial acetic acid mixture followed by heating at 100°C using heat gun for 2 minutes to detect the spots. The *n*-hexane and dichloromethane extracts had overlapping spots on the TLC plates suggesting they were homogeneous and were combined to form one extract. Part of the crude extracts from *n*-hexane/dichloromethane, ethyl acetate and methanol after extraction process were subjected to chromatographic methods of separation in order to obtain pure isolates.

3.4.1 Fractionation of *n*-hexane/dichloromethane extract

The *n*-hexane/DCM extract (23.0 g) was loaded onto *n*-hexane slurry of silica gel column and eluted stepwise with *n*-hexane: ethyl acetate gradient mixture starting with 100% *n*-hexane and increasing the polarity stepwise by 10% ethyl acetate after collection of every 1000 mL of eluent. The column was finally washed with 100% ethyl acetate. A total of 85 fractions each of volume 50 mL were collected. The 50 mL each, collected fractions were monitored by TLC using *n*-hexane: ethyl acetate (9:1, 4:1, 3:2, 1:1) solvent system and visualization was done using *p*-anisaldehyde reagent followed by heating at 100°C using heat gun for 2 minutes. Fractions collected were combined into three fractions based on the TLC spots and were pooled as fractions **A** (10-19), **B** (25-43) and **C** (43-65). The fractions combined were concentrated *in vacuo* using rotary evaporator. Fractions **A** (10-19; 1.00 g), **B** (25-43; 1.84 g) and **C** (43-65; 1.21 g) were loaded in three, 40 mm diameter columns separately and eluted with 500 ml portions of *n*-hexane: ethyl acetate solvent system, starting with 100% *n*-hexane and gradually introducing 15% ethyl acetate to increase the polarity then finally 100% ethyl acetate. Fraction **B** (25-43; 1.84 g), yielded 100 fractions of 20 mL each. Purification of fraction 70-85 with 15% ethyl acetate in *n*-hexane, yielded

a white amorphous substance, serialized as **28** (50 mg). The compound had a single spot on TLC with an R_f of 0.60 (15% ethyl acetate in *n*-hexane). Fraction **C** (43-65; 1.21 g) yielded 60 fractions collected in 20 mL each. Purification of fraction 6-13 with 15% ethyl acetate in *n*-hexane led to the isolation of a white powder, serialized as **29** (30 mg) which had a single spot on TLC with an R_f of 0.57 (15% ethyl acetate in *n*-hexane). Fraction **A** (10-19; 1.00 g) yielded 50 fractions of 20 mL each. Purification of fraction 30-45 with 25% ethyl acetate in *n*-hexane gave a white amorphous solid, serialized as **30** (40 mg) and had a single spot on TLC with an R_f of 0.56 (25% ethyl acetate in *n*-hexane). Compounds **28** and **29** were purified using 15% ethyl acetate in *n*-hexane, while **30** using 25% ethyl acetate in *n*-hexane on 40 mm diameter column, warmed and crystallized in dichloromethane.

3.4.2 Fractionation of ethyl acetate extract

The EtOAc extract (55.00 g) was loaded into a column and eluted with 1000 ml portions of solvent system, starting with 100% *n*-hexane and polarity was varied gradually by incremental addition of 10% ethyl acetate until 100% ethyl acetate had been added. The column was finally washed with 10% methanol in ethyl acetate. A total of 100 fractions, each of 50 mL were obtained. The 50 mL each, collected fractions were monitored on TLC using *n*-hexane: ethyl acetate (4:1, 3:2, 1:1, 2:3,1:4) solvent system and visualization done using *p*-anisaldehyde reagent followed by heating at 100°C for 2 minutes using heat gun. Fractions 30-63 had similar TLC profiles and were combined into one fraction pooled as **D** (30-63), concentrated under vacuum using a rotary evaporator. The fraction **D** (30-63; 1.50 g) was loaded into a 40 mm diameter column for further separation and eluted with 500 mL of *n*-hexane: ethyl acetate solvent systems of varying polarity starting with 4:1 ratio then finally adding up to 100% ethyl acetate. A total of 40 fractions each of 20 mL were collected. Purification of fractions 9-29 with 75% of ethyl acetate in *n*-hexane yielded

a pale yellow solid, serialized as **31** (30 mg) which showed a single spot on TLC with an R_f of 0.54 (75% of ethyl acetate in *n*-hexane). Purification of fraction 32-40 with 75% of ethyl acetate in *n*-hexane yielded a light yellow solid, serialized as **32** (20 mg) which showed a single spot on TLC with an R_f of 0.56 (75% of ethyl acetate in *n*-hexane).

3.4.3 Fractionation of methanol extract

A portion of aqueous MeOH extract (100.5 g) was adsorbed on silica gel, then loaded onto *n*-hexane slurry of silica gel column and eluted with 1000 mL portions of solvent system whose polarity was varied gradually by incremental addition of 20% of ethyl acetate, starting with 80% *n*-hexane in ethyl acetate. Ethyl acetate was introduced until 100% had been added and the polarity was further varied by incremental addition of 5% methanol in ethyl acetate which was added up to 100% methanol. The 50 mL each, collected fractions were monitored on TLC using *n*-hexane: ethyl acetate (2:1 and 1:1) and ethyl acetate: methanol (4:1 and 2:1) solvent system and visualization was done using *p*-anisaldehyde reagent followed by heating at 100°C for 2 minutes. A total of 120 fractions, each of 50 mL were obtained and they were spotted on TLC plates for combination of the fractions with similar profiles. Fractions 38-67 had similar TLC profiles and were pooled into one fraction as **E** (38-67), concentrated under vacuum using a rotary evaporator. The fraction **E** (38-67; 2.45 g) was further chromatographed over 40 mm diameter column using dichloromethane: methanol solvent system starting with 1:4 ratio then finally 1:9 collecting 20 mL each. A total of 30 fractions each of 20 mL were collected. Fractions 17-25 readily precipitated out and was further purified on sephadex LH-20 using methanol: dichloromethane (9:1) to yield a white amorphous solid, serialized as **33** (15 mg), that had one spot on TLC with R_f of 0.63 (9:1 methanol: dichloromethane).

3.5 Physical and spectroscopic data of isolated compounds

The physical data obtained for compounds **28**, **29**, **30**, **31**, **32** and **33** included the uncorrected melting points for the solids, appearance and retention factor. Spectrometric data determined were MS spectra while spectroscopic data determined for compounds were 1D (^{1}H, ^{13}C, DEPT) and 2D (COSY, NOESY, HSQC, HMBC) NMR spectra, attached in the Appendices (1.0-6.0) section.

3.5.1 Compound 28

White amorphous substance (*n*-hexane/DCM extract); yield (50 mg); single spot on TLC at R_f of 0.60 (15% EtOAc in *n*-hexane); m.p of 132-134°C; ^{1}H NMR ($CDCl_3$, δ_H (ppm), 500 MHz) δ_H 0.92 (m, H-19'), 1.74 (2H, m, H-1'), 2.21 (2H, dd, J = 14.2, 5.4 Hz, H-5), 4.70 (1H, m, 4-OH), 5.34 (2H, t, J = 4.8 Hz, H-14', 15'), 6.09 (1H, d, J = 10.1 Hz, H-2), 6.90 (1H, dd, J = 10.1, 3.6 Hz, H-3); ^{13}C NMR ($CDCl_3$, δ_C (ppm), 125 MHz), δ_C 14.0 (C-19'), 22.4 (C-18'), 22.9 (C-2'), 26.9 (C-16'), 27.2 (C-13'), 29.9 (C-3'-12'), 32.0 (C-17'), 39.1 (C-1'), 41.1 (C-5), 64.1 (C-4), 74.6 (C-6), 129.7 (C-15'), 129.8 (C-14'), 149.9 (C-3), 201.0 (C-1); EIMS *m/z*: 393 $[M+H]^+$, 375 $[M-H_2O]^+$. Appendices 1.0.

3.5.2 Compound 29

White powder (*n*-hexane/DCM extract); yield (30 mg); R_f of 0.57 (15% EtOAc in *n*-hexane); m.p of 136-138°C; ^{1}H NMR (CD_2Cl_2, δ_H (ppm), 500 MHz) δ_H 0.92 (3H, t, J = 7.1 Hz, H-19'), 1.70 (2H, dd, J = 14.8, 3.5 Hz, H-6), 1.76 (2H, d, J = 4.4 Hz, H-1'β), 2.97 (2H, dd, J = 12.3, 11.2 Hz, H-3), 3.99 (1H, m, 5-OH), 4.21 (1H, ddd, J = 11.0, 4.4, 3.1 Hz, 4-OH), 5.38 (2H, t, J = 4.7 Hz, H-14', H-15'); ^{13}C NMR (CD_2Cl_2, δ_C (ppm), 125 MHz), δ_C 13.8 (C-19'), 22.4 (C-18'), 23.1 (C-2'), 26.9 (C-16'), 27.2 (C-13'), 29.9 (C-3'-12'), 32.0 (C-17'), 39.5 (C-1'), 40.3 (C-6), 41.9 (C-3), 68.4 (C-4), 72.0 (C-5), 77.3 (C-2), 129.8 (C-15'), 129.9 (C-14'), 210.9 (C-1); EIMS *m/z*: 410 $[M]^+$, 392 $[M-H_2O]^+$. Appendices 2.0.

3.5.3 Compound 30

White amorphous solid (*n*-hexane/DCM extract); yield (40 mg); single spot on TLC at R_f of 0.56 (25% EtOAc in *n*-hexane); m.p 142-144°C; ^{1}H NMR ($CDCl_3$, δ_H (ppm), 500 MHz) δ_H 0.71 (3H, s, H-19), 0.85 (3H, d, *J* = 6.6 Hz, H-26), 0.97 (3H, d, *J* = 6.6 Hz, H-27), 1.04 (3H, t, *J* = 7.1 Hz, H-29), 1.21 (3H, d, *J* = 6.2 Hz, H-21), 1.27 (3H, s, H-18), 3.51 (1H, m, H-3), 5.08 (1H, dd, *J* = 18.0, 4.2 Hz, H-22), 5.18 (1H, m, H-23), 5.31 (1H, m, H-6); ^{13}C NMR $CDCl_3$, δ_C (ppm), 125 MHz) δ_C 12.2 (C-18, 29), 19.4 (C-19), 21.2 (C-26), 23.0 (C-21, 27), 24.4 (C-11, 15), 25.3 (C-28), 28.0 (C-16), 29.8 (C-2), 31.9 (C-7), 34.1 (C-25), 35.0 (C-10), 36.4 (C-1), 39.8 (C-12, 20), 42.0 (C-13), 42.0 (C-4), 51.1 (C-9, 24), 56.1 (C-17), 57.0 (C-14), 71.9 (C-3), 121.9 (C-6), 129.4 (C-23), 138.6 (C-22), 141.1 (C-5). Appendices 3.0.

3.5.4 Compound 31

Pale yellow solid (EtOAc extract); yield (30 mg); R_f of 0.54 (75% of EtOAc in *n*-hexane); m.p 200-201°C; ^{1}H NMR ($CDCl_3$, δ_H (ppm), 500 MHz) δ_H 1.42 (3H, s, H-5''), 1.43 (3H, s, H-6''), 2.83 (dd, *J* = 17.1, 3.3 Hz, H-3eq), 3.06 (dd, *J* = 17.1, 12.9 Hz, H-3ax), 5.44 (dd, *J* = 12.9, 3.3 Hz, H-2), 5.49 (1H, d, *J* = 10.0 Hz, H-3''), 6.01 (1H, s, H-6), 6.57 (1H, d, *J* = 10.0 Hz, H-4''), 7.46 (m, 2'-6'), 12.09 (s, 5-OH); ^{13}C NMR ($CDCl_3$, δ_C (ppm), 125 MHz) δ_C 28.2 (C-5''), δ_C 28.5 (C-6''), 43.3 (C-3), 78.1 (C-2), 79.1 (C-2''), 97.6 (C-8), 102.9 (C-6, 10), 115.5 (C-4''), 125.9 (C-3''), 126.4 (C-2', 6'), 128.7 (C-3', 5'), 138.5 (C-1'), 156.7 (C-5), 162.3 (C-9), 163.8 (C-7), 195.6 (C-4). Appendices 4.0.

3.5.5 Compound 32

Light yellow solid (EtOAc extract); yield (20 mg); R_f of 0.56 (75% of EtOAc in *n*-hexane); m.p 204-205°C; ^{1}H NMR ($CDCl_3$, δ_H (ppm), 500 MHz) δ_H 1.37 (3H, s, H-5''), 1.40 (3H, s, H-6''), 2.83 (dd, *J* = 17.1, 3.3 Hz, H-3eq), 3.06 (dd, *J* = 17.1, 12.9 Hz, H-3ax), 3.97 (s, 5-OCH_3), 5.29 (dd, *J* =

12.9, 3.3 Hz, H-2), 5.48 (1H, d, *J* = 10.0 Hz, H-3''), 6.01 (1H, s, H-6), 6.62 (1H, d, *J* = 10.0 Hz, H-4''), 7.50 (m, H-2'-6'); ^{13}C NMR ($CDCl_3$, δ_C (ppm), 125 MHz) δ_C 28.1 (C-5''), δ_C 28.4 (C-6''), 45.6 (C-3), 77.2 (C-2), 77.9 (C-2''), 93.7 (C-8), 105.6 (C-6, 10), 115.9 (C-4''), 125.8 (C-3''), 126.2 (C-2', 6'), 128.4 (C-3', 5'), 128.6 (C-4'), 138.9 (C-1'), 156.7 (C-5), 159.9 (C-9), 162.1 (C-7), 189.1 (C-4). Appendices 5.0.

3.5.6 Compound 33

White amorphous solid (MeOH extract); yield (15 mg); R_f of 0.60 (9:1 MeOH/DCM); m.p 147-149°C; ^{1}H NMR (CD_3OD, δ_H (ppm), 500 MHz) δ_H 0.77 (3H, d, *J* = 7.0 Hz, H-27), 0.79 (3H, d, *J* = 7.0 Hz, H-26), 0.83 (3H, t, *J* = 7.0 Hz, H-29) ,0.90 (1H, d, *J* = 6.5 Hz, H-21), 0.98 (1H, m, H-17), 3.40 (1H, m, 4'-OH), 3.62 (1H, m, 3'-OH), 3.83 (1H, m, H-2'), 4.05 (1H, d, *J* = 6.5 Hz, H-21), 4.46 (1H, dd, *J* = 12.3, 5.5 Hz) 3.13 (1H, m, H-5'), 4.46 (1H, dd, *J* = 12.3, 3.0 Hz, 6''-OH), 4.49 (1H, d, *J* = 8.8 Hz, H-1'), 4.49 (1H, dd, *J* = 12.3, 3.0 Hz, 6''-OH), 4.78 (1H, d, *J* = 8.8 Hz, 4''-OH), 4.89 (1H, d, *J* = 8.8 Hz, 4''-OH), 5.13 (1H, dd, *J* = 18.0, 8.1 Hz, H-23), 5.25 (1H, dd, *J* = 18.0, 4.2 Hz , H-22); ^{13}C NMR CD_3OD, δ_C (ppm), 125 MHz) δ_C 18.7 (C-29), 20.2 (C-27), 20.3 (C-18), 20.5 (C-19), 20.8 (C-21), 21.0 (C-26), 22.5 (C-11), 25.3 (C-15), 27.7 (C-28), 28.6 (C-16), 29.2 (C-25), 31.3 (C-2), 31.7 (C-8), 35.4 (C-7), 38.2 (C-1), 38.3 (C-10), 39.7 (C-12), 40.0 (C-20), 41.6 (C-13), 42.7 (C-4), 49.4 (C-9), 50.4 (C-17), 55.3 (C-24), 56.1 (C-14), 63.8 (C-6''), 65.3 (C-5'), 68.0 (C-5''), 69.6 (C-4'), 70.3 (C-2''), 73.4 (C-4''), 74.9 (C-2'), 76.6 (C-3''), 77.7 (C-3'), 82.3 (C-3), 101.3 (C-1''), 106.4 (C-1'), 121.1 (C-6), 128.2 (C-23), 137.9 (C-22), 140.3 (C-5); ESIMS *m/z*: 707.4 $[M]^+$. Appendices 6.0

3.6 *In-vitro* inhibition and kinetic analysis of modes of α-amylase inhibition

3.6.1 α-Amylase inhibition assay

The α-amylase inhibitory activity was determined using a modified assay of (McCue, 2004). The α-amylase was assayed using 500 µL of each sample extracts (0.0625, 0.125, 0.25, 0.5, 1.0 mg/mL), sample isolates (0.0625, 0.125, 0.25, 0.5, 1.0 mM) and standard drug metformin (0.05-1.0 mM) and a total of 500 µL of 0.02 M sodium phosphate buffer (pH 6.9) containing 0.5 mg/mL of α-amylase was pre-incubated at 25°C for 10 min. After the pre-incubation, 250 µL of a 1% starch solution in 0.02 M sodium phosphate buffer (pH 6.9) was added to each tube at timed intervals. The reaction was stopped using 500 µL of DNS acid colour reagent. The test tubes were incubated in a boiling water bath for 5 min and then cooled to room temperature. The reaction mixture was diluted by adding 5 mL distilled water and the absorbances measured at 540 nm using UV-Visible light spectrophotometer. The absorbance readings were compared with the negative controls that contained distilled water instead of sample. The percentage α-amylase inhibitory activity was calculated using the equation;

$$\%\ inhibition = \frac{Absorbance\ negative\ control\ (540) - Absorbance\ sample\ (540)}{Absorbance\ negative\ control\ (540)} \times 100$$

Concentration of samples resulting in 50% inhibition of enzyme activity (IC_{50}) was determined on probit plot of the % inhibition against the concentrations of the samples. The layout of experiment was completely randomized block design.

3.6.2 Modes of α-amylase inhibition

The kinetic analysis of modes of inhibition of α-amylase by active isolates was conducted using the isolates with lowest IC_{50} according to the modified method described (Ali, Houghton, &

Soumyanath, 2006). This was done in triplicates using completely randomized design. Amount of 250 µL of the isolate (5.0 mM) was pre-incubated with 250 µL of α-amylase solution for 10 min at 25°C in one set of six test tubes and in another set of six test tubes, α-amylase with (0.0 mM of isolate) was pre-incubated with 250 µL of phosphate buffer (pH 6.9). Amount of 250 µL of starch solution at increasing concentrations (0.3, 1.24, 2.18, 3.12, 4.06, 5.0 mg/mL) was added to both sets of test tubes to start the reaction. The mixture was then incubated for 10 min at 25°C and then boiled for 5 min after the addition of 500 µL of DNS to stop the reaction. The reactions were conducted for interval of 2 min for a particular substrate concentration [S] within 10 min in which the absorbances for each time interval was measured at 540 nm. The absorbances for different substrate concentration [S], for same reaction time of 10 min was also measured at 540 nm. The amount of reducing sugars (absorbance against time) released for different substrate concentration was determined spectrophotometrically using maltose standard curve and converted to reaction velocities. The mode of inhibition (i.e. competitive, mixed, non-competitive or uncompetitive) of the screened isolates was determined on the basis of the inhibitory effects on K_m (dissociation constant/Michaelis-Menten constant) and V_{max} (maximum reaction velocity, determined as reciprocal of y-intercept value) of the enzyme (Kakadiya, 2010), K_m is concentration of substrate at $1/2V_{max}$, determined as reciprocal of x-intercept value. A double reciprocal plot of 1/v $(mM/min)^{-1}$ versus 1/[S] $(mM)^{-1}$ where v is reaction velocity (mM/min) and [S] (mM) is substrate concentration was plotted. The modes of inhibition of the isolates on α-amylase activity were determined by analysis of the Lineweaver-Burk plot based on Michaelis-Menten kinetic parameters. The inhibition constants were calculated using the following equation (Segel, 1993): Where v is the initial velocity in absence and presence of inhibitor; S and I are concentration of substrate and inhibitor, respectively; K_i is the free enzyme binding inhibition constant (competitive

inhibition constant) and $K_{i'}$ is the enzyme-substrate binding inhibition constant (uncompetitive inhibition constant).

3.7 Statistical analysis

Enzyme activities in the presence of inhibitors were expressed as a percentage of the uninhibited enzyme activity. Concentration of samples resulting in 50% inhibition of enzyme activity (IC_{50}) was determined on probit plot of the % inhibition against the concentrations of the samples from the mean inhibitory values. The data on α-amylase inhibitory activities (IC_{50}) was subjected to a one –way analysis of variance (ANOVA) and results was expressed as mean ± standard deviation. Differences between means of samples and that of the control tests for the close dependency was compared using Tukey-Kramer Multiple Comparison range tests at $p \leq 0.05$ and LSD values obtained.

CHAPTER FOUR

RESULTS AND DISCUSSION

4.1 Crude extract yields

The amount of crude extracts obtained and percentage yields for *n*-hexane, dichloromethane, ethyl acetate and methanol extracts were recorded as in Table 3.

Table 3: Masses of sequential extraction of *Lannea schweinfurthii* stem bark and percentage yields

Extraction Solvent	Mass in grams	% yield
n-Hexane	12.0	0.300
Dichloromethane	15.0	0.375
Ethyl acetate	57.0	1.425
Methanol	150.7	3.768

Methanol extract had the highest percentage yield while *n*-hexane extract had the least. The results showed that the percentage yield increased with increase in polarity of the solvent used. This could be attributed to the fact that most metabolites were very polar.

4.2 Bioassay results of crude extracts

4.2.1 *In-vitro* α-amylase inhibition IC_{50} by the crude extracts

The *n*-hexane/dichloromethane, ethyl acetate and methanol extracts were tested against α-amylase to determine their inhibitory activities and IC_{50} results presented as in Figure 1. Methanol extract showed high inhibitory activity against α-amylase (IC_{50} = 0.497 mg/mL) which showed no significant difference ($p>0.05$) relative to the positive control (metformin; IC_{50} = 0.468 mg/mL). The inhibition by the ethyl acetate extract was moderate (IC_{50} = 0.578 mg/mL) and had no significant difference ($p>0.05$) relative to positive control (metformin; IC_{50} = 0.468 mg/mL). The methanol extract and ethyl acetate extract showed no significant difference ($p>0.05$) to each other whereas *n*-hexane/dichloromethane extract (IC_{50} = 1.024 mg/mL) showed low inhibitory activities ($p<0.05$) relative to metformin (IC_{50} = 0.468 mg/mL).

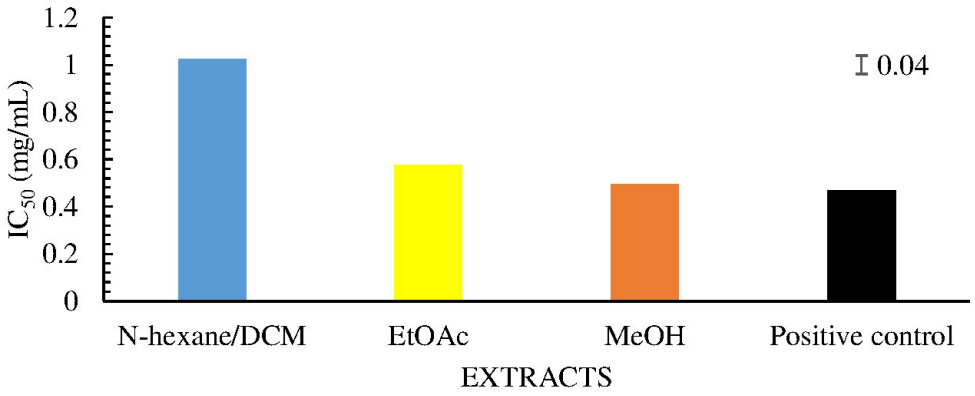

Figure 1: Mean IC_{50} of different extracts of *Lannea schweinfurthii* stem bark on α-amylase. Positive control = Metformin; LSD value = 0.04 at P<0.05.

The fact that methanol and ethyl acetate extracts showed activity against α-amylase indicated ingredient of these fractions were closely related except that concentration of highly potent compounds were more in methanol extract. Following the observations of inhibitory effects on α-amylase, it was considered that one or a combination of the polar compounds of *Lannea schweinfurthii* stem bark had high *in-vitro* inhibitory effects against hydrolytic activities of α-amylase. The implication of such results was that suppose these extracts could reduce the rate of starch breakdown to glucose consequently, reducing glucose level in the blood stream. Drugs such as metformin, voglibose, acarbose miglitol and many other plants extracts had been established to control post-prandial hyperglycemia by suppressing the hydrolysis of carbohydrates (Tarling, et al., 2008) and so anticipated for *Lannea schweinfurthii* stem bark extracts as indicated by the results of the study.

4.3 Structure elucidations

4.3.1 (4*R*,6*S*)-4,6-dihydroxy-6-((*Z*)-nonadec-14'-en-1-yl)cyclohex-2-en-1-one (28)

Compound **28** was isolated as a white amorphous substance from *n*-hexane/DCM extract; yield (50 mg); single spot on TLC, R_f of 0.60 (15% EtOAc in *n*-hexane); m.p of 132-134°C. The ^{1}H and

^{13}C NMR spectral data (Table 4; Appendices 1.1 and 1.2) were used to deduce the structure of compound **28**. The signals at δ_H 6.09 (1H, d, J = 10.1 Hz), δ_C 126.7; δ_H 6.90 (1H, dd, J = 10.1, 3.6 Hz), δ_C 149.9 and δ_H 5.34 (1H, t, J = 4.8 Hz), δ_C 129.8, δ_C 129.7 were observed. Based on the previous studies (Kapche, 2007; Okoth, Akala, Jonson, & Koorbanally, 2016; Yaouba, et al., 2017) , these NMR data indicated the presence of two alkenyl functionalities which were supported by ^{13}C NMR signals at δ_C 126.7, δ_C 129.8, δ_C 129.7, δ_C 149.9 and HSQC (Appendix 1.4) spectra showing correlation of signals at δ_C 201.0 for a keto carbon, δ_C 74.6 for hydroxylated carbon and δ_H 4.70 (1H, m), δ_C 64.1 for hydroxylated carbon.

Further analysis of HMBC spectrum (Appendix 1.5) revealed the connectivity between one of the alkenic protons at δ_H 6.09 (d, H-2, J = 10.1 Hz) to the keto carbon at δ_C 201.0 (C-1) which in turn showed two HMBC correlations (^3J) to the two hydroxylated carbons at δ_C 64.1 (C-4) and δ_C 74.6 (C-6). The hydroxymethine proton at δ_H 4.70 (m, H-4) on the carbon at δ_C 64.1 (C-4) showed ^2J and ^3J correlation with the alkenic carbon at δ_C 149.9 (C-3) and δ_C 126.7 (C-2), respectively. Furthermore, the other alkenic proton at δ_H 6.90 (dd, H-3, J = 10.1, 3.6 Hz) on δ_C 149.9 carbon displayed ^3J correlation with the keto carbon at δ_C 201.0 (C-1) and a methylene carbon at δ_C 41.1 (C-5), that had proton at δ_H 2.21 (dd, H-5α, J = 5.4, 14.2 Hz) and δ_H 2.18 (dd, H-5β, J = 5.4, 14.2 Hz) which in turn showed similar correlation to the alkenic carbon at δ_C 149.9 (C-3) and the keto carbon at δ_C 201.0 (C-1). Such correlation depicted a CH_2(OH)HCHC=HC-C(O)-C(OH) arrangement which indicated a six membered cyclic system with an α,β-unsaturated carbonyl group. The EIMS (Appendix 1.7) showed a quasimolecular ion peak $[M+H]^+$ at *m/z* 393 of a long chain alkenyl cyclohexenone, an alkenyl cyclohexenone derivative, together with NMR spectral data (Table 4; Appendix 1.0), molecular formula was established as $C_{25}H_{44}O_3$ and a characteristic fragment ion $[M-H_2O]^+$ at m/z 374 indicative of hydroxyl substituents.

The other alkene group appeared to be on a straight chain alkenyl type due to the multiplicity pattern and its presence was confirmed from the fragment ion peak at *m/z* 97 $[C_7H_{13}]^+$ resulting from allylic cleavage of hept-2-en-1-ylium in agreement with placement of the double bond at C-14'. The close ^{13}C NMR chemical shift values (δ_C 129.8 and δ_C 129.7) for the olefinic carbons C-14' and C-15' of compound **28** was consistent with assignment of *Z*-configuration to the double bond at C-14' of the alkenyl chain (Kapche, 2007; Okoth, Akala, Jonson, & Koorbanally, 2016; Okoth & Koorbanally, 2015). The orientation of the alkene substituent was assigned as 14'-(*Z*)-nonadecenyl based on the observed small coupling constant of J = 4.8 Hz (Kapche, 2007; Okoth, Akala, Jonson, & Koorbanally, 2016). The position of the double bond and its *Z*-configuration indicated that it is biosynthetically derived from fatty acid [5ω]-hexadecenoic-*cis*-hexadecenoic acid, through a similar mechanism as proposed for related compounds

The substitution pattern in the cyclohexenone ring was established from the ^1H-^1H COSY (Appendix 1.3) and HMBC (Appendix 1.5) experiment, where ^3J correlation of signal at δ_H 6.09 (d, H-2, J = 10.1 Hz) with signal at δ_C 64.1 (C-4) and δ_C 74.6 (C-6); signal at δ_H 6.90 (dd, H-3, J = 10.1, 3.6 Hz) with signals at δ_C 201.0 (C-1) and δ_C 41.1 (C-5) and signal at δ_H 2.21 (dd, H-5α, J = 5.4, 14.2 Hz) and δ_H 2.18 (dd, H-5β, J = 5.4, 14.2 Hz) with signals at δ_C 201.0 (C-1) and δ_C 149.9 (C-3) were observed. The placement of the alkenyl group at C-6 was also supported by the HMBC correlation of signal at δ_H 1.74 (2H, m, H-1') with signals at δ_C 201.0 (C-1) and δ_C 41.1 (C-5) as observed in related compounds (Okoth, Akala, Jonson, & Koorbanally, 2016).

The planar structure of compound **28** was the same as the ones reported by (De Jesus Correa, David, David, Chai, Pezzuto, & Cordelll, 2001; Okoth, Akala, Jonson, & Koorbanally, 2016; Yaouba, et al., 2017) and also based on the comparable NMR spectral data and the coupling patterns, it followed then that from the configurational assignment compound **28** was (4*R*,6*S*). The

compound **28** was characterized as (4*R*,6*S*)-4,6-dihydroxy-6-((*Z*)-nonadec-14'-en-1-yl)cyclohex-2-en-1-one, reported from *Lannea schweinfurthii* for the first time.

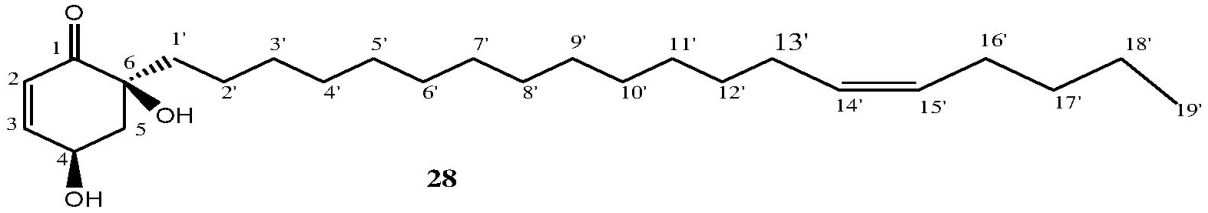

28

Table 4:^{1}H (500 MHz) and ^{13}C (125 MHz) NMR spectral data of compound **28** in $CDCl_3$

	Compound **28**	(Yaouba, et al., 2017)	Compound **28**	(Yaouba, et al., 2017)
Position	δ_H (*J* in Hz)	δ_H (*J* in Hz)	δ_C (ppm)	δ_C (ppm)
1			201.0	200.9
2	6.09 (d, *J* = 10.1 Hz)	5.96 (d, *J* = 10.1 Hz)	126.7	126.6
3	6.90 (dd, *J* = 10.1, 3.6 Hz)	6.80 (dd, *J* = 10.1,3.6 Hz)	149.9	149.4
4	4.70 (m)	4.62 (m)	64.1	64.0
5	2.21 (dd, *J* = 5.4, 14.2 Hz, H-5α) 2.18 (dd, *J* = 5.4, 14.2 Hz, H-5β)	2.20 (dd, *J* = 5.4,14.2 Hz) 2.15 (dd, *J* = 5.4,14.2 Hz)	41.1	41.0
6			74.6	74.5
1'	1.74 (m)	1.72 (m)	39.2	39.0
2'	1.24 (m)	1.25 (m)	22.9	22.9
3'-12'	1.20 (br, s)	1.17 (br, s)	29.9-29.2	29.8-29.2
13'	2.01 (m)	1.95 (m)	27.2	27.1
14',15'	5.34 (t, *J* = 4.8 Hz, H-14', H-15')	5.28 (t, *J* = 4.8 Hz)	129.8 129.7	129.8 129.7
16'	2.01 (m)	1.95 (m)	26.9	26.8
17'	1.24 (m)	1.25 (m)	32.0	31.8
18'	1.24 (m)	1.25 (m)	22.4	22.2
19'	0.92 (m)	0.83 (m)	14.0	13.9

4.3.2 (2*S*,4*R*,5*S*)-2,4,5-trihydroxy-2-((*Z*)-nonadec-14'-en-1-yl)cyclohexan-1-one (29)

Compound **29** was isolated as a white powder from *n*-hexane/DCM extract; yield (30 mg); R_f of 0.57 (15% EtOAc in *n*-hexane); m.p of 136-138°C. EIMS spectrum (Appendix 2.6) analysis showed a weak molecular ion peak $[M]^+$ at *m/z* 410 and a more stable fragment ion $[M\text{-}H_2O]^+$ at *m/z* 392.Comparison of the MS and NMR spectral data of this compound **29** (Table 5; Appendices 2.1 and 2.2) with those of compound **28** (Table 4; Appendices 1.1 and 1.2) indicated that the compound could be a hydroxylated-derivative of **28** with a molecular formula of $C_{25}H_{46}O_4$. The

EIMS data showed a close similarity between compound **28** and **29**, although NMR spectral data (Table 5; Appendices 2.1 and 2.2) of compound **29** indicated lack of one alkenyl functionality except an additional hydroxyl group.

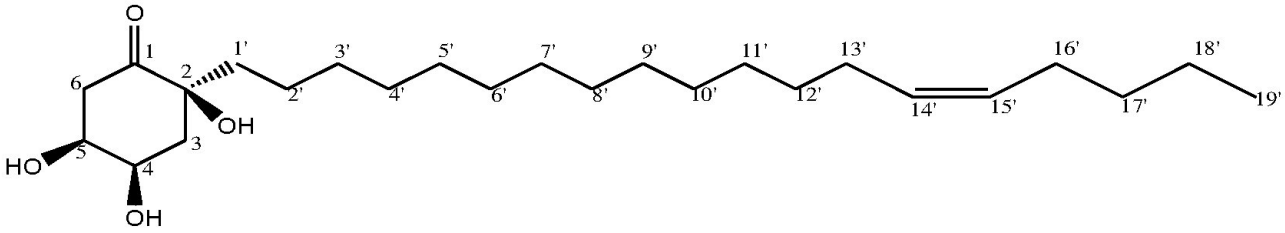

29

The NMR spectral data showed three hydroxylated carbons; one quaternary which appeared at δ_C 77.3 and two oxymethines at δ_C 68.4, δ_H 4.21(1H, ddd, J = 11.0, 4.5, 3.1 Hz) and δ_C 72.0, δ_H 3.99 (1H, m,) which were deduced based on the HSQC results (Appendix 2.4). The substitution pattern in the cyclohexanone ring was established from the HMBC spectrum (Appendix 2.5) correlation of signal at δ_H 2.97 (dd, H-3ax, J = 12.3, 11.2 Hz) and δ_H 2.71 (m, H-3eq) with signal at δ_C 210.9 (C-1) and δ_C 72.0 (C-5); signal at δ_H 4.21 (ddd, H-4, J = 11.0, 4.5, 3.1 Hz) with signal at δ_C 77.3 (C-2) and δ_C 40.3 (C-6); signal at δ_H 3.99 (2H, m, H-5) with signal at δ_C 210.9 (C-1) and δ_C 41.9 (C-3); signals at δ_H 2.41 (dd, H-6ax, J = 14.8, 4.1 Hz) and δ_H 1.70 (dd, H-6eq, J = 14.8, 3.5 Hz) with signals at δ_C 77.3 (C-2) and δ_C 68.4 (C-4) and signals at δ_H 1.76 (d, H-1'β, J = 4.4 Hz) and δ_H 2.05 (m, H-1'α) with signals at δ_C 210.9 (C-1) and δ_C 41.94 (C-3). This substitution was further supported by ^{1}H-^{1}H COSY correlation (Appendix 2.3) that depicted a CH_2-3↔H-4↔H-5↔CH_2-6 connectivity and proved a trisubstituted cyclohexanone. The observation indicated that two of the hydroxyl groups were located on adjacent carbon atoms, signals at δ_C 68.4 (C-4) and δ_C 72.0 (C-5). The side chain at δ_C 77.3 (C-2) in compound **29** was

established to be nonadec-14'-en-1-yl (Okoth & Koorbanally, 2015; Quieroz, Kuhl, Terreaux, Mavi, & Hostettmann, 2003) group based on the EIMS, molecular ion $[M]^+$ at *m/z* 410 and the fragment ion $[C_7H_{13}]^+$ at *m/z* 97 formed as a result of allylic cleavage of hept-2-en-1-ylium group consistent with the placement of the double bond at δ_C 129.9 (C-14'). The HMBC spectrum showed correlation of signal at δ_H 0.92 (3H, t, H-19', J = 7.1 Hz) with a sp^3 carbon atoms signals at δ_C 22.4 (C-18') and δ_C 32.0 (C-17'), showing that the double bond was not located two bonds away from the terminal methyl group as found in some other alkenyl cyclohexanone derivatives The HMBC correlation of signal at δ_H 2.05 (m, H-13') and δ_H 2.05 (m, H-16') with signal at δ_C 129.8 (C-15') and δ_C 129.9 (C-14'), confirmed the location of the double bond at δ_C 129.9 (C-14'). Comparison of the ^1H and ^{13}C NMR spectral data with those of compound **28** and related compounds having similar long alkenyl chain suggested *Z*-configuration at C-14' (Groweiss, Cardellina, Pannell, Uyakul, Kashman, & Boyd, 1997; Kapche, 2007; Okoth, Akala, Jonson, & Koorbanally, 2016). The two olefinic protons on the side chain, H-14' and H-15', appeared overlapping at δ_H 5.38 (t, J = 4.7 Hz) showed HMBC correlations with the signals at δ_C 27.2 (C-13') and δ_C 26.9 (C-16') of allylic carbon. These ^{13}C NMR chemical shift values were consistent with a *Z*-configuration for the double bond on the side chain, as a double bond with *E*-configuration was expected to appear at higher signal values (δ_C 32.0) for the allylic carbon atoms (Roumy, Fabre, Portet, Bourdy, Acebey, Vigor, et al., 2009).

The large coupling constant between H-3ax δ_H 2.97 (1H, dd, J = 12.3, 11.2 Hz) and H-4 δ_H 4.21 (ddd, J = 11.0, 4.5, 3.1 Hz) required that H-4 was axial and hence OH-4 should be equatorial. On the other hand, the small coupling constant between H-4 and H-5 required that H-5 be equatorial while OH-5 to be axially oriented. These observations were consistent with the two hydroxy groups being *cis*-oriented. The relative stereochemical co-occurrence of compound **29**

with **28** indicated that they were biogenetically related, and it was likely that the configurations at C-2 (C-6 in compound **28**) and C-4 in compound **29** were same as in **28**. In compound **29** (where the cyclohexanone ring was rigid, stabilized by hydrogen bonding between C=O and OH-2, OH-4 must be equatorial (α-oriented), OH-5 should be axial (β-oriented). Thus, relative configuration of **29** was likely to be (2*S*,4*R*,5*S*) from the literature studies as described by (Yaouba, et al., 2017). Hence the compound **29** was characterized as (2*S*,4*R*,5*S*)-2,4,5-trihydroxy-2-((*Z*)-nonadec-14'-en-1-yl)cyclohexan-1-one, reported for the first time from *Lannea schweinfurthii*.

Table 5: ^{1}H (500MHz) and ^{13}C (125MHz) NMR spectral data of compound **29** in CD_2Cl_2

	Compound **29**	(Yaouba, et al., 2017)	Compound **29**	(Yaouba, et al., 2017)
Position	δ_H (*J* in Hz)	δ_H (*J* in Hz)	δ_C (ppm)	δ_C (ppm)
1			210.9	210.9
2			77.3	77.3
3	2.97 (dd, *J* = 12.3, 11.2 Hz, H-3ax) 2.71 (m, H-3eq)	2.98 (dd, *J* = 12.3,11.2 Hz) 2.70 (m)	41.9	41.8
4	4.21 (ddd, *J* = 11.0, 4.4, 3.1 Hz)	4.20 (ddd, *J* = 11.0, 4.4,3.1)	68.4	68.5
5	3.99 (m)	4.00 (m)	72.0	71.9
6	2.41 (dd, *J* = 14.8, 4.1 Hz, H-6ax) 1.70 (dd, *J* = 14.8, 3.5 Hz, H-6eq)	2.40 (dd, *J* = 14.8, 4.1 Hz) 1.71 (dd, *J* = 14.8, 3.5 Hz)	40.3	40.4
1'	2.05 (m, H-1'α) 1.76 (d, *J* = 4.4 Hz, H-1'β)	2.06 (m, H-1'α) 1.77 (d, *J* = 4.4 Hz, H-1'β)	39.5	39.5
2'	1.36 (m)	1.36 (m)	23.1	23.1
3'-12'	1.29 (br, s)	1.29 (br, s)	29.9-29.3	29.8-29.3
13'	2.05 (m)	2.06 (m)	27.2	27.2
14', 15'	5.38 (t, *J* = 4.7 Hz, H-14', H-15')	5.36 (t, *J* = 4.7 Hz)	129.9 129.8	129.8 129.7
16'	2.05 (m)	2.06 (m)	26.9	26.9
17'	1.36 (m)	1.36 (m)	32.0	32.0
18'	2.05 (m)	2.06 (m)	22.4	22.4
19'	0.92 (t, *J* = 7.1 Hz)	0.94 (t, *J* = 7.1 Hz)	13.8	13.7

4.3.3 Stigmasterol (30)

Compound **30** was isolated as a white amorphous solid from *n*-hexane/dichloromethane extract; yield (40 mg); single spot on TLC, R_f of 0.56 (25% EtOAc in *n*-hexane); m.p 142-144°C. The ^{1}H and ^{13}C NMR spectral data (Table 6) were used to deduce the structure of compound **30**. The ^{1}H

NMR spectrum (Appendix 3.1) showed signals between δ_H 0.71 and δ_H 5.1, consisting of six high intensity peaks which indicated the presence of six methyl groups at δ_H 0.71, 0.85, 0.97, 1.04, 1.21 and 1.53. Three signals appeared as doublets at δ_H 0.85 (3H, d, J = 6.6 Hz), 0.97 (3H, d, J = 6.6 Hz) and δ_H 1.21 (3H, d, J = 6.2 Hz) were ascribed to H-26, H-27 and H-21, respectively, while the signal at δ_H 1.04 (3H, t, J = 7.1 Hz) appeared as a triplet was assigned to H-29. In addition, the spectrum revealed the existence of three signals that appeared downfield at δ_H 5.08, 5.18 and 5.31, this suggested the presence of olefinic protons of a sterol structure (Habib, Nikkon, Rahman, Haque, & Karim, 2007). The signals at δ_H 5.18 (1H, m) and δ_H 5.31 (1H, m) appeared as a multiplet, suggested the presence of two alkenic methine protons. Two signals appeared as singlets at δ_H 1.27, and 0.71 for angular methyl protons were assigned to C-18 and C-19, respectively. Furthermore, the spectrum showed a signal that appeared as a multiplet at δ_H 3.51 (1H, m) that corresponded to protons of H-3 of sterol moiety and OH-3.

^{13}C NMR spectrum (Appendix 3.2) of compound **30** showed recognizable signals at δ_C 141.1 and 121.9 which were assigned to C-5 double bonded to C-6 (C5=C6) as in Δ^5 spirostene. Two signals at δ_H 138.6 and 129.4 assigned for C-22 double bonded to C-23 (C22=C23). The C-5, C-6, C-22 and C-23 appeared as alkene carbons based on the spectrum. The signal at δ_C 71.9 of an oxymethine group for C-3 observed from the spectrum, indicated a β-hydroxyl (Habib *et al.*, 2007). In addition, signals at δ_C 19.4 and 12.2 corresponded to angular methyl carbon atoms for C-19 and C-18, respectively. The spectrum showed twenty-nine carbon signals consisting of six methyls, nine methylenes, eleven methines and three quaternary carbons. Based on the spectral data, compound **30** was identified as stigmasterol.

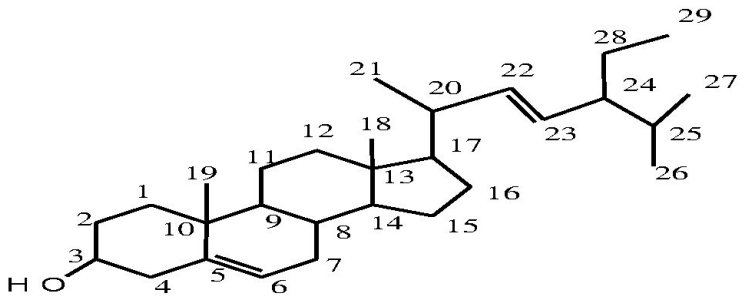

30

Table 6: ^{1}H (500 MHz) and ^{13}C (125 MHz) NMR spectral data of compound **30** in $CDCl_3$

	Compound **30**	(Habib, Nikkon, Rahman, Haque, & Karim, 2007)	Compound **30**	(Habib, Nikkon, Rahman, Haque, & Karim, 2007)
Position	δ_H (J in Hz)	δ_H (J in Hz)	δ_C (ppm)	δ_C (ppm)
1			36.4	36.7
2			29.8	31.6
3	3.51 (m, 1H)	3.53 (m, 1H)	71.9	71.8
4			42.0	42.2
5			141.1	141.0
6	5.31 (m, 1H)	5.38 (m, 1H)	121.9	121.6
7			31.9	31.8
8			29.8	30.9
9			51.1	50.1
10			35.0	36.5
11			24.4	24.3
12			39.8	39.7
13			42.0	40.4
14			57.0	56.9
15			24.4	24.3
16			28.0	28.9
17			56.1	56.0
18	1.27 (s, 3H)	1.29 (s, 3H)	12.2	12.0
19	0.71 (s, 3H)	0.74 (s, 3H)	19.4	19.0
20			39.8	39.8
21	1.21 (d, 3H, J = 6.2 Hz)	1.20 (d, 3H, J = 6.2 Hz)	23.0	23.1
22	5.08 (dd, 1H, J = 18.0, 4.2)	5.07 (dd, 1H, J =18.0,4.2)	138.6	138.4
23	5.18 (1H, m)	5.20 (1H, m)	129.4	129.3
24			51.1	51.2
25			34.1	34.0
26	0.85 (d, 3H, J = 6.6 Hz)	0.84 (d, 3H, J = 6.6 Hz)	21.2	21.1
27	0.97 (d, 3H, J = 6.6 Hz)	0.97 (d, 3H, J = 6.6 Hz)	23.0	22.8
28			25.3	25.3
29	1.04 (t, 3H, J = 7.1 Hz)	1.04 (t, 3H, J = 7.1 Hz)	12.2	12.0

4.3.4 5-hydroxy-7,8-(2'',2''-dimethylchromene)-flavanone (31)

Compound **31** was isolated as a pale yellow solid from EtOAc extract; yield (30 mg); R_f of 0.54 (75% of EtOAc in *n*-hexane); m.p of 200-201°C. The EIMS spectrum (Appendix 4.6) of the compound indicated a peak $[M+CH_2]^+$ at *m/z* 335.1949 together with ^1H, ^{13}C NMR spectral data (Table 7), exact molecular structure and molecular formula of $C_{20}H_{18}O_4$ was established.

The ^1H NMR spectrum (Appendix 4.1) showed signals at δ_H 5.44 (1H, dd, *J* = 12.9, 3.3 Hz), δ_H 3.06 (1H, dd, *J* = 17.1, 12.9 Hz) and δ_H 2.83 (1H, dd, *J* = 17.1, 3.3 Hz). From the ^1H-^1H COSY (Appendix 4.3), there was a correlation of signal at δ_H 5.44 (1H, dd, *J* = 12.9, 3.3 Hz) to signal at δ_H 3.06 (1H, dd, *J* = 17.1, 12.9 Hz) and δ_H 2.83 (1H, dd, *J* = 17.1, 3.3 Hz), a spin system indicative of a flavanone structure (Rocio, Maria, Peter, & Luis, 2005). The HMBC correlation (Appendix 4.4) of signals at δ_H 5.44 (1H, dd, *J* = 12.9, 3.3 Hz), δ_H 3.06 (1H, dd, *J* = 17.1, 12.9 Hz) and δ_H 2.83 (1H, dd, *J* = 17.1, 3.3 Hz) with ^{13}C NMR signals at δ_C 78.1 and δ_C 125.9, further confirmed the presence of the flavanone structure. The ^1H NMR spectrum showed a five protons multiplet signal at δ_H 7.46 (5H, m) of an aromatic group, a characteristic of phenyl moiety and signals at δ_H 5.49 (d, *J* = 10.0 Hz), δ_H 6.57 (1H, dd, *J* = 10.0 Hz) of benzopyran aromatic ring protons together with a signal at δ_H 12.09 (s) ascribed to a chelated phenolic proton. These observations were predictive of flavanone skeleton with trisubstituted benzopyran ring and non-substituted ring C. Moreover, there was a pair of signals for alkenic protons at δ_H 5.49 (1H, dd, *J* = 10.0 Hz) and δ_H 6.57 (1H, dd, *J* = 10.0 Hz), with coupling constant of *J* = 10.0 Hz, the coupling constant lower than 12.0 Hz indicative of a *cis*-configuration. The ^1H NMR spectrum showed two methyl protons signals at δ_H 1.42 and δ_H 1.43 (2 ×CH_3) that showed HMBC correlation to signal δ_C 125.9 of the alkene moiety and ^1H -^1H COSY correlation to the alkene proton. Such connectivity displayed the existence of prenylated *O*-pyran group possibly cyclized on the aryl ring A.

The ^{13}C NMR spectrum (Appendix 4.2) consisted of eighteen carbon signals with fourteen signals being in aromatic or double bond region and a chelated carbonyl signal at δ_C 195.6 consistent with the structure of flavonoid. Four signals out of the fourteen signals were between δ_C 146.5 and δ_C 195.6 attributed to the four oxygenated carbon atoms at δ_C 146.5, δ_C 156.7, δ_C 163.8 and δ_C 162.3. Nine signals in the olefinic and aromatic region between δ_C 97.6 and δ_C 138.8 were attributed to δ_C 138.5, δ_C 102.8, δ_C 97.6, δ_C 125.9, δ_C 126.4, δ_C 128.7, δ_C 128.8, δ_C 115.5 and δ_C 125.9. The germinal dimethyl signals occurred at δ_C 28.2 and δ_C 28.5.

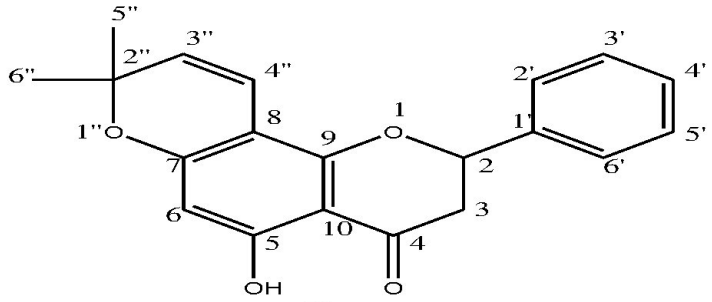

31

The proton signal at δ_H 5.49 (d, H-3'', J = 10.0 Hz) showed HMBC correlations to the methyl carbon signal at δ_C 28.2 (C-5''), δ_C 28.5 (C-6'') and the oxygenated carbon of the prenylated pyran group signal at δ_C 79.1 (C-2''). The proton signal at δ_H 6.01 (s, H-6) showed HMBC correlations to the aromatic carbon signal at δ_C 102.9 (C-6). The fact that this signal was seen also coupled to the chelated hydroxyl proton of OH-5 indicated a connectivity between C-4'', C-8 and C-7 rather than C-4'' and C-6. This confirmed the connectivity of 2'',2''-dimethylpyran/chromene at C-7 and C-8. The signal at δ_H 6.57 (H-4'') showed HMBC correlations to signals at δ_C 163.8 (C-7), δ_C 97.6 (C-8) and δ_C 162.3 (C-9). The signal at δ_H 6.01 (H-6) showed HMBC correlation to signals at δ_C 163.8 (C-7) and δ_C 156.7 (C-5). It followed from the spectral data that compound **31** was identified as 5-hydroxy-7,8-(2'',2''-dimethylchromene)-flavanone.

Table 7: ^{1}H (500MHz) and ^{13}C (125MHz) NMR spectral data of compound **31** in $CDCl_3$

	Compound **31**	(Rocio, Maria, Peter, & Luis, 2005)	Compound **31**	(Rocio, Maria, Peter, & Luis, 2005)
Position	δ_H (*J* in Hz)	δ_H (*J* in Hz)	δ_C (ppm)	δ_C (ppm)
2	5.44 (dd, *J* = 12.9, 3.3 Hz)	5.41 (dd, *J* = 13.0, 3.0)	78.1	79.4
3	3.06 (dd, *J* = 17.1, 12.9 Hz, H-3ax) 2.83 (dd, *J* = 17.1, 3.3 Hz, H-3eq)	3.08 (dd, *J* = 17.0,13.0) 2.83 (dd, *J* = 17.0, 3.0)	43.3	43.6
4			195.6	196.0
5	12.09 (s, OH)	12.28 (s, OH)	156.7	158.7
6	6.01 (s)	5.90 (s)	102.9	105.0
7			163.8	162.4
8			97.6	96.5
9			162.3	162.6
10			102.8	105.0
1'			138.5	138.7
2'	7.46 (m)	7.45 (m)	126.4	126.3
3'	7.46 (m)	7.45 (m)	128.7	129.8
4'	7.46 (m)	7.45 (m)	128.8	129.8
5'	7.46 (m)	7.45 (m)	128.7	129.8
6'	7.46 (m)	7.45 (m)	126.4	126.3
2''			79.1	79.10
3''	5.49 (d, *J* = 10.0 Hz)	5.51 (d, *J* = 10.0 Hz)	125.9	126.5
4''	6.57 (d, *J* = 10.0 Hz)	6.63 (d, *J* = 10.0 Hz)	115.5	115.5
5''	1.42 (s)	1.45 (s)	28.2	28.6
6''	1.43 (s)	1.46 (s)	28.5	28.7

4.3.5 5-methoxy-7,8-(2'',2''-dimethylchromene)-flavanone (32)

Compound **32** was isolated as a light yellow solid from EtOAc extract; yield (20 mg); R_f of 0.56 (75% of EtOAc in *n*-hexane); m.p of 204-205°C. The EIMS (Appendix 5.7) indicated molecular ion $[M]^+$ at *m/z* of 336.1181 corresponding to $C_{21}H_{20}O_4$ showing addition of 12 a.m.u, which implied compound **32** was a derivative of compound **31** except for additional methyl group. The additional methyl group was supported by the appearance of an intense singlet signal at δ_H 3.97 on ^{1}H NMR (Table 8) which showed the presence of a methoxy group. The absence of a highly deshielded proton signal at δ_H 12.09 as observed in compound **31** and ascribed to chelated proton OH-5 signified methylation of the 5-OH in compound **32**. This assertion was confirmed by the HMBC (Appendix 5.5) correlation between the methoxy proton signal at δ_H 3.97 and carbon signal at δ_C 156.7 (C-5).

The ^{1}H NMR spectrum (Appendix 5.1) showed signals at δ_H 5.29 (1H, dd, J = 12.9, 3.3 Hz), δ_H 3.06 (1H, dd, J = 17.1, 12.9 Hz) and δ_H 2.83 (1H, dd, J = 17.1, 3.3 Hz). From the ^{1}H-^{1}H COSY (Appendix 5.4), there was a correlation of signal at δ_H 5.29 (1H, dd, J = 12.9, 3.3 Hz) to signal at δ_H 3.06 (1H, dd, J = 17.1, 12.9 Hz) and δ_H 2.83 (1H, dd, J = 17.1, 3.3 Hz), showing a flavanone structure (Rocio, Maria, Peter, & Luis, 2005). The HMBC correlation of signals at δ_H 5.29 (1H, dd, J = 12.9, 3.3 Hz), δ_H 3.06 (1H, dd, J = 17.1, 12.9 Hz) and δ_H 2.83 (1H, dd, J = 17.1, 3.3 Hz) with ^{13}C NMR signal at δ_C 138.9, further confirmed the presence of the flavanone structure. The ^{1}H NMR spectrum of compound **32** was very similar to that of compound **31** with the proton signals and splitting patterns of the five protons multiplet signals at δ_H 7.50 (5H, m) of aromatic group, a characteristic of phenyl protons were observed on the ^{1}H NMR spectrum. Two additional doublet signals at δ_H 6.62 (1H, d, J = 10.0 Hz), δ_H 5.48 (1H, d, J = 10.0 Hz) and two singlet signals at δ_H 1.37 (3H, s) and δ_H 1.40 (3H, s) were also observed in the ^{1}H NMR spectrum, all being very close to those signals of compound **31**. The ^{1}H NMR spectrum showed a pair of doublet signals at δ_H 5.48 (1H, d, J = 10.0 Hz) and δ_H 6.62 (1H, d, J = 10.0 Hz) indicating a cyclized prenylated *O*-pyran group and two methyl protons signals at δ_H 1.37 and δ_H 1.40 (2 $\times CH_3$), with two methyl carbon signals at δ_C 28.1 and δ_C 28.4. In addition, a multiplet signal at δ_H 7.50 (5H, m) of a five-proton aromatic group characteristic of phenyl protons and signals at δ_H 5.48, δ_H 6.62 of a benzopyran ring were observed. The ^{13}C NMR spectrum (Appendix 5.2) showed nineteen carbon signals with fourteen signals being in aromatic or double bond region and a carbonyl signal at δ_C 189.1, which showed no chelation as in compound **31**, this was consistent with the structure of flavonoid.

The signals at δ_H 6.62 (1H, d, H-4'', J = 10.0 Hz) and δ_H 5.48 (1H, dd, H-3'', J = 10.0 Hz), both olefinic protons of the cyclized prenylated pyran group were seen coupled in the ^{1}H-^{1}H COSY

spectrum. The signal at δ_H 6.62 (H-4'') showed HMBC correlations to signals at δ_C 162.1 (C-7), δ_C 93.7 (C-8) and δ_C 159.9 (C-9). The signal at δ_H 6.01 (H-6) showed HMBC correlation to signal at δ_C 105.6 (C-6) indicated a connectivity between C-4'', C-8 and C-7 rather than C-4'' and C-6. This confirmed the connectivity of 2'',2''-dimethylpyran/chromene at C-7 and C-8. Based on the spectral data and literature comparison, compound **32** was identified as 5-methoxy-7,8-(2'',2''-dimethylchromene)-flavanone, reported for the first from *Lannea schweinfurthii*.

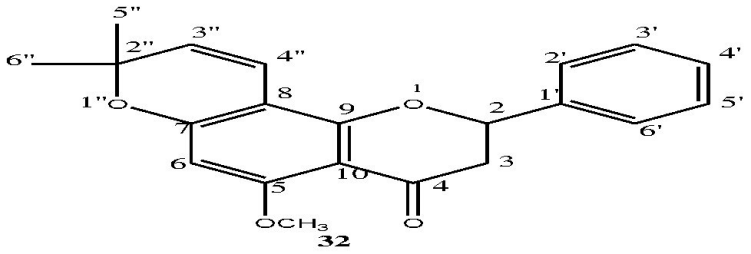

32

Table 8: ^{1}H (500MHz) and ^{13}C (125MHz) NMR spectral data of compound **32** in $CDCl_3$

	Compound **32**	(Rocio, Maria, Peter, & Luis, 2005)	Compound **32**	(Rocio, Maria, Peter, & Luis, 2005)
Position	δ_H (J in Hz)	δ_H (J in Hz)	δ_C (ppm)	δ_C (ppm)
2	5.29 (dd, J = 12.9, 3.3 Hz)	5.03 (dd, J = 12.0, 3.3)	77.2	83.3
3	3.06 (dd, J = 17.1, 12.9 Hz,H-3ax) 2.83 (dd, J = 17.1, 3.3 Hz,H-3eq)	4.46 (dd, J = 17.1,12.0) 2.83 (dd, J = 17.1, 3.3)	45.6	72.8
4			189.1	190.4
5			156.7	161.3
6	6.01 (s)	6.08 (s)	105.6	105.2
7			162.1	155.6
8			93.7	92.0
9			159.9	163.6
10			105.6	102.9
1'			138.9	136.5
2'	7.50 (m)	7.57 (m)	126.2	127.5
3'	7.50 (m)	7.48 (m)	128.4	128.7
4'	7.50 (m)	7.48 (m)	128.6	129.2
5'	7.50 (m)	7.48 (m)	128.4	128.7
6'	7.50 (m)	7.57 (m)	126.2	127.5
2''			77.9	77.2
3''	5.48 (d, J = 10.0 Hz)	5.52 (d, J = 10.0 Hz)	125.8	126.6
4''	6.62 (d, J = 10.0 Hz)	6.55 (d, J = 10.0 Hz)	115.9	115.8
5''	1.37 (s)	1.38 (s)	28.1	27.8
6''	1.40 (s)	1.40 (s)	28.4	28.1
OCH_3	3.97 (s)	3.84 (s)	56.1	55.6

4.3.6 3-*O*-[β-Glucopyranosyl-(1''→2')-*O*-β-xylopyranosyl]-β-stigmasterol (33)

Compound **33** was isolated as a white amorphous solid from MeOH extract; yield (15 mg); R_f of 0.60 (9:1 MeOH/DCM); m.p 147-149°C. The ^{1}H NMR spectrum of compound **33** (Table 9; Appendix 6.1) displayed three regions, characteristic of hydroxymethines, alkenic and aliphatic protons signals (Rai, Adhikari, Paudel, Masuda, Mckelvey, & Manandhar, 2006). The ^{1}H-^{1}H COSY showed a correlation between the hydroxymethine signal at δ_H 3.62 (1H, m) and hydroxymethine signal at δ_H 3.40 (1H, m) which strongly suggested a glucopyranosyl moiety. The signals at δ_H 5.25 (1H, dd, J = 18.0, 4.2 Hz) and δ_H 5.13 (1H, dd, J = 18.0, 8.1 Hz) suggested the presence of a *trans*/E oriented alkene system. The other alkene signal appeared as multiplet at δ_H 5.33 (1H, m) and showed a ^{1}H-^{1}H COSY correlation to methylene proton signals at δ_H 1.47 (2H, m) and δ_H 1.67 (2H, m). This suggested a cyclic allylic system. Signals for six methyl groups consisting of two tertiary methyls at δ_H 0.96 (3H, s), δ_H 0.65 (3H, s), three secondary methyls at δ_H 0.90 (1H, d, J = 6.5 Hz), δ_H 0.79 (3H, d, J = 7.0 Hz), δ_H 0.77 (3H, d, J = 7.0 Hz) and one primary methyl at δ_H 0.83 (3H, t, J = 7.0 Hz) together with two alkenic signals at δ_H 5.25 (1H, dd, J = 18.0, 4.2 Hz) and δ_H 5.13 (1H, dd, J = 18.0, 8.1 Hz) signified characteristic peaks for stigmastane triterpenoid (Rai, Adhikari, Paudel, Masuda, Mckelvey, & Manandhar, 2006). A combination of such a set of six methyl groups and two alkenes moieties as confirmed by ^{13}C NMR spectra (Table 9; Appendix 6.2) that showed δ_C 140.3 and δ_C 121.1 undoubtedly indicated compound **33** to have stigmasterol aglycone.

A stigmastane triterpenoid would be expected to have a hydroxyl group at C-3, with a proton signal at δ_H 3.50 to 3.65, however, for compound **33**, this was not the case, and instead it showed a series of hydroxymethine protons. The signal for the proton at C-3 was at δ_H 3.92 (1H,

m) which was shifted downfield instead of δ_H 3.50 to 3.65, indicated presence of a different functional group other than the expected hydroxyl group. The downfield shift was similarly observed on ^{13}C NMR for the carbon that showed HSQC correlation to the proton at δ_H 3.92 as δ_C 82.3, the possible explanation to this occurrence was the existence of sugar moiety confirmed by the additional twelve hydroxymethine protons.

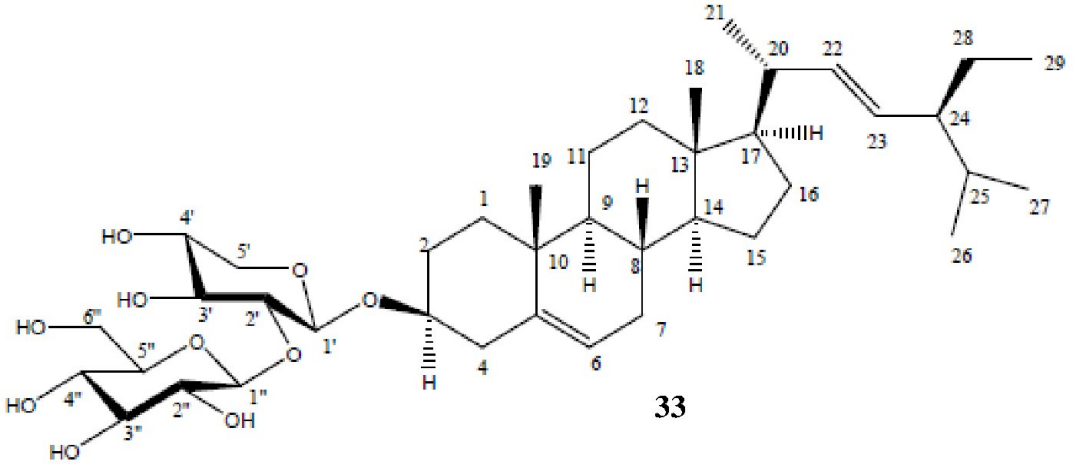

33

The appearance of two signals at δ_C 106.4 and δ_C 101.3 signified two anomeric carbons, one oxymethylene signal at δ_C 63.8 and eight oxymethine signals at δ_C 69.6, δ_C 68.0, δ_C 74.9, δ_C 76.6, δ_C 65.3, δ_C 73.4, δ_C 70.3 and δ_C 77.7 implied more than one simple sugar moiety but a di-sugar groups. Existence of eleven sugar carbons suggested a pentose and hexose sugar moieties identified by comparing their ^{13}C and ^{1}H NMR spectra with those of the literature (Orsini, Pelizzoni, & Verotta, 1991; Tapondjou, Miyamoto, Mirjolet, Guilbaud, & Lacaille-Dubois, 2005; Toukam, Maurice, Lauve, Gakul, Nabin, Alembert, et al., 2018). Based on the aforementioned ^{1}H NMR and ^{13}C NMR spectral data (Table 9) and the ESIMS spectrum (Appendix 6.5) analysis which showed a stable quasimolecular ion $[M+H]^+$ at *m/z* 707.4450 alongside fragment ions at *m/z*

413.2356 and 411.4105 that corresponded to loss of a pentose and hexose units, respectively, that corresponded to a molecular formula of $C_{40}H_{66}O_{10}$. Both sugar units connected to aglycone were predicted to be β-oriented based on the fact that the anomeric protons H-1' showed coupling constants J = 8.8 Hz consistent with β-orientation and not α-orientation which was characterized with J = 2.5–4.0 Hz (Altona & Haasnoot, 1980). The predictions were based on cyclohexane ring orientation placed all the proton substituents axial, implied the anomeric H-1' and H-2' were both anti-oriented, thus experienced the 180° dihedral angle and displayed larger coupling constant as opposed to H-2' axial coupling to H-1'equatorial.

The HMBC (Appendix 6.4) showed correlation of signal at δ_H 4.49 (1H, d, H-1', J = 8.8 Hz) with signal at δ_C 82.3 (C-3), δ_C 74.9 (C-2'), δ_C 76.6 (C-3'') which confirmed the connectivity of the pentose unit to the stigmasterol at C-3. The other anomeric proton signal at δ_H 4.89 (1H, d, H-1'', J = 8.8 Hz) showed HMBC correlation with signals at δ_C 77.7 (C-3'), δ_C 70.3 (C-2'') and δ_C 76.6 (C-3'') which confirmed the linkage between hexose unit to pentose unit was at C-2'. Moreover, HMBC correlations observed between signal at δ_H 4.89 (1H, d, H-1'', J = 8.8 Hz) and signal at δ_C 74.9 (C-2'), in turn signal at δ_H 3.83 (1H, m, H-2') correlated to signal at δ_C 101.3 (C-1'') confirmed the linkage between the two sugars to be possibly at 1''→2'. The two proton signals at δ_H 4.46 (1H, dd, H-6''α, J = 12.3, 3.0 Hz); δ_H 4.49 (1H, dd, H-6''β, J = 12.3, 3.0 Hz) both attached to δ_C 63.8 (C-6'') on HSQC (Appendix 6.3) showed hydroxylated methylene was attached to hexose moiety which that represented glucopyranosyl group and the pentose moiety was xylose unit. Based on these spectral data, the compound **33** was identified as 3-*O*-[β-glucopyranosyl-(1''→2')-*O*-β-xylopyranosyl]-β-stigmasterol, reported for the first time from *Lannea schweinfurthii*.

Table 9: ^{1}H (500 MHz) and ^{13}C (125 MHz) NMR spectral data of compound **33** in CD_3OD

	Compound **33**	(Toukam, et al., 2018)	Compound **33**	(Toukam, et al., 2018)
Position	δ_H (*J* in Hz)	δ_H (*J* in Hz)	δ_C (ppm)	δ_C (ppm)
1	1.14 (2H, m) 1.20 (2H, m)	1.59 (2H, m) 1.08 (2H, m)	38.2	26.7
2	1.80 (2H, m) 1.78 (2H, m)	1.94 (2H, m) 1.64 (2H, m)	31.3	31.9
3	3.92 (1H, m)	3.62 (1H, m)	82.3	81.4
4	2.92 (2H, m)	2.92 (2H, m)	42.7	41.0
5			140.3	142.8
6	5.33 (1H, m)	5.38 (1H, m)	121.1	124.3
7	1.47 (2H, m) 1.67 (2H, m)	1.99 (2H, m) 1.58 (2H, m)	35.4	34.3
8	2.50 (1H, m)	1.47 (1H, m)	31.7	34.4
9	2.38 (1H, m)	0.93 (1H, m)	49.4	52.7
10			38.3	39.2
11	1.49 (2H, m) 1.74 (2H, m)	1.44 (2H, m) 1.18 (2H, m)	22.5	27.8
12	2.10 (2H, m) 1.96 (2H, m)	2.02 (2H, m) 1.19 (2H, m)	39.7	42.2
13			41.6	44.6
14	1.23 (1H, m)	0.94 (1H, m)	56.1	48.3
15	1.15 (2H, m) 2.23 (2H, m)	1.88 (2H, m) 1.09 (2H, m)	25.3	39.7
16	1.02 (2H, m) 2.20 (2H, m)	1.73 (2H, m) 1.30 (2H, m)	28.6	31.4
17	0.98 (1H, m)	1.03 (1H, m)	50.4	59.4
18	0.65 (3H, s)	0.71 (3H, s)	20.3	14.2
19	0.96 (3H, s)	1.06 (3H, s)	20.5	21.5
20	1.51 (1H, m)	2.05 (1H, m)	40.0	43.0
21	0.90 (1H, d, *J* = 6.5 Hz)	1.04 (1H, d, 3.4 Hz)	20.8	23.4
22	5.25 (1H, dd, *J* = 18.0, 4.2 Hz)	5.17 (1H, dd, *J* = 15.1, 6.1 Hz)	137.9	140.9
23	5.13 (1H, dd, *J* = 18.0, 8.1 Hz)	5.04 (1H, dd, *J* = 15.1, 6.3 Hz)	128.2	131.7
24	1.45 (1H, m)	1.55 (1H, m)	55.3	53.8
25	1.43 (1H, m)	1.15 (1H, m)	29.2	58.4
26	0.79 (3H, d, *J* = 7.0 Hz)	0.85 (3H, m)	21.0	23.2
27	0.77 (3H, d, *J* = 7.0 Hz)	0.79 (3H, m)	20.2	21.1
28	1.23-1.34 (2H, m)	1.24-1.52 (2H, m)	27.7	23.5
29	0.83 (3H, t, *J* = 7.0 Hz)	0.82 (3H, m)	18.7	14.2
1'	4.49 (1H, d, *J* = 8.8 Hz)	4.45 (1H, d, *J* = 7.8 Hz)	106.4	103.1
2'	3.83 (1H, m)	3.40 (1H, m)	74.9	75.3
3'	3.62 (1H, m)	3.53 (1H, m)	77.7	89.9
4'	3.40 (1H, m)	3.48 (1H, m)	69.6	71.3
5'	4.46 (1H, dd, *J* = 12.3, 5.5 Hz) 3.13 (1H, m)	3.73 (1H, dd, *J* = 11.9, 5.2 Hz) 3.89 (1H, m)	65.3	64.1
1''	4.89 (1H, d, *J* = 8.8 Hz)	4.53 (1H, d, *J* = 7.8 Hz)	101.3	106.6
2''	4.22 (1H, d, *J* = 8.8 Hz)	3.36 (1H, m)	70.3	79.2
3''	4.05 (1H, d, *J* = 8.8 Hz)	3.35 (1H, m)	76.6	76.5
4''	4.78 (1H, d, *J* = 8.8 Hz)	3.43 (1H, m)	73.4	78.9
5''	3.48 (1H, m)	3.34 (1H, m)	68.0	72.6
6''	4.46 (1H, dd, *J* = 12.3, 3.0 Hz) 4.49 (1H, dd, *J* = 12.3, 3.0 Hz)	3.91 (1H, m) 3.67 (1H, dd, *J* = 11.9, 5.9 Hz)	63.8	63.9

4.4 Bioassay of isolated compounds

4.4.1 *In-vitro* α-amylase inhibition IC_{50} by the compounds

Compounds **28**, **29**, **30**, **31, 32** and **33** were subjected to *in-vitro* α-amylase inhibition assay. The results obtained on *in-vitro* inhibitory activities were as plotted in the Figure 2. The dose dependent *in-vitro* α-amylase inhibitory activities of these compounds were processed on long probit analysis to establish the IC_{50} values. Compounds **31** and **33** showed high inhibitory activities on α-amylase ($p>0.05$) (IC_{50} = 0.665 mM and 0.580 mM, respectively) relative to metformin (IC_{50} = 0.468 mM). Compound **33** had a significantly higher inhibitory activity on α-amylase, followed with compound **31**, whereas compounds **28, 30** and **29** showed a significant difference ($p<0.05$) in their low inhibitory activities on α-amylase (IC_{50} = 1.245 mM, 1.125 mM and 1.037 mM, respectively) relative to metformin (IC_{50} = 0.468 mM). Compound **32** showed moderate inhibitory activity on α-amylase (IC_{50} = 0.826 mM) relative to metformin (IC_{50} = 0.468 mM).

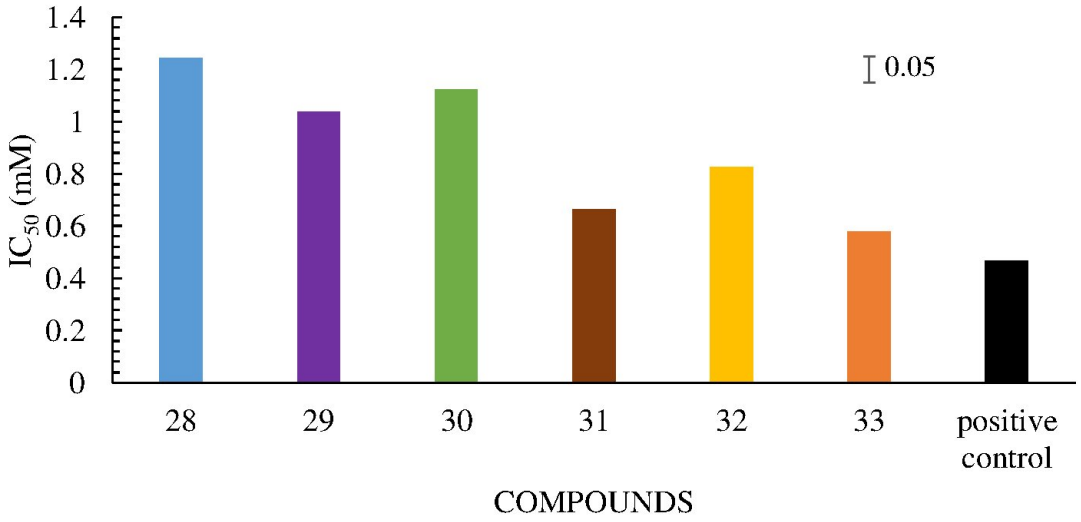

Figure 2: IC_{50} of isolated compounds **28**, **29**, **30**, **31, 32** and **33** of *Lannea schweinfurthii* stem bark on α-amylase. Positive control = Metformin; (4*R*,6*S*)-4,6-dihydroxy-6-((*Z*)-nonadec-14'-en-1-yl)cyclohex-2-en-1-one(**28**); (2*S*,4*R*,5*S*)-2,4,5-trihydroxy-2-((*Z*)-nonadec-14'-en-1-yl)cyclohexan-1-one (**29**); stigmasterol (**30**); 5-hydroxy-7,8-(2'',2''-dimethylchromene)-flavanone (**31**); 5-methoxy-7,8-(2'',2''-dimethylchromene)-flavanone (**32**); 3-*O*-[β-glucopyranosyl-(1''→2')-*O*-β-xylopyranosyl]-β-stigmasterol (**33**); LSD value = 0.05 at $P<0.05$.

The relative inhibitory potential of 3-*O*-[β-glucopyranosyl-(1''→2')-*O*-β-xylopyranosyl]-β-stigmasterol (**33**) isolated from *Lannea schweinfurthii* stem bark could be attributed to presence of hydroxyl groups which might have interacted with active site of enzyme via hydrogen bonding as had previously been postulated that hydrogen bonding between the residues of the active sites of α-amylase with the hydroxyl groups based on molecular docking studies (Bahadoran, Golzarand, Mirmiran, Saadati, & Azizi, 2013; Perera, Premadasa, & Poongunran, 2016). The same assertion could still be inferred on compounds **28**, **29**, **30**, **31** and **32** which have more structural potential to hydrophilicity. These compounds could possibly reduce post-prandial hyperglycemia by suppressing hydrolysis of carbohydrates through modulating the α-amylase functions (Kazeem, 2013b; Tundis, Loizzo, & Menichini, 2010). The results indicated high inhibitory activity of compound **33** from *Lannea schweinfurthii* stem bark on α-amylase. Compound **33** could be relevant for use in management of post-prandial hyperglycemia and as template for anti-hyperglycemic drug based on its high inhibitory activity comparable to metformin on α-amylase.

4.4.2 *In-vitro* modes of α-amylase inhibition by the active compounds

Compounds **31**, **32,** and **33** showed relatively high inhibitory activities on α-amylase and were subjected to *in-vitro* inhibitory kinetic analysis test on α-amylase to determine their modes of inhibition based on Michaelis-Menten parameters. The Lineweaver-Burk plots (1/V $[mM/min]^{-1}$ against 1/S $[mM]^{-1}$), obtained from inhibitory kinetic analysis on α-amylase for compounds **31**, **32** and **33** (Figure 3, 4 and 5) were used to establish the possible modes of inhibition. Figure 3, depicted two inhibition constants, K_i = 1.186 mM (R^2 = 0.9965) and $K_{i'}$ = 4.184 mM (R^2 = 0.9918) for compound **33**, determined from the slope and y-intercept of the Lineweaver-Burk plot which indicated that the inhibitor interacted with both the free enzyme and enzyme-substrate complex implying mixed inhibition, common among natural products (Priscilla, Roy, Suresh, & Kumar,

2014; Xu, 2010). The smaller inhibition constant K_i = 1.186 mM signified a stronger binding affinity on the active site of the free enzyme. The results showed a decrease in the apparent affinity of enzyme to substrate (K_m apparent > K_m), meaning that dissociation constant (K_m) value increased so the inhibitor was able to bind favorably to the free enzyme (Zhang, Wang, & Dong, 2014) . It was also noted that V_{max} value changed, because the inhibitor was capable of preventing catalysis regardless of whether the substrate was bound to the enzyme or not (Figure 3).

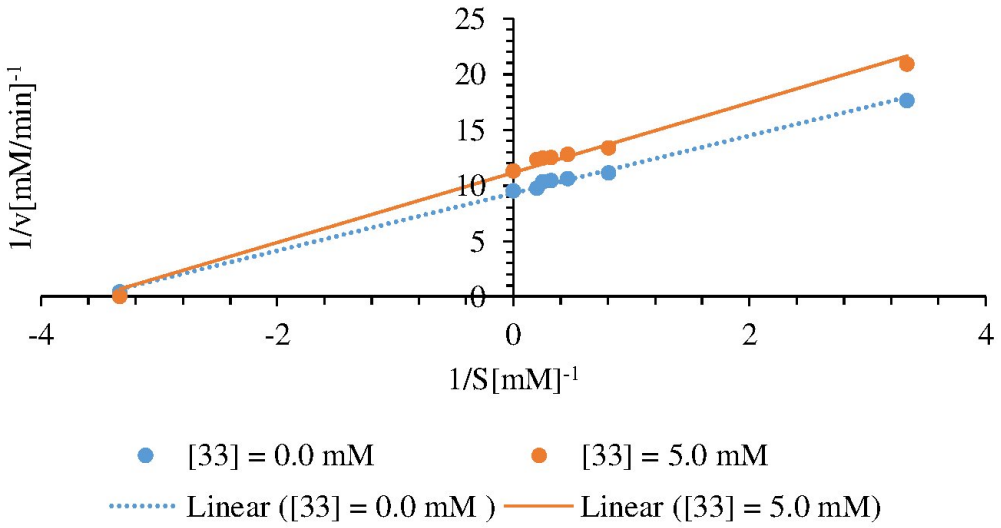

Figure 3: 1/v [mM/min]$^{-1}$ verses 1/S [mM]$^{-1}$ of negative control (no inhibitor) and compound **33** of *Lannea schweinfurthii* on α-amylase. 3-*O*-[β-glucopyranosyl-(1''→2')-*O*-β-xylopyranosyl]-β-stigmasterol (**33**). Mixed mode of inhibition observed with inhibition constants K_i = 1.186 mM and $K_{i'}$ = 4.184 mM; K_m apparent > K_m and V_{max} apparent< V_{max}.

From the Lineweaver-Burk plot in Figure 4, the apparent K_m (1.667 mM) increased in the presence of compound **31** relative to K_m (0.7143 mM) in the absence of compound **31**, which implied it raised the concentration of the substrate required for the reaction velocity. However, the apparent V_{max} (0.1543 mM/min) was unchanged in the presence of compound **31** relative to V_{max} (0.1543 mM/min) in the absence of compound **31**, which indicated that once substrate bound to the enzyme, the reaction proceeded normally, and therefore V_{max} depended only on the maximum possible enzyme-substrate complex. The inhibition constant of compound **31** was determined as

K_i = 24.29 mM (R^2 = 0.9516) which together with a constant V_{max} qualified its binding to be a competitive inhibitor of α-amylase towards hydrolysis of starch. The results implied that α-amylase had lower affinity for substrate carbohydrate in the presence of compound **31**.

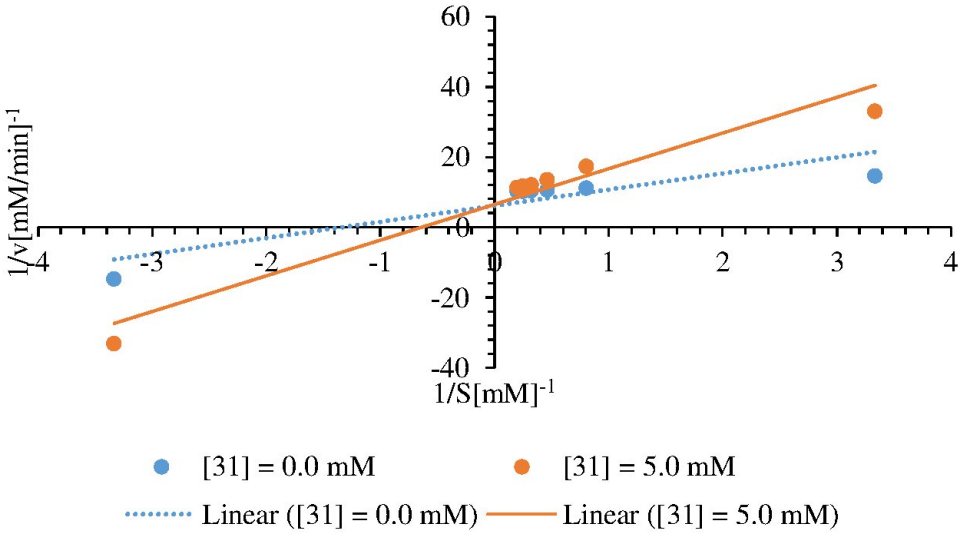

Figure 4: 1/v $[mM/min]^{-1}$ verses 1/S $[mM]^{-1}$ of negative control (no inhibitor) and compound **31** of *Lannea schweinfurthii* on α-amylase. 5-hydroxy-7,8-(2'',2''-dimethylchromene)-flavanone (**31**). Competitive mode of inhibition observed with inhibition constant K_i = 24.29 mM; K_m apparent > K_m and V_{max} apparent = V_{max}.

From Figure 5, the apparent K_m value of 3.333 mM was higher in the presence of compound **32** compared to K_m value of 0.7143 mM in the absence of compound **32**, however, the apparent V_{max} value of 0.1606 mM/min was unchanged in the presence of compound **32** relative to V_{max} value of 0.1606 mM/min in the absence of compound **32**. From the Lineweaver-Burk plot, one inhibition constant, K_i = 37.9 mM (R^2 = 0.9909) was determined from the slope of the Lineweaver-Burk plot and this revealed compound **32** bound to free enzyme only, thus confirming a competitive mode of inhibition on α-amylase towards hydrolysis of starch. The results implied that α-amylase had lower affinity for the substrate carbohydrate in the presence of compound **32** and thus the compound displayed competitive mode of inhibition on α-amylase towards hydrolysis of starch.

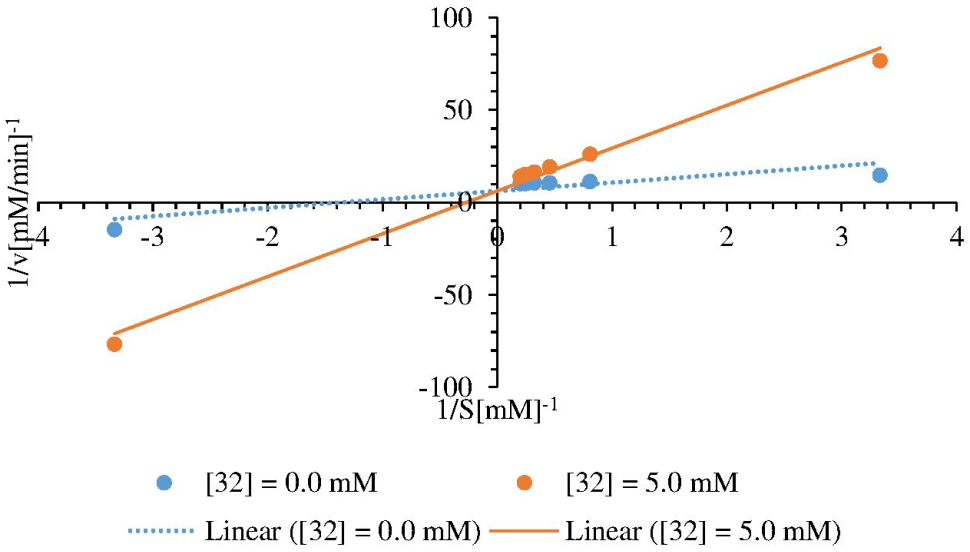

Figure 5: 1/v $[mM/min]^{-1}$ verses 1/S $[mM]^{-1}$ of negative control (no inhibitor) and compound **32** of *Lannea schweinfurthii* on α-amylase. 5-methoxy-7,8-(2'',2''-dimethylchromene)-flavanone (**32**). Competitive mode of inhibition observed with inhibition constant $K_i = 37.9$ mM; K_m apparent > K_m and V_{max} apparent = V_{max}.

The mixed mode of inhibition by compound **33**, implied that the compound bound on both free enzyme and enzyme-substrate complex, thus delayed breakdown of starch to smaller sugars. Compounds **31** and **32** competitively inhibited α-amylase activity, which indicated they contested with the substrate for the active site of the enzyme. Inhibitory action of all these three compounds therefore both diminished the substrate up take and prevented enzyme-substrate complex formation which ultimately slowed down rate of breakdown of polysaccharides to disaccharides by α-amylase (Breitmeier, Günther, & Heymann, 1997). The competitive and mixed inhibitors from *Lannea schweinfurthii* just like had been observed in other plant isolates (Fatai, Anofi, & Ashafa, 2018; Shai, et al., 2010) had therefore been noted to be capable of modifying the activity of the free enzyme and enzyme-substrate complex.

CHAPTER FIVE

SUMMARY, CONCLUSION AND RECOMENDATIONS

Phytochemicals are useful in effective control of hyperglycemia thus currently receiving more attention due to their effectiveness in the management of the blood glucose level as well as mitigating many of the side effects caused by conventional anti-hyperglycemic agents. This study focused on evaluation of phytochemicals from *Lannea schweinfurthii* stem bark on α-amylase inhibition and their modes of inhibition. The following summary, conclusion, recommendations, significance of the study, limitations of the study and suggestions for further studies were made.

5.1 Summary

The *n*-hexane/dichloromethane, ethyl acetate and methanol extracts from *Lannea schweinfurthii* stem bark showed *in-vitro* inhibitory activities against α-amylase, with IC_{50} values of 1.024 mg/mL, 0.578 mg/mL and 0.497 mg/mL, respectively relative to standard drug metformin (IC_{50} = 0.468 mg/mL). Two alkenyl cyclohexenone derivatives; (4*R*,6*S*)-4,6-dihydroxy-6-((*Z*)-nonadec-14'-en-1-yl)cyclohex-2-en-1-one (**28**) and (2*S*,4*R*,5*S*)-2,4,5-trihydroxy-2-((*Z*)-nonadec-14'-en-1-yl)cyclohexan-1-one (**29**), two flavonoids; 5-hydroxy-7,8-(2'',2''-dimethylchromene)-flavanone (**31**) and 5-methoxy-7,8-(2'',2''-dimethylchromene)-flavanone (**32**) and two sterols; stigmasterol (**30**) and 3-*O*-[β-glucopyranosyl-(1''→2')-*O*-β-xylopyranosyl]-β-stigmasterol (**33**) were isolated from *Lannea schweinfurthii* stem bark. The compounds 3-*O*-[β-glucopyranosyl-(1''→2')-*O*-β-xylopyranosyl]-β-stigmasterol (**33**) and 5-hydroxy-7,8-(2'',2''-dimethylchromene)-flavanone (**31**) showed high inhibitory activities on α-amylase (IC_{50} = 0.580 mM and 0.665 mM, respectively) while (4*R*,6*S*)-4,6-dihydroxy-6-((*Z*)-nonadec-14'-en-1-yl)cyclohex-2-en-1-one (**28**), 5-methoxy-7,8-(2'',2''-dimethylchromene)-flavanone (**32**), stigmasterol (**30**) and (2*S*,4*R*,5*S*)-2,4,5-trihydroxy-2-((*Z*)-nonadec-14'-en-1-yl)cyclohexan-1-one (**29**) showed moderate to mild

inhibitory activities relative to standard drug metformin. The compound 3-*O*-[β-glucopyranosyl-(1''→2')-*O*-β-xylopyranosyl]-β-stigmasterol (**33**) showed mixed inhibition (K_i = 1.186 mM and $K_{i'}$ = 4.1846 mM) on α-amylase while 5-hydroxy-7,8-(2'',2''-dimethylchromene)-flavanone (**31**) and 5-methoxy-7,8-(2'',2''-dimethylchromene)-flavanone (**32**) showed competitive inhibition (K_i = 24.29 mM and K_i = 37.9 mM, respectively) on α-amylase.

5.2 Conclusion

i. Methanol extract of *Lannea schweinfurthii* stem bark showed high *in-vitro* inhibitory activities (IC_{50} = 0.497 mg/mL), ethyl acetate extract showed moderate inhibitory activity while *n*-hexane/dichloromethane extract had low inhibitory activity (IC_{50} = 1.024 mg/mL) on α-amylase relative to standard drug metformin (IC_{50} = 0.468 mg/mL). Methanol extract was the most active against α-amylase due to more polar metabolites.

ii. The compounds isolated from *L*annea *schweinfurthii* stem bark were two alkenyl cyclohexenone derivatives; (4*R*,6*S*)-4,6-dihydroxy-6-((*Z*)-nonadec-14'-en-1-yl)cyclohex-2-en-1-one (**28**) and (2*S*,4*R*,5*S*)-2,4,5-trihydroxy-2-((*Z*)-nonadec-14'-en-1-yl)cyclohexan-1-one (**29**), two flavonoids; 5-hydroxy-7,8-(2'',2''-dimethylchromene)-flavanone (**31**) and 5-methoxy-7,8-(2'',2''-dimethylchromene)-flavanone (**32**) and two sterols; stigmasterol (**30**) and 3-*O*-[β-glucopyranosyl-(1''→2')-*O*-β-xylopyranosyl]-β-stigmasterol (**33**). The compounds isolated were known compounds.

iii. The compounds 3-*O*-[β-glucopyranosyl-(1''→2')-*O*-β-xylopyranosyl]-β-stigmasterol (**33**) from methanol extract and 5-hydroxy-7,8-(2'',2''-dimethylchromene)-flavanone (**31**) from ethyl acetate extract showed high inhibitory activities on α-amylase (IC_{50} = 0.580 mM and 0.665 mM, respectively) relative to standard drug metformin (IC_{50} = 0.468 mM). Compound **33** was the most active against α-amylase shown by its least IC_{50} value.

iv. The compound 3-*O*-[β-glucopyranosyl-(1''→2')-*O*-β-xylopyranosyl]-β-stigmasterol (**33**) showed mixed inhibition (K_i = 1.186 mM and $K_{i'}$ = 4.184 mM) on α-amylase while 5-hydroxy-7,8-(2'',2''-dimethylchromene)-flavanone (**31**) and 5-methoxy-7,8-(2'',2''-dimethylchromene)-flavanone (**32**) showed competitive inhibition (K_i = 24.29 mM and K_i = 37.9 mM, respectively) on α-amylase. The compounds had inhibitory activity against α-amylase, compound **33** was the most active against α-amylase due to its small calculated inhibition constants (K_i = 1.186 mM and $K_{i'}$ = 4.184 mM) relative to compounds **31** and **32** (K_i = 24.29 mM and K_i = 37.9 mM, respectively).

5.3 Recommendations

i. The observed *in-vitro* inhibitory activity against α-amylase by the crude extracts from *Lannea schweinfurthii* stem bark indicated the potential of the extracts to manage post-prandial hyperglycemia and the plant stem bark may be used as herbal formulation to manage high blood glucose level is supported subject to safety and efficacy considerations.

ii. The extracts from *Lannea schweinfurthii* stem bark contain bioactive compounds particularly, 5-hydroxy-7,8-(2'',2''-dimethylchromene)-flavanone (**31**), 5-methoxy-7,8-(2'',2''-dimethylchromene)-flavanone (**32**) and 3-*O*-[β-glucopyranosyl-(1''→2')-*O*-β-xylopyranosyl]-β-stigmasterol (**33**) which may be used in medicinal application of the plant subject to pharmacological establishment of their efficacies.

iii. The molecular information of the compounds may serve as templates for development of molecular scaffolds that are earmarked for anti-hyperglycemic alternatives, upon *in-vivo* verification of the potential of isolates.

5.4 Significance of the study

The anti-hyperglycemic activity of crude extracts and identified active compounds from *Lannea schweinfurthii* supports use of the plant in management of diabetes. The established molecular structures of active compounds against α-amylase generated compounds against post-prandial hyperglycaemia that provides a basic inference for the activities and templates for future drug development.

5.5 Limitations of the study

Though crude extracts and isolated compounds from *Lannea schweinfurthii* showed *in-vitro* inhibitory activities against α-amylase and the modes of inhibition of the isolated active compounds established, it remained unknown if they have *in-vivo* activities against α-amylase.

5.6 Suggestions for further studies

i. A sequential inhibition study of extracts and compounds from *Lannea schweinfurthii* stem bark against carbohydrate hydrolytic enzymes such as maltase, glucosidases and sucrase is necessary to determine inhibitory activities and modes of action for the phytochemicals.

ii. Structural mechanism and molecular interaction (docking) studies on 5-hydroxy-7,8-(2'',2''-dimethylchromene)-flavanone (**31**), 5-methoxy-7,8-(2'',2''-dimethylchromene)-flavanone (**32**), 3-*O*-[β-glucopyranosyl-(1''→2')-*O*-β-xylopyranosyl]-β-stigmasterol (**33**) and their analogues on enzymes protein active sites is necessary to establish their affinity for α-amylase thereby mechanism and molecular interaction between enzyme-inhibitor-substrate complex.

iii. *In-vivo* and toxicological cytotoxicity tests to be done to ascertain the efficacy and toxicity of the isolated compounds.

REFERENCES

Abdul, M., Hirak, D., Mohibur, R., Jerin, J., Aziza, S., Mahabuba, R., & Mohammed, R. (2010). Antihyperglycemic activity evaluation of *Leucas aspera* (Wild.) link leaf and stem and *Lannea coromandelica* (Houtt.) Merr. Bark extract in mice. *Advances in Natural and Applied Sciences, 4*, 385-388.

Adewusi, E. A., & Steenkamp V. (2011). *In vitro* screening for acetylcholinesterase inhibition and antioxidant activity of medicinal plants from Southern Africa. *Asian Pacific Journal of Tropical Medicine, **4***, 829-835.

Adoum, O. A. (2009). Determination of toxicity levels of some Savannah plants using brine shrimp test (BST). *Bayesian Journal of Pure and Applied sciences, 2*, 135-138.

Akhilesh, K. (2012). Inhibition of alpha-glucosidase by *Acacia nilotica* prevents hyperglycemia along with improvement of diabetic complications via aldose reductase inhibition. *Journal of Diabetes Metabolism, 6*, 1-7.

Akinsinde, K. A., & Olukoya, D. K. (1995). Vibriocidal activities of some local herbs. *Journal of Diarrhoeal Disease Research, 13*, 127-129.

Akter, R., Uddin, S. J., Grice, I. D., & Tiralongo, E. (2013). Cytotoxic activity screening of Bangladeshi medicinal plant extracts. *Journal of Natural Medicine, 68*(1), 246-252.

Alam, R., A.B., R., Moniruzzaman, K. M. F., A., H., R.U.H., M., M.R., A., & Ratan, L. (2012). Evaluation of antidiabetic phytochemicals in Syzygium cumini (L.) Skeels (Family: Myrtaceae). *Journal of Applied Pharmaceutical Science, 2*(10), 094-098.

Ali, H., Houghton, P. J., & Soumyanath, A. (2006). A-amylase inhibitory activity of some Malaysian plants used to treat diabetes with particular reference to *Phyllanthus amurus*. *Journal of Ethnopharmacology, 107* (3), 449-445.

Allabi, A. C., Busia, K., Ekanmian, V., & Bakiono, F. (2011). The use of medicinal plants in self-care in the Agonlin region of Benin. *Journal of Ethnopharmacology, 133*, 234-243.

Allenki, V., Vasantha, G., Chitturi, D., & K., V. (2014). Antidiabetic activity of Lannea coromandelica Houtt. Leaves in alloxan induced diabetic rats. *International Journal of Pharmacy and Biological Sciences, 4*, 108-114.

Altona, C., & Haasnoot, C. A. (1980). Prediction of anti and gauche vicinal proton-proton coupling constants in carbohydrates: a simple additivity rule for pyranose rings. *Journal of Magnetic Resonance, 13*, 417-429.

Asano, N. (2003). Glycosidase inhibitors: update and perspectives on practical use. *Glycobiology 1, 3*(10), 93-104.

Bahadoran, Z., Golzarand, M., Mirmiran, P., Saadati, N., & Azizi, F. (2013). The association of dietary phytochemical index and cardiometabolic risk factors in adults: Tehran lipid and glucose study. *Journal of Human Nutrition and Dieteticsv, 26*, 145-153.

Bationo, J. H., Hilou, A., Savadogo, P. W., & Nacoulma, O. G. (2012). Content of polyphenolic constituents and the antioxidant and antimicrobial activities of extracts from leaves and fruits of *Lannea microcarpa* Engl. & K. Kraus (Anacardiaceae). *Current Research Journal of Biological Sciences, 4*, 290-296.

Bischoff, H. (1994). Pharmacology of alpha-glucosidase inhibition. *European Journal of Clinical Investigation, 24*, 3-10.

Breitmeier, D., Günther, S., & Heymann, H. (1997). Acarbose and 1-deoxynojirimycin inhibit maltose and maltooligosaccharide hydrolysis of human small intestinal glucoamylasemaltase in two different substrate-induced modes. *Archives of Biochemistry and Biophysics, 346*(1), 7-14.

Burkill, H. M. (1985). The useful plants of West Tropical Africa. 2nd Edition. Volume 1, Families A–D. *Royal Botanic Gardens, Kew, Richmond, UK, 1*.

Chehade, J. M., & Mooradian, A. D. (2000). A rational approach to drug therapy of type 2 diabetes mellitus. *Drugs, 60*(1), 95-113.

Cheng, A. Y. Y., & Fantus, I. G. (2005). Oral antihyperglycemic therapy for type 2 diabetes mellitus. *Canadian Medical Association Journal, 172*(2), 213-226.

Chinsembu, K. C., & Hedimbi, M. (2010). An ethnobotanical survey of plants used to manage HIV/AIDS opportunistic infections in Katima Mulilo, Caprivi region, Namibia. *Journal of Ethnobiology and Ethnomedicine, 6*, 25-34.

Clarkson, C., Maharaj, V. J., Crouch, N. R., Grace, W. M., Pillay, P., Matsabisa, M. G., & Olajubu, F. A. (2010). Antimicrobial activity of *Lannea welwitschii* stem bark against wound pathogens. *Journal of Ethnopharmacology, 28*, 110-116.

De Jesus Correa, S., David, J. M., David, J. P., Chai, H. B., Pezzuto, J. M., & Cordelll, G. A. (2001). Alkyl phenols and derivatives from *Tapirira obtusa*. *Phytochemistry, 56*, 781-784.

Deutschländer, M., Lall, N., & van de Venter, M. (2009). Plant species used in the treatment of diabetes by South African traditional healers: An inventory. *Pharmaceutical Biology, 47*, 348-365.

Diallo, A. K., Eklu-hachegkeku, A., Agbonon, K., Aklikokou, E. E., Creppy, M., & Gbeasser, B. (2010). Acute and subchronic (28-day) oral toxicity studies of hydrochloric extract of *Lannea kerstingii* Engl. Aad K.Krause (Anacardiaceae) stem bark. *Journal of Pharmacological and Toxicological Methods, 5*(7), 343-349.

Eckel, R. H., Grundy, S. M., & Zimmet, P. Z. (2005). The metabolic syndrome. *Lancet, 365*, 1415–1428.

Eichler, H. G., Korn, A., Gasic, S., Prison, W., & Businger, J. (1984). The effect of new specific α-amylase inhibitor on post-prandial glucose and insulin excursions in normal subjects and Type 2 (non-insulin dependent) diabetic patients. *Diabetologia, 26*(4), 278-281.

Elya, B., Basah, K., Munim, A., Yuliastuti, W., Bangung, A., & Septriana, K. (2012). Screening of α-glucosidase inhibitory activity from some plants of Apocynaceae, Clusiaceae, Euphorbiaceae, and Rubiaceae. *Journal of Biomedicine and Biotechnology, 4*, 1-6.

Etuk, E. U., Ugwah, M. O., Jagbonna, O. P., & Onyeyili, P. A. (2009). Ethnobotanical survey and preliminary evaluation of medicinal plants with antidiarrhoeal properties in Sokoto state, Nigeria. *Journal of Medicinal Plants Research, 3*, 763-766.

Ezure, Y., Murao, S., Miyazaki, K., & Kawamata, M. (1985). Molanoline (1-deoxynojirimycin) fermentation and its improvement. *Agricultural and Biological Chemistry, 49*, 1111-1125.

Fadeyi, S. A., Fadeyi, O., Adejumo, A., Okoro, C., & Myles, E. L. (2013). In vitro anticancer screening of 24 locally used Nigerian medicinal plants. *BMC Complementary Medicine and Therapies, 13*, 79-84.

Fatai, O. B., Anofi, O., & Ashafa, T. (2018). Oxidative stress mitigation, kinetics of carbohydrate-enzymes inhibition and cytotoxic effects of flavonoids-rich leaf extract of *Gazania krebsiana* (Less.): An in vitro evaluation. *Asian Pacific Journal of Tropical Medicine, 8*(1), 52-58.

Fernandez-Mej, C. (2013). Oxidative stress and chronic degenerative diseases role for antioxidants. *Mexico City: InTech.*

Gardner, D., & Shoback, D. (2011). *Greenspan's Basic and Clinical Endocrinology* (9th ed.). *McGraw-Hill medical, New York.*

Gathirwa, J. W., Rukunga, G. M., Njagi, E. N. M., Omar, S. A., Mwitari, P. G., Guantai, A. N., & Ndiege, I. O. (2008). The *in vitro* anti-plasmodial and in vivo antimalarial efficacy of combinations of some medicinal plants used traditionally for treatment of malaria by the Meru community in Kenya. *Journal of Ethnopharmacology, 115*, 223-231.

Geissler, P. W., Harris, S. A., Prince, R. J., Olsen, A., Achieng', O. R., Oketch, R. H., & MΦlgaard, P. (2002). Medicinal plants used by Luo mothers and children in Bondo District, Kenya. *Journal of Ethnopharmacology, 83*, 39-44.

Groweiss, A., Cardellina, J. H., Pannell, L. K., Uyakul, D., Kashman, Y., & Boyd, M. R. (1997). Novel cytotoxic, alkylated hydroquinones from *Lannea welwitschii*. *Journal of Natural Products, 60*, 116-121.

Gulati, R., Serena, R. K., & Gupta, R. S. (2017). A rapid plate assay for screening-asparaginase producing microorganisms. *The Society for Applied Bacteriology Letters in Applied Microbiology, 24*, 23-26.

Habib, M. R., Nikkon, F., Rahman, M., Haque, M. E., & Karim, M. R. (2007). Isolation of stigmasterol and β-sitosterol from methanolic extract of root of bark of Calotropis gigantean (Linn.). *Pakistan Journal of Biological Sciences, 10*, 4174-4176.

Haule, E. E., Moshi, M.J., Nondo, R.S.O., Mwangomo, D.T., & Mahunnah, R.L.A. (2012). A study of antimicrobial activity, acute toxicity and cytoprotective effect of a polyherbal extract in a rat ethanol-HCl gastric ulcer model. *BMC Research Notes, 5*, 546-550.

Horii, S., Fukase, H., Matsuo, T., Kameda, Y., Asano, N., & Matsui, K. (1986). Synthesis and a-D-glucosidase inhibitory activity of Nsubstituted valiolamine derivatives as potential oral antidiabetic agents. *Journal of Medicinal Chemistry, 29*, 1038-1046.

Inoue, S., Tsuruoka, T., & Niida, T. (1966). The structure of nojirimycin, a piperidinose sugar antibiotic. *Journal of Antibiotics, 19*, 288-292.

Jeon, C. Y., Lokken, R.P., Hu, F.B., & van Dam, R.M. (2007). Physical activity of moderate intensity and risk of type 2 diabetes: a systematic review. *Diabetes care, 30(3)*, 744-752.

Jeruto, P., Lukhoba, C., Ouma, G., Otieno, D., & Mutai, C. (2008). An ethnobotanical study of medicinal plants used by the Nandi people in Kenya. *Journal of Ethnopharmacology, 116*, 370-376.

Johansen, J. S., Harris, A.K., Rychly, D.J., & Ergul, A. (2005). Oxidative stress and the use of antioxidants in diabetes: Linking basic science to clinical practice. *Cardiovascular Diabetology, 6*, 4-5.

Johns, T., Faubert, G.M., Kokwaro, J.O., Mahunnah, R.L.A., & Kimanani, E.K. (1995). Anti-giardial activity of gastrointestinal remedies of the Luo of East-Africa. *Journal of Ethnopharmacology, 46*, 17-23.

Joubert, P. H., Venter, H.L., & Foukaridis, G.N. (1990). The effect of miglitol and acarbose after an oral glucose load: a novel hypoglycaemic mechanism. *Brazilian Journal of Clinical Pharmacology, 30*, 391-396.

Junge, B., Matzke, M., & Stltefuss, J. (1996). *Chemistry and structureactivity relationships of glucosidase inhibitors. Handbook of experimental pharmacology* (Vol. 119). New York: Springer-Verlag.

Kakadiya, J., Shah, M., & Shah, N.J. (2010). Effect of nobivolol on serum diabetic marker and lipid profile in normal and streptozotocinnicotinamide induced diabetic rats. *Research Journal of Pharmaceutical Biology and Chemical Sciences, 1*, 329-334.

Kameda, Y., Asano, N., Yoshikawa, M., Takeuchi, M., Yamaguchi, T., Matsui, K., … Fukase, H. (1984). Valiolamine, a new aglucosidase inhibiting aminocyclitol produced by Streptomyces hygroscopicus. *Journal of Antibiotics, 37*, 1301-1307.

Kapche, G. D. W. F., Laatsch, H., Fotso, S., Kouam, S.F., Wafo, P., Ngadjui, B.T., & Abegaz, B.M. (2007). Lanneanol: A new cytotoxic dihydroalkylcyclohexenol and phenolic compounds from Lannea nigritana (Sc. Ell.) Keay. *Biochemical Systematics and Ecology, 35*, 539-543.

Kazeem, M. I., Raimi, O.G., Balogun, R.M., & Ogundajo, A.L. (2013b). Comparative study on the α-amylase and α-glucosidase inhibitory potential of different extracts of Blighia sapida (Koenig). *American, Journal of Research Community, 1(7)*, 178-192.

Kazembe, T., Munyarari, E., & Charumbira, I. (2012). Use of traditional herbal medicines to cure malaria. *Bulletin of Environment, Pharmacology & Life Sciences, 1*, 63-85.

Kihagi, R. G., Alex, K.M., & Alphonce, W.W. (2016). *Antibacterial, antifungal and phytochemical screening of the plant species Lannea schweinfurthii.* kenyatta University.

Kisangau, D. P., Hosea, K.M., Lyaruu, H.V.M., Joseph, C.C., Mbwambo, Z.H., Masimba, P.J., … Sewald, N. (2009). Screening of traditionally used Tanzanian medicinal plants for antifungal activity. *Pharmaceutical Biology, 47*, 708-716.

Kisangau, D. P., Lyaruu, H.V.M., Hosea, K.M., & Joseph, C.C. (2007). Use of traditional medicines in the management of HIV/AIDS opportunistic infections in Tanzania: a case in the Bukoba rural district. *Journal of Ethnobiology And Ethnomedicine, 3*, 29-33.

Kokwaro, J. O. (2009). *Medicinal Plants of East Africa.* Nairobi: University of Nairobi Press.

Kone, W. M., Atindehou, K.K., Terreaux, C., Hostettmann, K., Traore, D., & Dosso, M. (2004). Traditional medicine in North Cote-d'Ivoire: screening of 50 medicinal plants for antibacterial activity. *Journal of Ethnopharmacology, 93*, 43-49.

Kone, W. M., Koffi, A.G., Bomisso, E.L., & Bi, F.H.T. (2012). Ethnomedical study and iron content of some medicinal herbs used in traditional medicine in Cote d'Ivoire for the treatment of anaemia. *African Journal of Traditional Complimentary and Alternative Medicine, 9*, 81-87.

Krentz, A. J., & Bailey, C.J. (2005). Oral antidiabetic agents: current role in type 2 diabetes mellitus. *Drugs, 63(3)*, 385-411.

Krentz, A. J., Ferner, R.E., & Bailey, C.J. (1994). Comparative tolerability profiles of oral antidiabetic agents. *Drug Saf, 11*, 223-241.

Krishnaswamy, N. R. (2003). *Chemistry of natural products: A Laboratory Handbook.* Hyderabad, India: Orient Blackswan publisher.

Lamien-Meda, A., Lamien, C.E., Compaore, M.M.Y., Meda, R.N.T., Kiendrebeogo, M., Zeba, B., Millogo, J.F., & Nacoulma, O.G. (2008). Polyphenol content and antioxidant activity of fourteen wild edible fruits from Burkina Faso. *Molecules, 13*, 581-594.

Lin, Y., & Sun, Z. (2010). Current views on type 2 diabetes. *Journal of Endocrinology, 204*, 1-11.

Magassouba, F. B., Diallo, A., Kouyate, M., Mara, F., Mara, O., Bangoura, O., … Baldé, A. (2007). Ethnobotanical survey and antibacterial activity of some plants used in Guinean traditional medicine. *Journal of Ethnopharmacology, 114*, 44-53.

Maiga, A., Malterud, K.E., Mathisen, G.H., Paulsen, R.E., Thomas-Oates, J., Bergstrom, E., … Paulsen, B.S. (2007). Cell protective antioxidants from the root bark of Lannea velutina. A. Rich. *A Malian Medicinal Plants Research, 1*, 66-79.

Maregesi, S. M., Ngassapa, O.D., Pieters, L., & Vlietinck, A.J. (2007). Ethnopharmacological survey of the Bunda district, Tanzania: Plants used to treat infectious diseases. *Journal of Ethnopharmacology, 113*, 457-470.

Marles, R. J., & Farnsworth, N.R. (1995). Antidiabetic plants and their active constituents. *Phytomedicine Elseir GmbH Newyork, 2(2)*, 137-189.

Maroyi, A. (2011). An ethnobotanical survey of medicinal plants used by the people in Nhema communal area, Zimbabwe. *Journal of Ethnopharmacology, 136*, 347-354.

Marquet, M., & Jansen, P.C.M (2005). *Lannea microcarpa Engl. & K.Krause In: Jansen, P.C.M. & Cardon, D. (Editors). PROTA 3: Dyes and tannins/colorants ettanins. [CDRom].* PROTA, Wageningen, Netherlands.

Maundu, P. M., Tengnäs, B., Muema, N., & Birnie, A. (2005). Useful Trees and Shrubs for Kenya. *World Agroforestry Centre, Eastern and Central Africa Regional Programme, Nairobi.*

McCue, P. P., & Shetty, K. (2004). Inhibitory effects of rosmarinic acid extraction porcine pancreatic amylase in vitro. *Asia Pacific Journal of clinical Nutrition, 13(1)*, 101-106.

Mothana, R. A., Lindequist, U., Gruenert, R., & Bednarski, P. J. (2009). Studies of the in vitro anticancer, antimicrobial and antioxidant potentials of selected medicinal plants from the island Soqotra. *BMC Complementary and Alternative Medicine, 9*, 7-13.

Mukherjee, P. K., Maiti, K., Mukherjee, K., & Houghton, P. J. (2006). Leads from Indian medicinal plants with hypoglycemic potentials. *Journal of Ethnopharmacology, 106*(1), 1-28.

Mukherjee, P. K., Pandey, D. M., & A.S., V. (2012). Molecular dynamics simulation of Rap 1 Myb-type domain in *Saccharomyces cerevisiae. Bionformation, 8*(8), 881-885.

Murao, S., & Miyata, S. (1980). Isolation and characterization of a new trehalase inhibitor, S-GI. *Agricultural and Biological Chemistry, 44*, 219-221.

Muraoka, O., Xie, W., Tanabe, G., Amer, M., Minematsu, T., & Yoshikawa, M. (2008). On the structure of the bioactive constituent from ayurvedic medicine *Salacia reticulata*: Revision of the literature. *Tetrahedron Letters, 49*, 7315-7317.

Nasri, H., Shirzad, H., Baradaran, A., & Rafieian-kopaei, M. (2015). Antioxidant plants and diabetes mellitus. *Journal of Research in Medical Sciences, 20*, 491-502.

Nathan, D. M., Genuth, S., Lachin, J., Cleary, P., Crofford, O., Davis, M., & C., S. (2003). The effect of intensive treatment of diabetes on the development and progression of long-term complications in insulin-dependent Diabetes mellitus. *New England Journal of Medicine, 329*(14), 977-986.

Nibret, E., Ashour, M. L., Rubanza, C. D., & Wink, M. (2010). Screening of some Tanzanian medicinal plants for their trypanocidal and cytotoxic activities. *Phytotherapy Research, 24*, 945-947.

Niwa, T., Inoue, S., Tsuruoka, T., Koaze, Y., & Niida, T. (1970). Nojirimycin'' as a potent inhibitor of glucosidase. *Agricultural and Biological Chemistry, 34*, 966-968.

Nyarko, A. K., Okine, L. K. N., Wedzi, R. K., Addo, P. A., & Ofosuhene, M. (2005). Subchronic toxicity studies of the antidiabetic herbal preparation ADD-199 in the rat: absence of organ toxicity and modulation of cytochrome P450. *Journal of Ethnopharmacology, 97*, 319-325.

Nyarko, A. K., Okine, L.K.N., Wedzi, R.K., Addo, P.A., & Ofosuhene, M. (2005). Subchronic toxicity studies of the antidiabetic herbal preparation ADD-199 in the rat: absence of organ toxicity and modulation of cytochrome P450. *Journal of Ethnopharmacology, 97*, 319-325.

Okoth, D. A., Akala, H. M., Jonson, J. D., & Koorbanally, N. A. (2016). Alkyl phenols: Alkenyl cyclohexenones and other phytochemical constituents from *Lannea rivae (Chiov.) secleu*x (Anacardiaceae) and their bioactivity. *Medicinal Chemistry Research, 25*, 690-703.

Okoth, D. A., Chenia, H. Y., & Koorbandly, N. A. (2013). Antibacterial and antioxidant activities of flavonoids from *Lennea alata* (Engl) Engl. (Anacardiaceae). *Phytochemistry Letters, 6*, 476-481.

Okoth, D. A., & Koorbanally, N. A. (2015). Cardanols, long chain cyclohexenones and cyclohexanols from *Lannea schimperi* (Anacardiaceae). *Natural Product Communication 10*, 103-106.

Olatokunboh, A. O., Mofomosara, S. H., & Ekene, O. A. (2010). Evaluation of the antidiarrhoeal effect of *Lannea welwitschii* Hiern (Anacardiaceae) bark extract. *African Journal of Pharmacy and Pharmacology, 4*, 165-169.

Olukoya, D. K., Idika, N., & Odugbemi, T. (1993). Antibacterial activity of some medicinal plants from Nigeria. *Journal of Ethnopharmacology, 39*, 69-72.

Orsini, F., Pelizzoni, F., & Verotta, L. (1991). Saponins from Albizzia lucida. *Phytochemistry, 30*, 4111-4115.

Osadebe, P. O., Omeje, E. O., Uzor, P. F., David, E. K., & Obiorah, D. C. (2013). Seasonal variation for the antidiabetic activity of *Loranthus micranthus* methanol extract. *Asian Pacific Journal of tropical Medicine, 3*(3), 196-199.

Ouattara, L., Koudou, J., Karou, D. S., Giaco, L., Capelli, G., Simpore, J., & Traore, A. S. (2011a). *In vitro* anti *Mycobacterium tuberculosis* H37Rv activity of *Lannea acida* from Burkina Faso. *Pakistanian Journal of Biological Sciences, 14*, 47-52.

Ouattara, L., Koudou, J., Karou, D.S., Giaco, L., Capelli, G., Simpore, J., … Traore, A. S. (2011a). In vitro anti Mycobacterium tuberculosis H37Rv activity of Lannea acida A. Rich from Burkina Faso. *Pakistan Journal of Biological Science, 14*, 47-52.

Pari, L., Latha, M., & Rao, C. A. (2004). Effect of Scorparia dulcis extract on insulin receptors in streptozocin induced rats. Studies on insulin binding to erythrocytes. *Journal of Basic Clinical Basic Clinical Physiology and Pharmacology, 15*, 223-240. .

Perera, H. K. I., Premadasa, W. K., & Poongunran, J. (2016). α-Glucosidase and glycation inhibitory effects of *Costus speciosus* leaves. *BMC Complementary and Alternative Medicine, 16*(2), 1-9.

Picerno, P., Mencherini, T., Della Loggia, R., Meloni, M., Sanogo, R., & Aquino, R. P. (2006). An extract of *Lannea microcarpa*: Composition, activity and evaluation of cutaneous irritation in cell cultures and reconstituted human epidermis. *Journal of Pharmacy and Pharmacology, 58*, 981-988.

Poongunran, J., Perera, H. K. I., Fernando, W. I. T., Jayasinghe, L., & Sivakanesan, R. (2015). α-Glucosidase and α-amylase inhibitory activities of nine Sri Lankan anti diabetic plants. *British Journal of Pharmaceutical Research, 7*(5), 365-374.

Priscilla, D. H., Roy, D., Suresh, A., & Kumar, V. (2014). Thirumurugan, K. Naringenin inhibits α-glucosidase activity: A promising strategy for the regulation of postprandial hyperglycemia in high fat diet fed streptozotocin induced diabetic rats. *Chemico-Biological Interactions, 210*, 77-85.

Puls, W., Keup, U., Krause, H. P., Thomas, G., & Hoffmeister, F. (1977). Glucosidase inhibition. A new approach to the treatment of diabetes, obesity and hyperlipoproteinaemia. *Naturwissenshaften, 64*, 536-537.

Quieroz, E. F., Kuhl, C., Terreaux, C., Mavi, S., & Hostettmann, K. (2003). New dihydroalkylhexenones from *Lannea edulis*. *Journal of Natural Products, 66*, 578-580.

Rabasa-Lhoret, R., & Chiasson, J. L. (1998). Potential of alpha-glucosidae inhibitors in elderly patients with diabetes mellitus and impaired glucose tolerance. *Drug Aging, 13*, 131-143.

Rahmatullah, M., Azam, M. N. K., Khatun, Z., Seraj, S., Islam, F., Rahman, M. A., & Aziz, M. S. (2012). Medicinal plants used for treatment of diabetes by the Marakh sect of the Garo tribe living in Mymensingh district, Bangladesh. *African Journal of Traditional, Complementary and Alternative Medicines, 9*, 3800-3385.

Rai, N. P., Adhikari, B. B., Paudel, A., Masuda, K., Mckelvey, R. D., & Manandhar, M. D. (2006). Phytochemical constituents of the flowers of *Sarcococca coriacea* of Nepalese origin. *Journal of the Chemical Society, 21*, 1-7.

Reddy, A. K., Joy, J. M., & Kumar, C. K. A. (2011). *Lannea coromandelica*: The researcher's tree. *Journal of Pharmacy Research, 4*, 577-579.

Rocio, B. R., Maria, E. P. D., Peter, G. W., & Luis, M. P. R. (2005). Additional Flavonoids from *Lonchocarpus yucatanensis* and *L. Xuul*. *Journal of Brazilian Chemical Society, 5*, 1078-1081.

Roumy, V., Fabre, N., Portet, B., Bourdy, G., Acebey, L., Vigor, C., & …Moulis, C. (2009). Four anti-protozoal and anti-bacterial compounds from *Tapirira guianensis*. *Phytochemistry, 70*, 305-311.

Runyoro, D. K. B., Matee, M. I. N., Ngassapa, O. D., Joseph, C. C., & Mbwambo, Z. H. (2006). Screening of Tanzanian medicinal plants for anti-Candida activity. *BMC Complementary and Alternative Medicine, 6*, 11-13.

Saravanam, S., Dhasarathan, P., Indira, V., & Venkataraman, R. (2010). Screening of antiinflammatory potential of chosen medicinal plants using Swiss albino mice. *Australian Journal of Basic and Applied Sciences, 4*, 6065-6068.

Sathish, R. (2010). Evaluation of wound healing and antimicrobial activity of Lannea coromandelica (Houtt) Merr. *Journal of Pharmaceuitical Research, 3*, 1225-1228.

Scheen, A. J., & Paquot, N. (2013). Metformin revisited: a critical review of the benefits-risk balance in at-risk patients with Type-2 diabetes. *Diabetes Metabolism, 39*, 179.

Schenk, S., Saberi, M., & Olefsky, J. M. (2008). Insulin sensitivity: modulation by nutrients and inflammation. *Journal Clinical Investigation, 118*(9), 2992-3000.

Schmidt, D. D., Frommer, W., Muller, L., Junge, B., Wingender, W., & Truscheit, E. (1977). α-Glucosidase inhibitors, new complex oligosaccharides of microbial origin. *Naturwissenshaften, 64*, 535-536.

Schmidt, D. D., Frommer, W., Muller, L., & Truscheit, E. (1979). Glucosidase inhibitors from bacilli. *Naturwissenshaften, 66*, 584-585.

Segawa, P., & Kasenene, J. M. (2007). Medicinal plant diversity and uses in the Sango bay area, Southern Uganda. *Journal of Ethnopharmacology, 113*, 521-540.

Segel, I. H. (1993). *Enzyme Kinetics: Behavior and Analysis of Rapid Equilibrium and Steady-State Enzyme Systems. John Wiley & Sons: New York, NY, USA.*

Shai, L. J., Masoko, P., Mokgotho, M. P., Magano, S. R., Mogale, A., Boaduo, N., & Eloff, J. N. (2010). Yeast alpha-glucosidase inhibitory and antioxidant activities of six medicinal plants collected in Phalaborwa, South Africa. *South African Journal Botany, 76*, 465-470.

Sim, L. (2010). Structural and inhibition studies of human intestinal glucosidases. *PhD thesis submitted at Graduate Department of Medical Biophysics, University of Toronto.*

Sim, L. (2010a). *Structural and inhibition studies of human intestinal glucosidases.* University of Toronto.

Singh, S., Bhat, J., & Wang, P. H. (2013). Cardiovascular effects of antidiabetic medications of Type 2 diabetes mellitus. *Current Cardiology Reports, 15*.

Sohni, Y. R., Davis, C. L., Deschamps, A. B., & Kale, P. G. (1995). Frameshift mutations in Salmonella induced by the extracts of medicinal herbs *Lannea edulis* (Sond) Engl and *Monotes glaber* Sprague. *Environmental and Molecular Mutagenesis, 25*, 77-82.

Sowemimo, A., van de Venter, M., Baatjies, L., & Koekemoer, T. (2009). Cytotoxic activity of selected Nigerian plants. *African Journal of Traditional Complemetary and Alternative medicine, 6*, 526-528.

Spiller, H. A., & Sawyer, T. S. (2006). Toxicology of oral antidiabetic medications. *American Journal of Health-System Pharmacy, 63* (10), 929-938.

Stuttz, A. E. (1999). *Iminosugars as glycosidase inhibitors: Nojirimycin and beyond. Weinheim; New York: Wiley-VCH.*

Tapondjou, A. L., Miyamoto, T., Mirjolet, J. F., Guilbaud, N., & Lacaille-Dubois, M. A. (2005). Pursaethosides A-E, triterpene saponins from *Entada pursaetha. Journal Natural Product, 68*, 1185-1190.

Tapsoba, H., & Deschamps, J. P. (2006). Use of medicinal plants for the treatment of oral diseases in Burkina Faso. *Journal of Ethnopharmacology, 104*, 68-78.

Tarling, C. A., Woods, K., Zhang, R., Brastianos, H. C., Brayer, G. D., Andersen, R. J., & Withers, S. G. (2008). The Search for Novel Human Pancreatic α-Amylase Inhibitors: High-Throughput Screening of Terrestrial and Marine Natural Product Extracts. *Chemistry and BioChemistry, 9*, 433-438.

Toukam, P. D., Maurice, F. T., Lauve, R. T. Y., Gakul, B., Nabin, C. B., Alembert, T. T., & Joseph, T. M. (2018). Novel saponin and benzofuran isoflavonoid with *in vitro* anti-inflammatory and free radical scavenging activities from the stem bark of *Pterocarpus erinaceus* (Poir). *Phytochemistry Letters, 28*, 69-75.

Trojan-Rodrigues, M., Alves, T., Soares, G., & M., R. (2012). Plants used as antidiabetics in popular medicine in Rio Grande do Sul, southern Brazil. *Journal of Ethnopharmacology, 139*, 155-163.

Tshikalange, E. T. (2007). In vitro antidiabetic and anti-HIV-1 properties of ethnobotanically selected South African plants used in the treatment of sexually transmitted diseases and diabetes mellitus. *PhD Thesis, University of Pretoria, Pretoria*, 1-12.

Tundis, R., Loizzo, M. R., & Menichini, F. (2010). Natural products of alpha-amylase and alpha-glucosidase inhibitors and their hypoglycaemic potential in the treatment of diabetes: up date. *Medicinal Chemistry, 10*(4), 315-331.

Van Wyk, B. E., Van Oudtshoom, B., & Gericke, N. (2005). *Medicinal plants of South Africa. Briza publications, Pretoria*, 301-304.

Van Wyk, B. E., van Oudtshoorn, B., & Gericke, N. (1997). *Lannea edulis. In medicinal plants of South Africa Briza Publications, Pretoria, South Africa,* 164-165.

W.H.O. (2003). Global report on diabetes. *World Health Organization, Geneva.*

W.H.O. (2016). Global report on diabetes. *World Health Organization, Geneva.*

Whiting, D. R., Guariguata, L., Weil, C., & Shaw, J. (2011). IDF Diabetes Atlas: Globalestimates of the prevalence of diabetes for 2011 and 2030. *Diabetes Research and Clinical Practice, 94*, 311-321.

Wild, S., Roglic, G., Green, A., Sicree, R., & King, H. (2004). Global prevalence of diabetes: Estimates for the year 2000 and projections for 2030. *Diabetes care, 27*(5), 1047-1053.

Xu, H. (2010). Inhibition kinetics of flavonoids on yeast α-glucosidase merged whit docking simulations. *Protein & Peptide Letters, 17*, 1270-1279.

Yagi, M., Kouno, T., Aoyagi, Y., & Murai, H. (1976). The structure of molanoline, a piperidine alkaloid from *Morus* species. *Nippon Nogei Kagaku Kaishi, 50*, 571-572.

Yaouba, S., Andreas, K., Erick, M. G., Solomon, D., Beatrice, I., Matthias, H., & Abiy, Y. (2017). Alkenyl cyclohexanone derivatives from Lannea rivae and Lannea schweinfurthii. *Phytochemistry Letters*, 1-8.

Yeo, C. R., Lee, S. M., & Popovich, D. G. (2011). Ginseng (Panax quinquefolius) reducess cell growth, lipid acquisition and increase adiponectin expression in 3T3-L1. *Evidence-Based Complementary and Alternative Medicine.*

Yoshikawa, M., Murakami, T., Shimada, H., Matsuda, H., Yamahara, J., Tanabe, G., & Muraoka, O. (1997). Alacinol, potent antidiabetic principle with unique thiosugar sulfonium sulfate structure from the Ayurvedic traditional medicine Salacia reticulata. *Tetrahedron Letters, 38*, 8367-8370.

Yoshikawa, M., Murakami, T., Yashiro, K., & Matsuda, H. (1998). Kotalanol, a potent alphaglucosidase inhibitor with thiosugar sulfonium sulfate structure, from antidiabetic ayurvedic medicine *Salacia reticulata*. *Chemical and Pharmaceutical Bulletin, 46*, 1339-1340.

Zhang, H., Wang, G., & Dong, J. (2014). Inhibitory properties of aqueous ethanol extracts of propolis on alpha-glucosidase. *Evidence-Based Complementary and Alternative Medicine, 2015*, 1-8.

APPENDICES

1.0: Spectra for compound **28**; (4*R*,6*S*)-4,6-dihydroxy-6-((*Z*)-nonadec-14'-en-1-yl)cyclohex-2-en-1-one

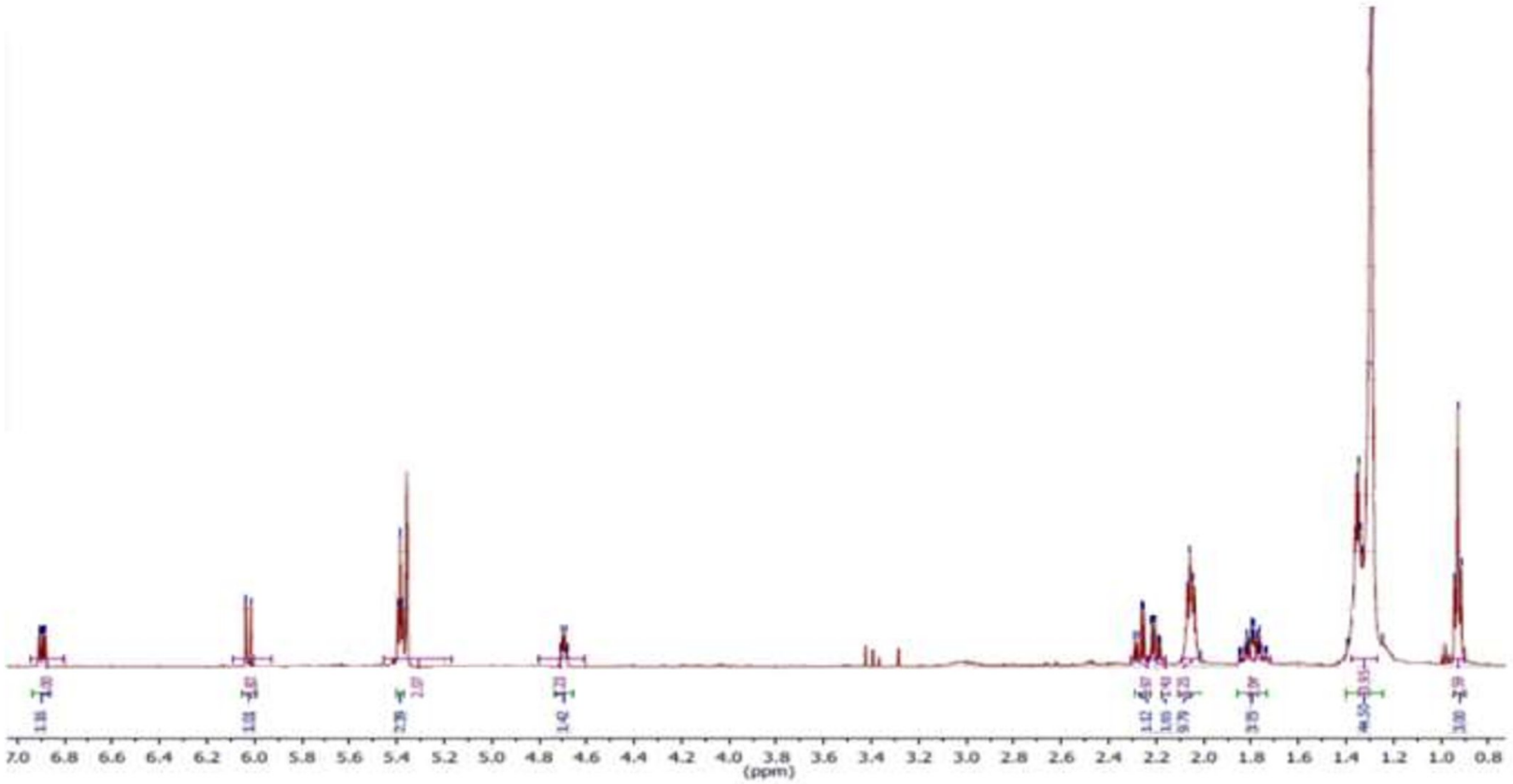

1.1: ^{1}H NMR spectrum of compound 28

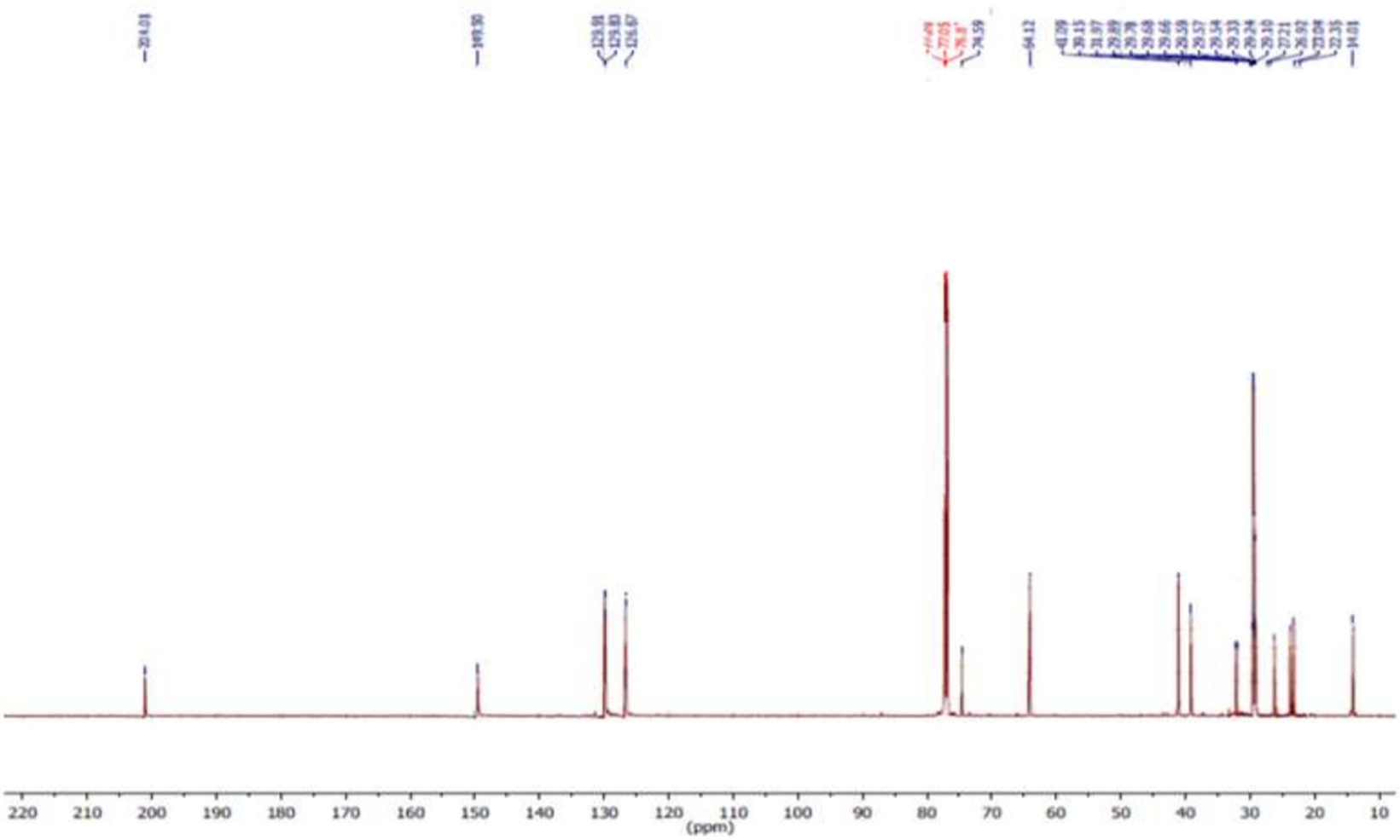

1.2: ^{13}C NMR Spectrum of Compound 28

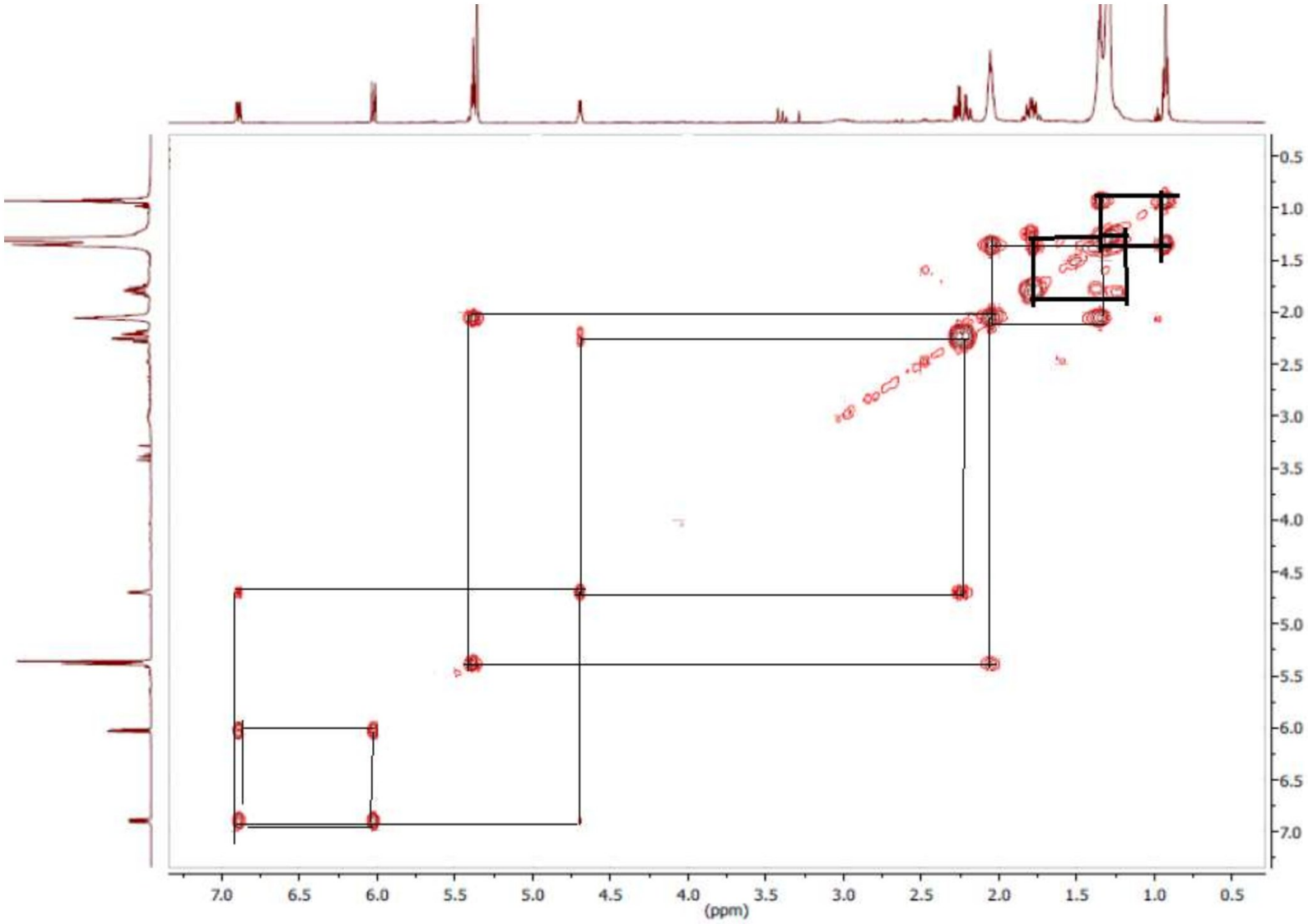

1.3: COSY spectrum of compound 28

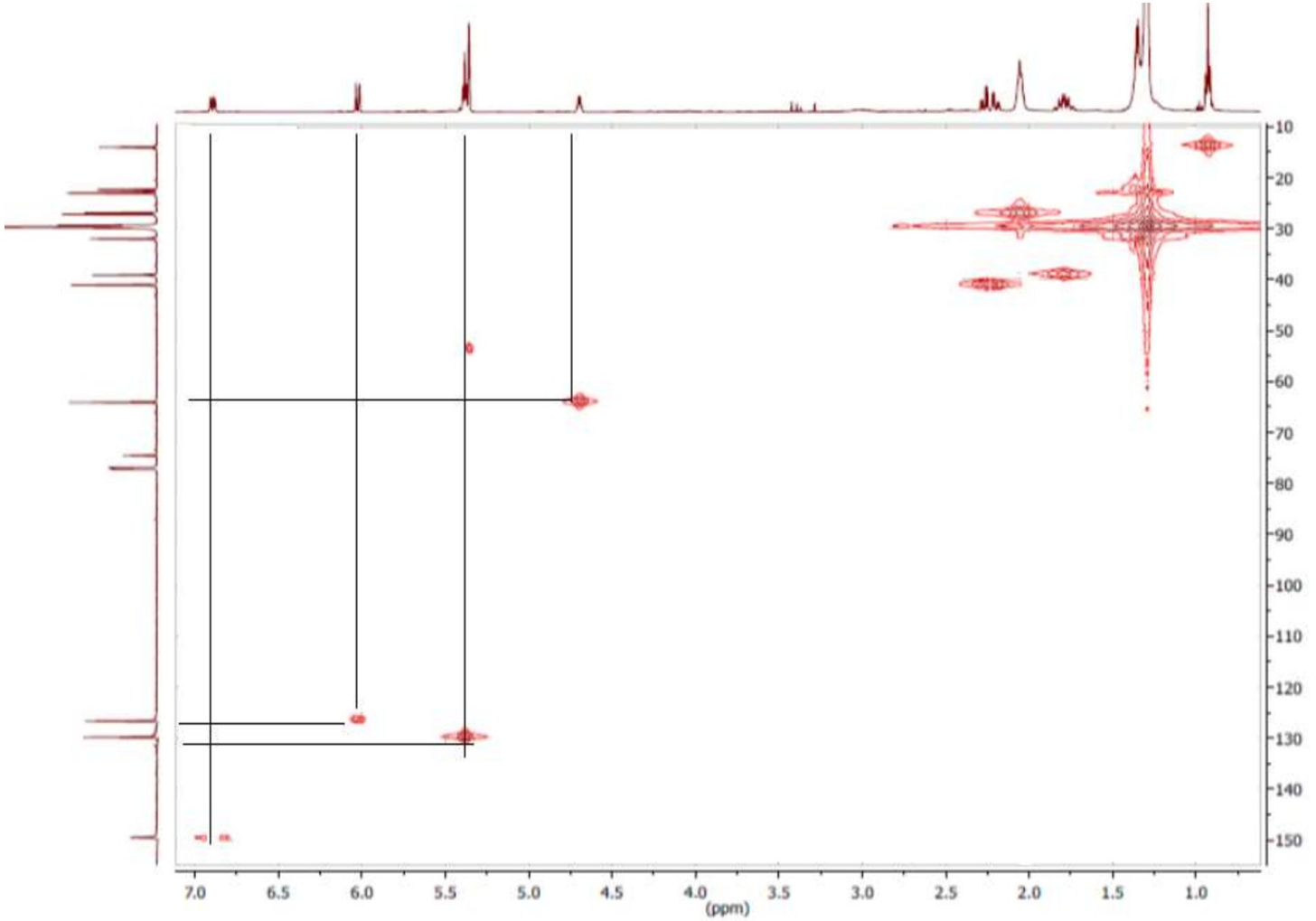

1.4: HSQC spectrum of compound 28

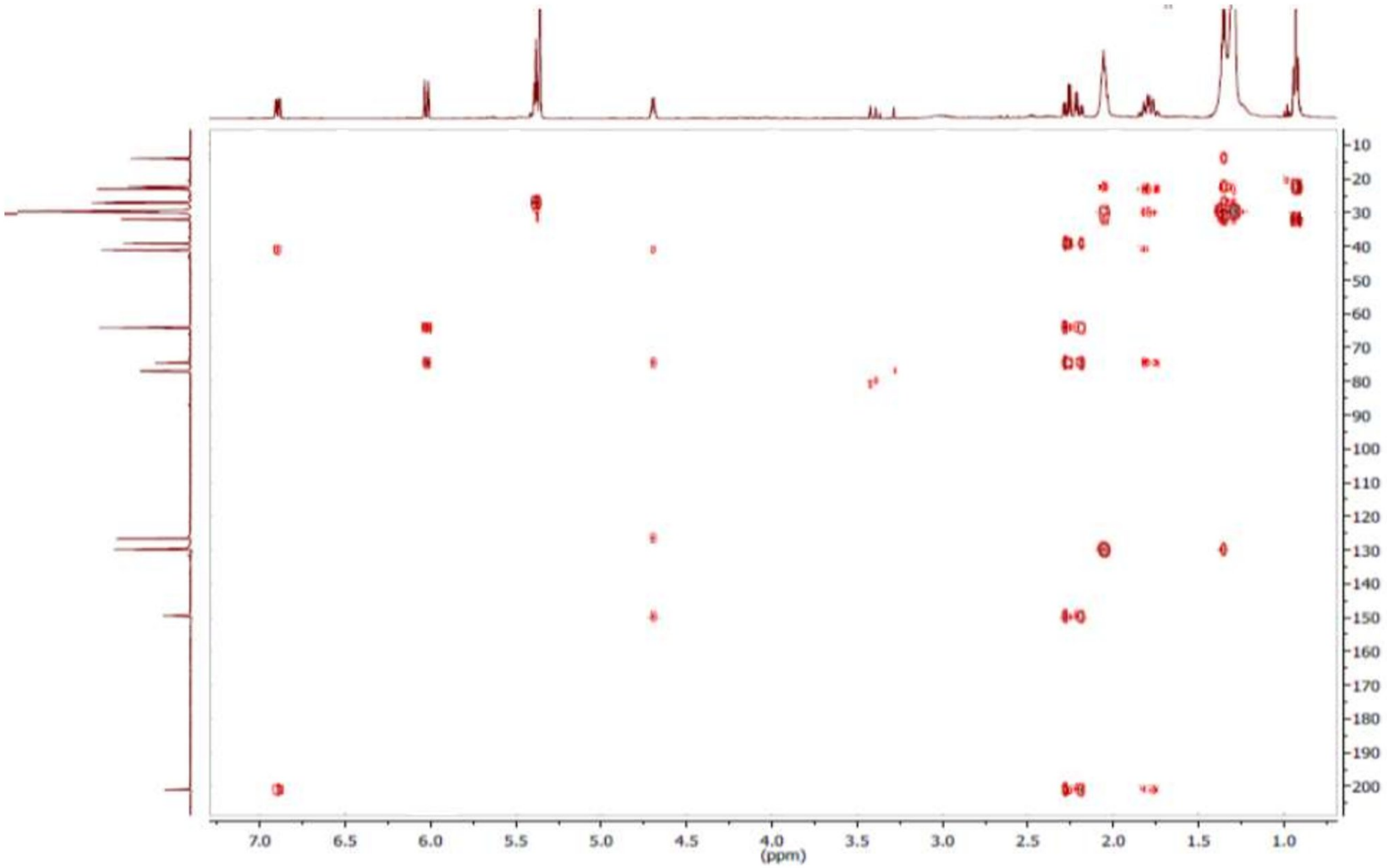

1.5: HMBC spectrum of compound 28

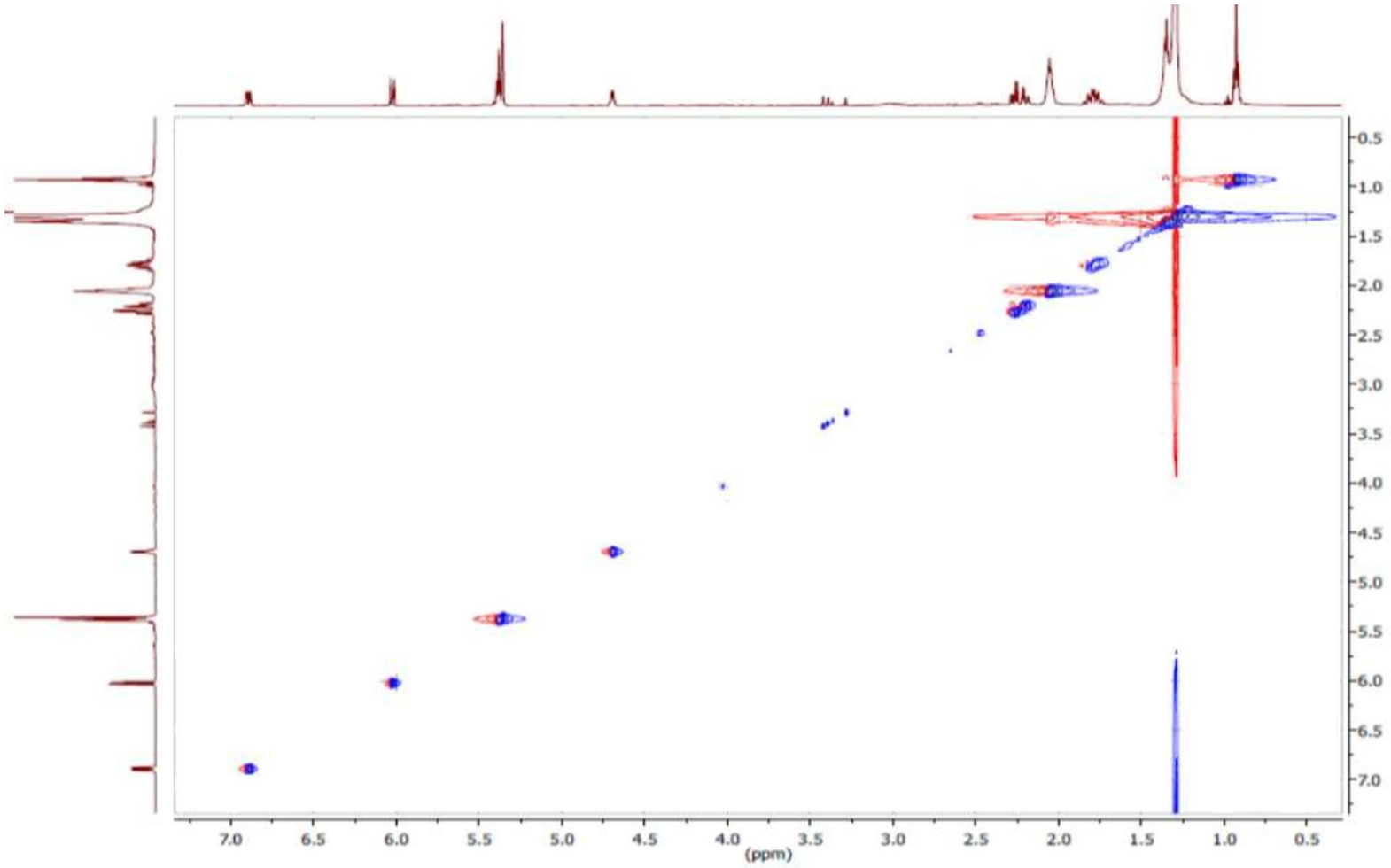

1.6: NOESY spectrum of compound 28

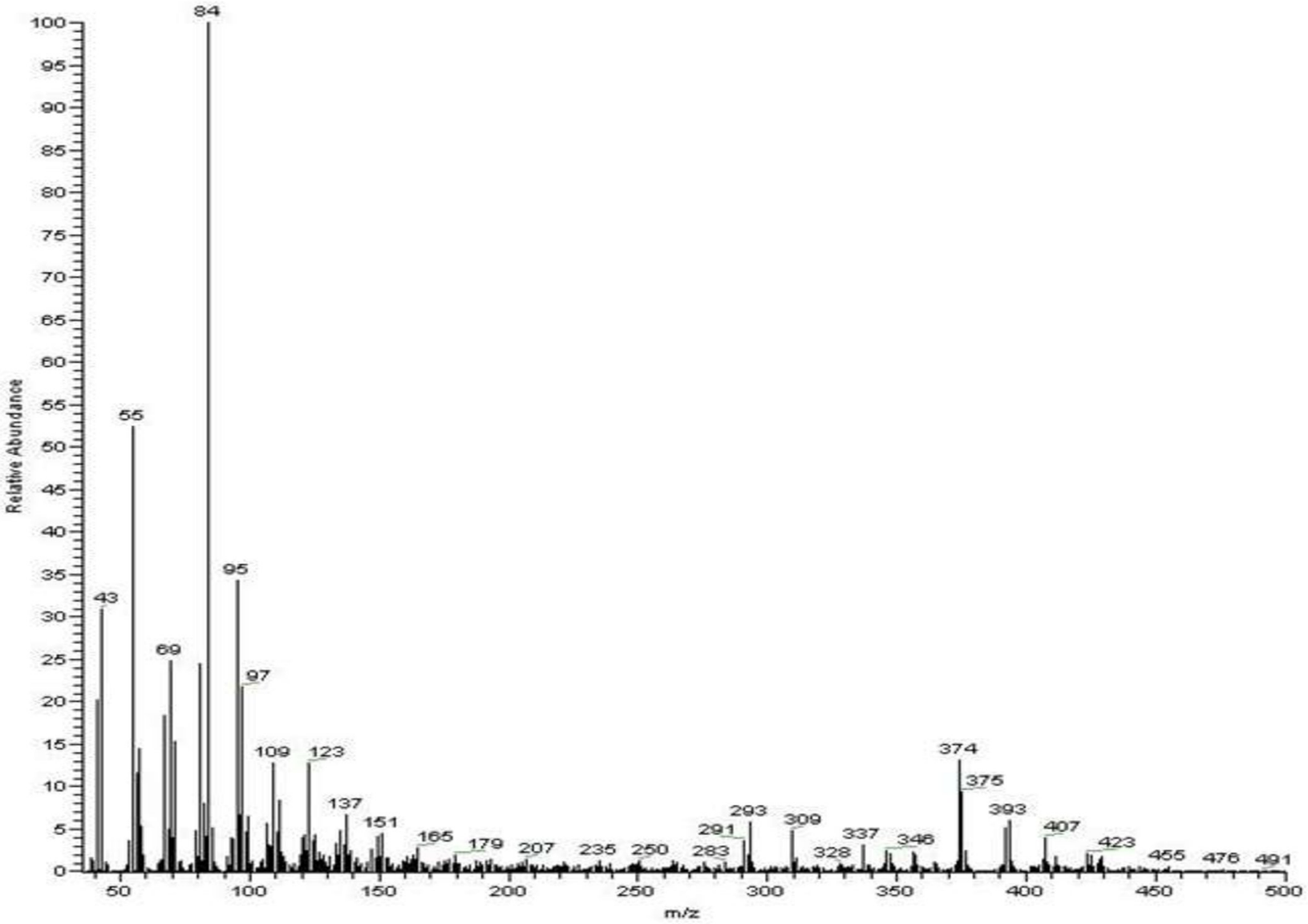

1.7: EIMS spectrum of compound 28

2.0: Spectra for compound **29**; (2*S*,4*R*,5*S*)-2,4,5-trihydroxy-2-((*Z*)-nonadec-14'-en-1-yl)cyclohexan-1-one

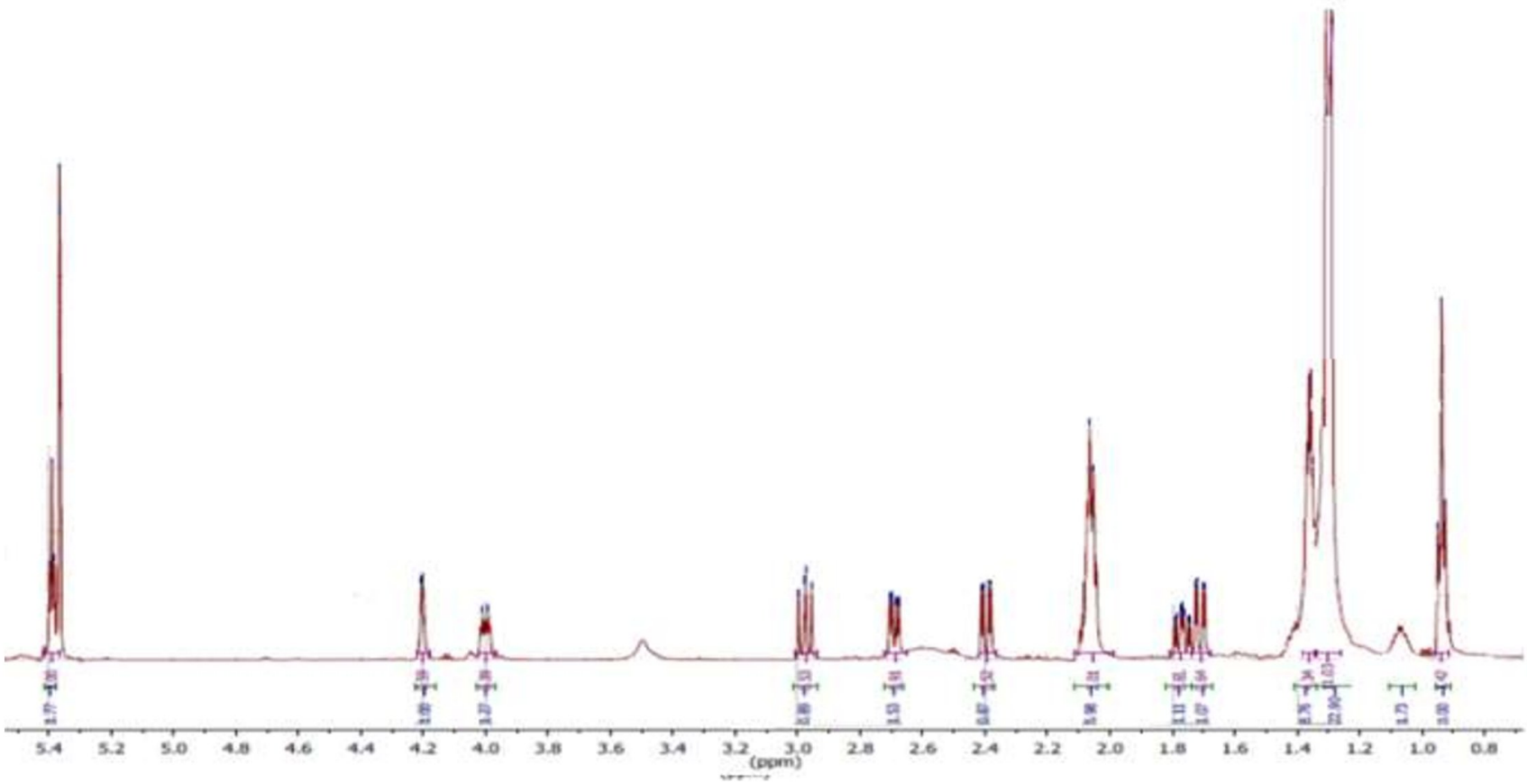

2.1: ^{1}H NMR spectrum of compound 29

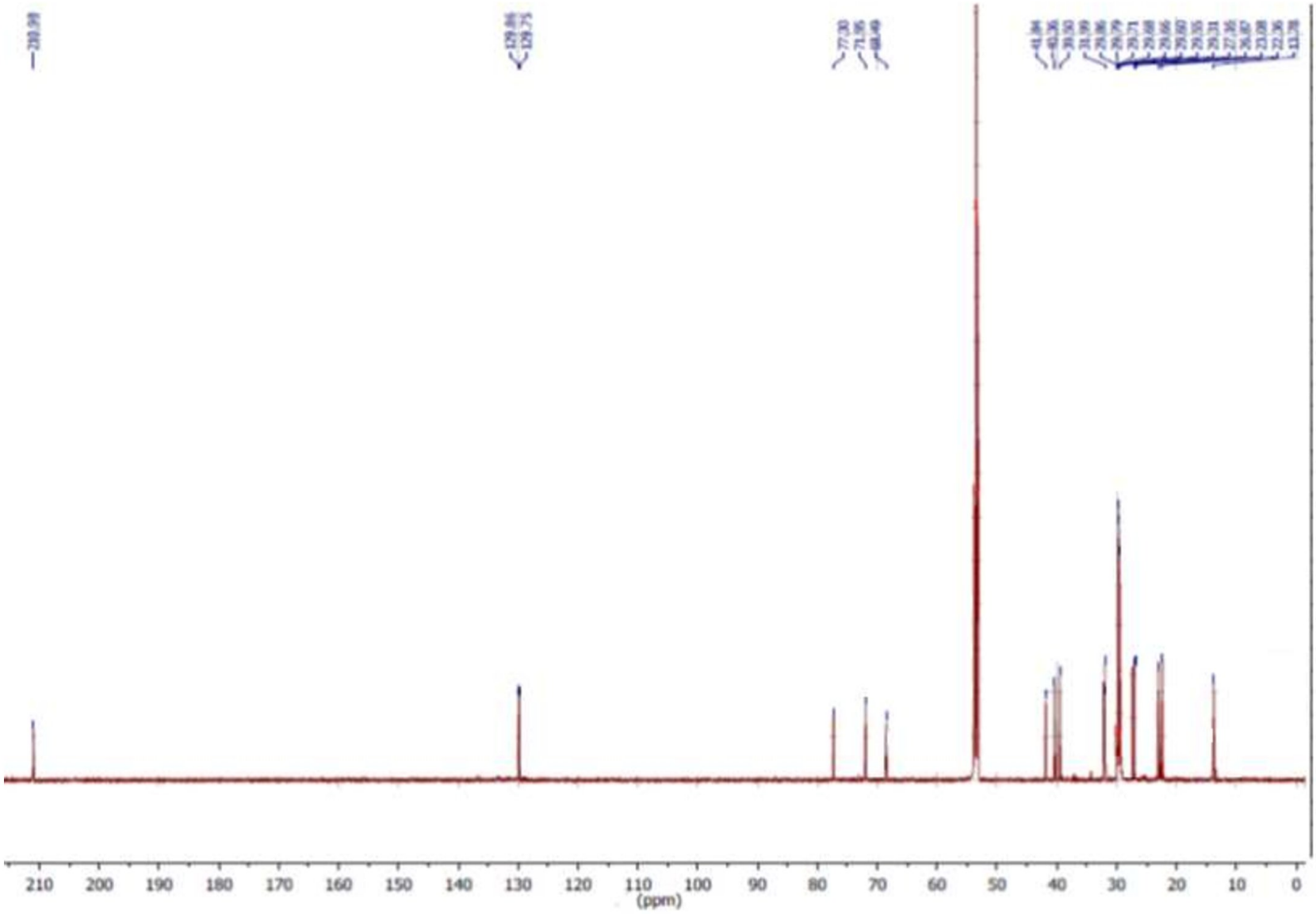

2.2: ^{13}C NMR spectrum of compound 29

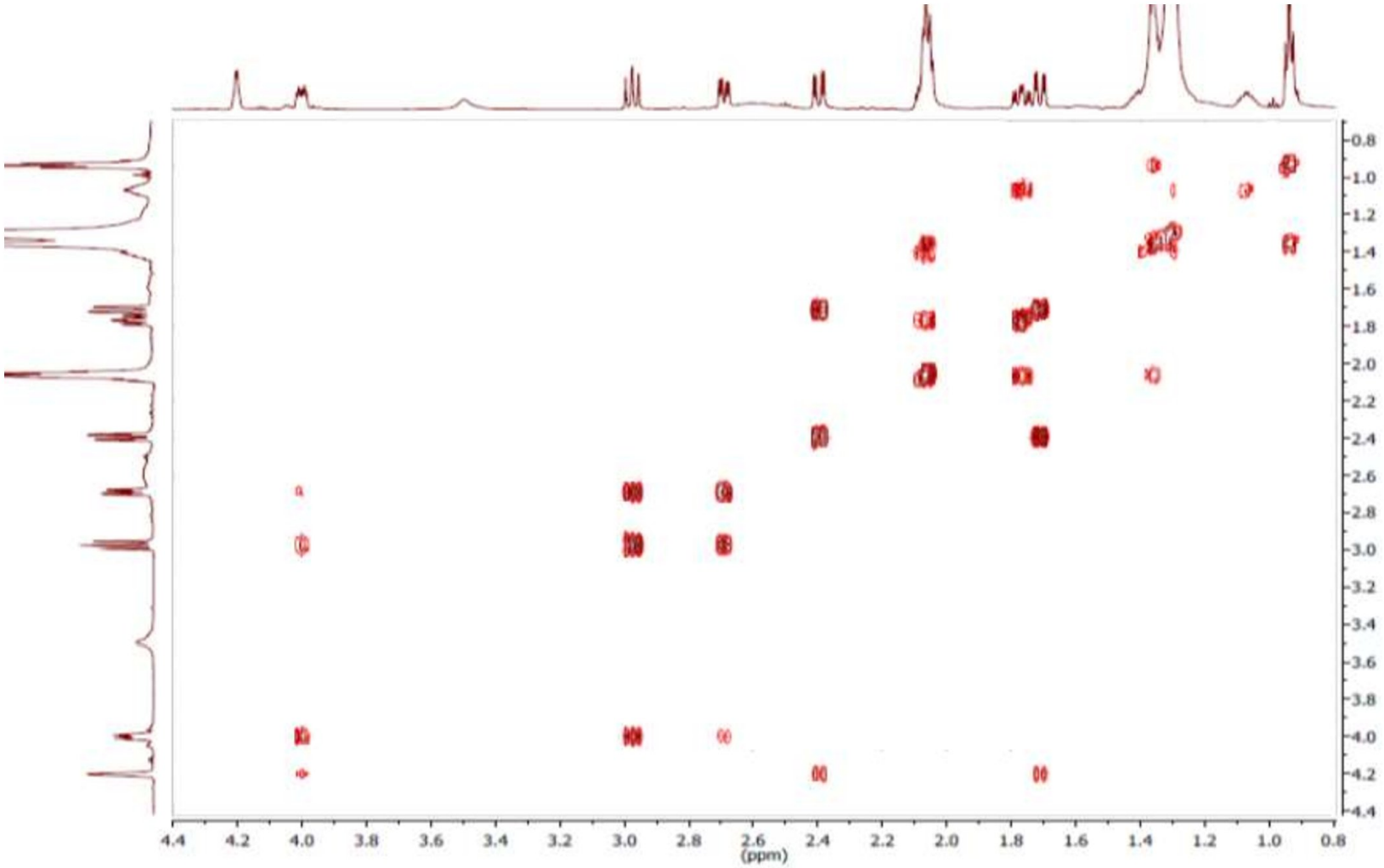

2.3: COSY spectrum of compound 29

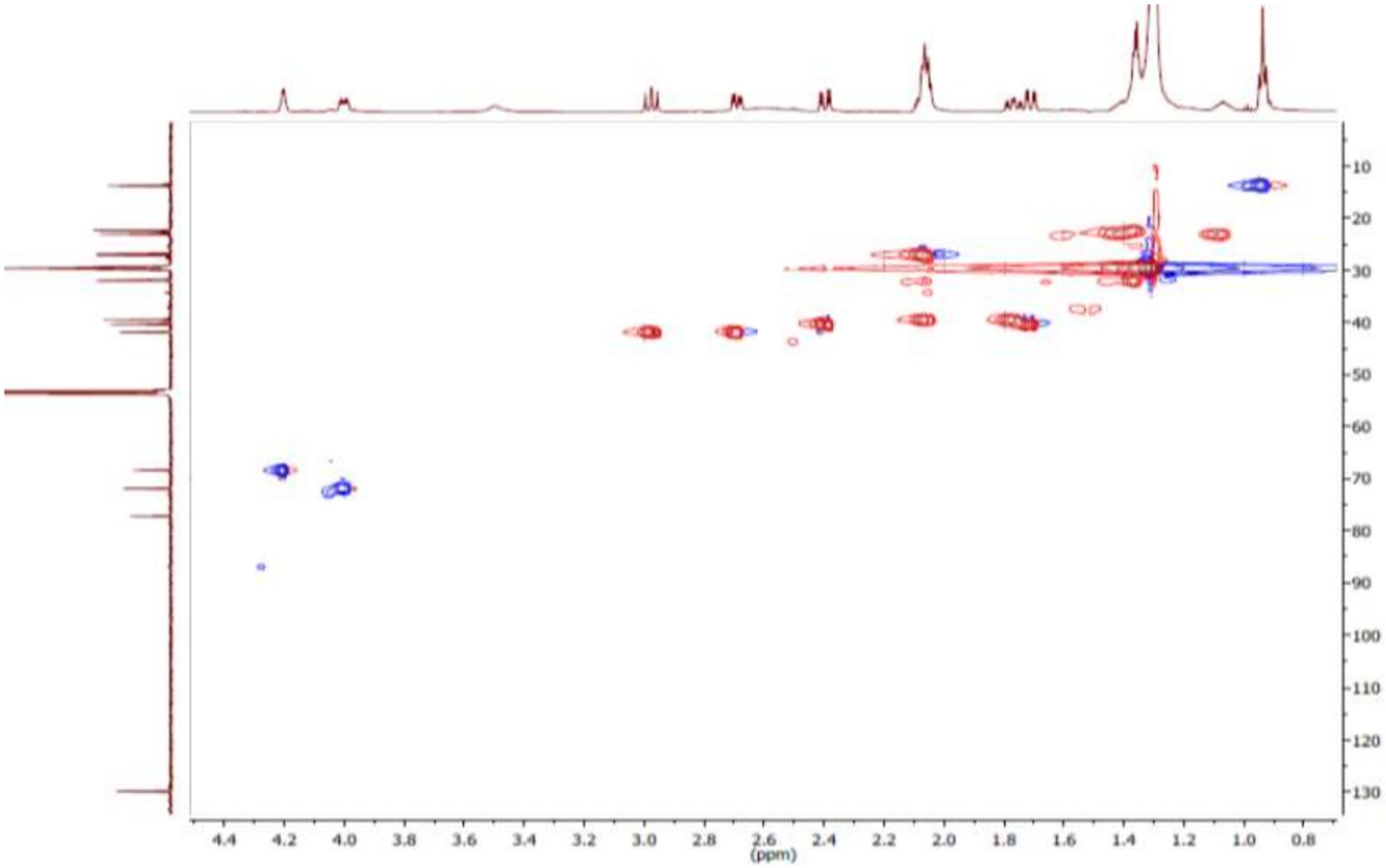

2.4: HSQC spectrum of compound 29

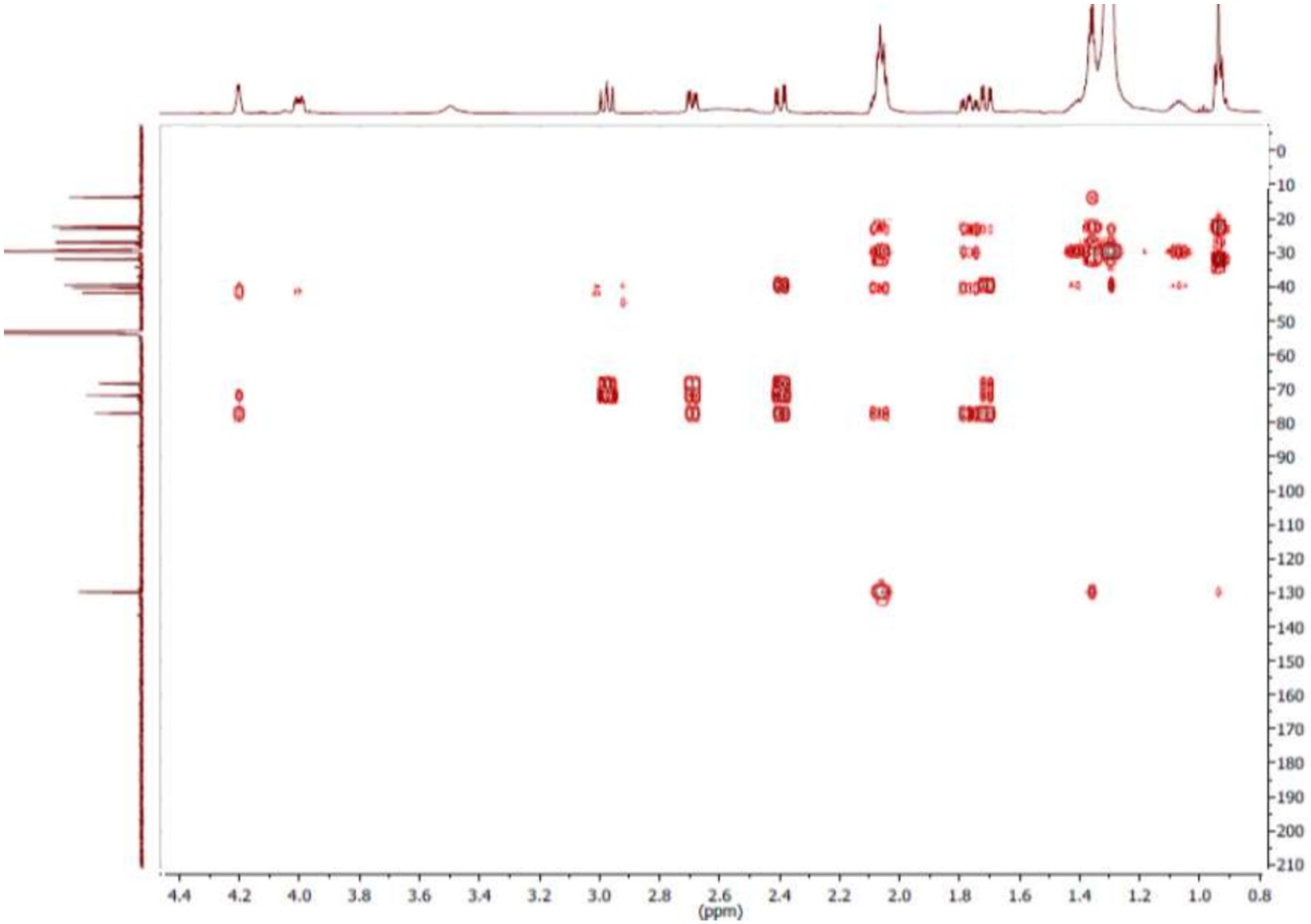

2.5: HMBC spectrum of compound 29

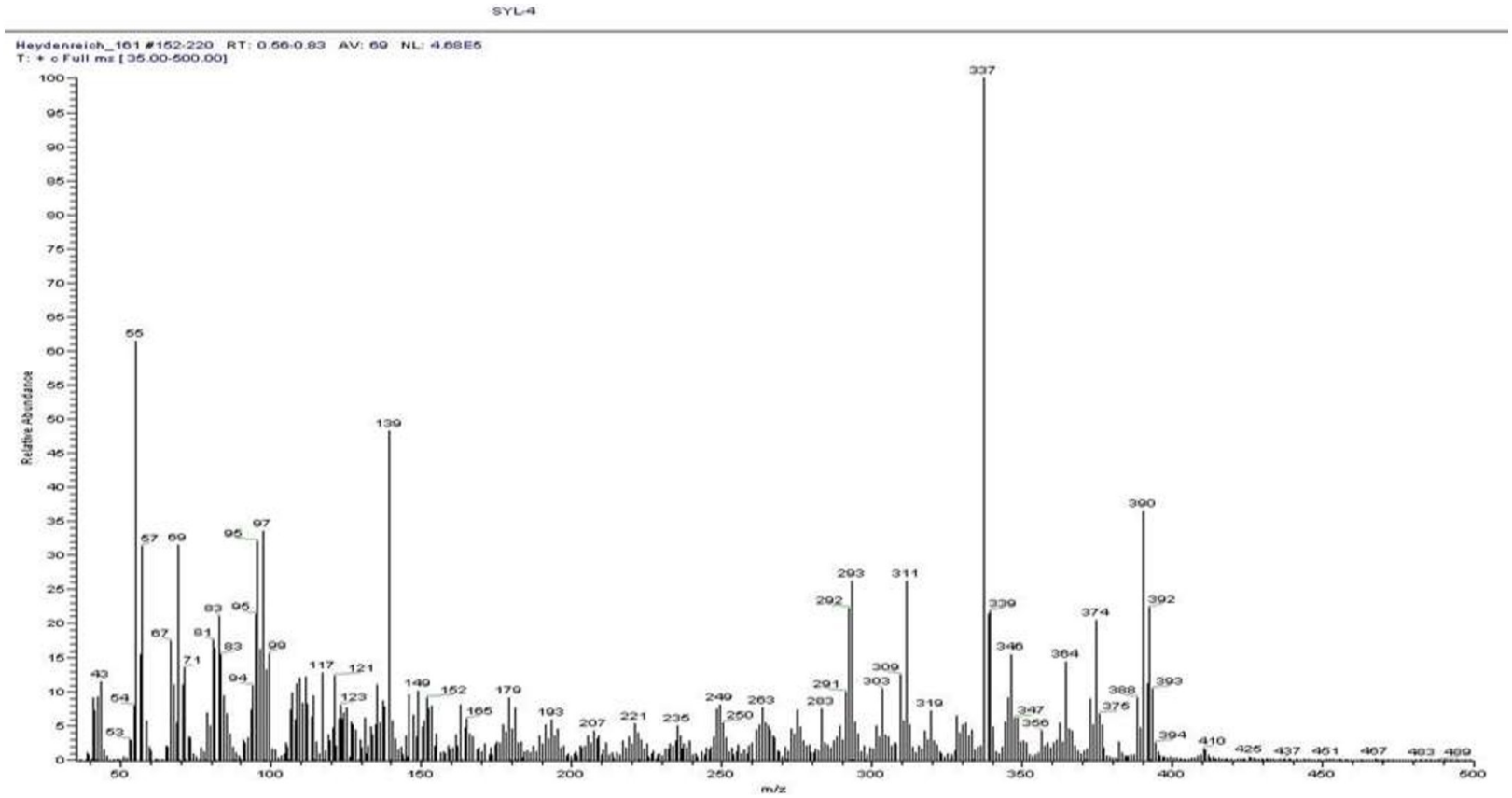

2.6: EIMS spectrum of compound 29

3.0: Spectra for compound **30**; stigmasterol

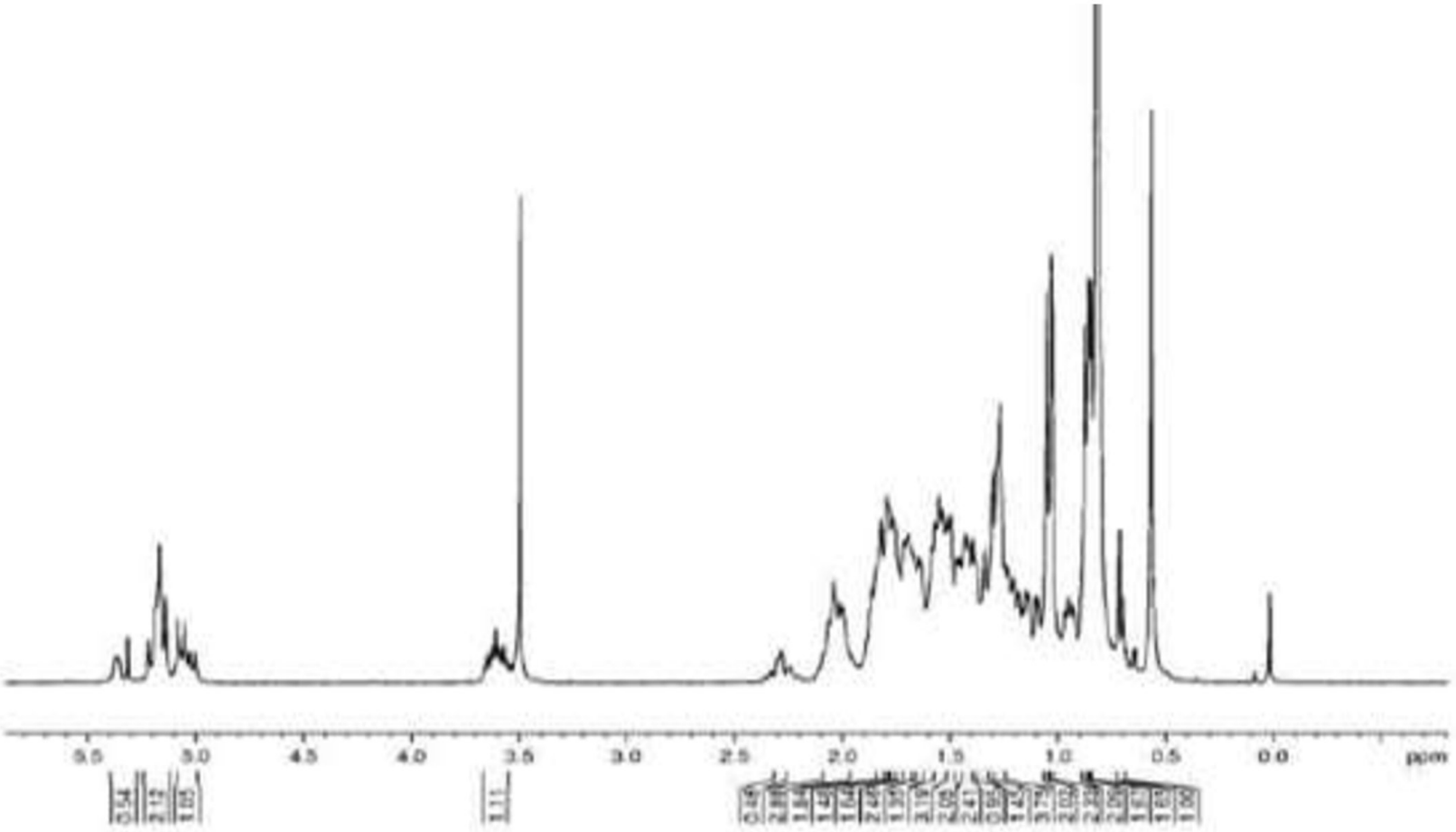

3.1: ^{1}H NMR spectrum of compound 30

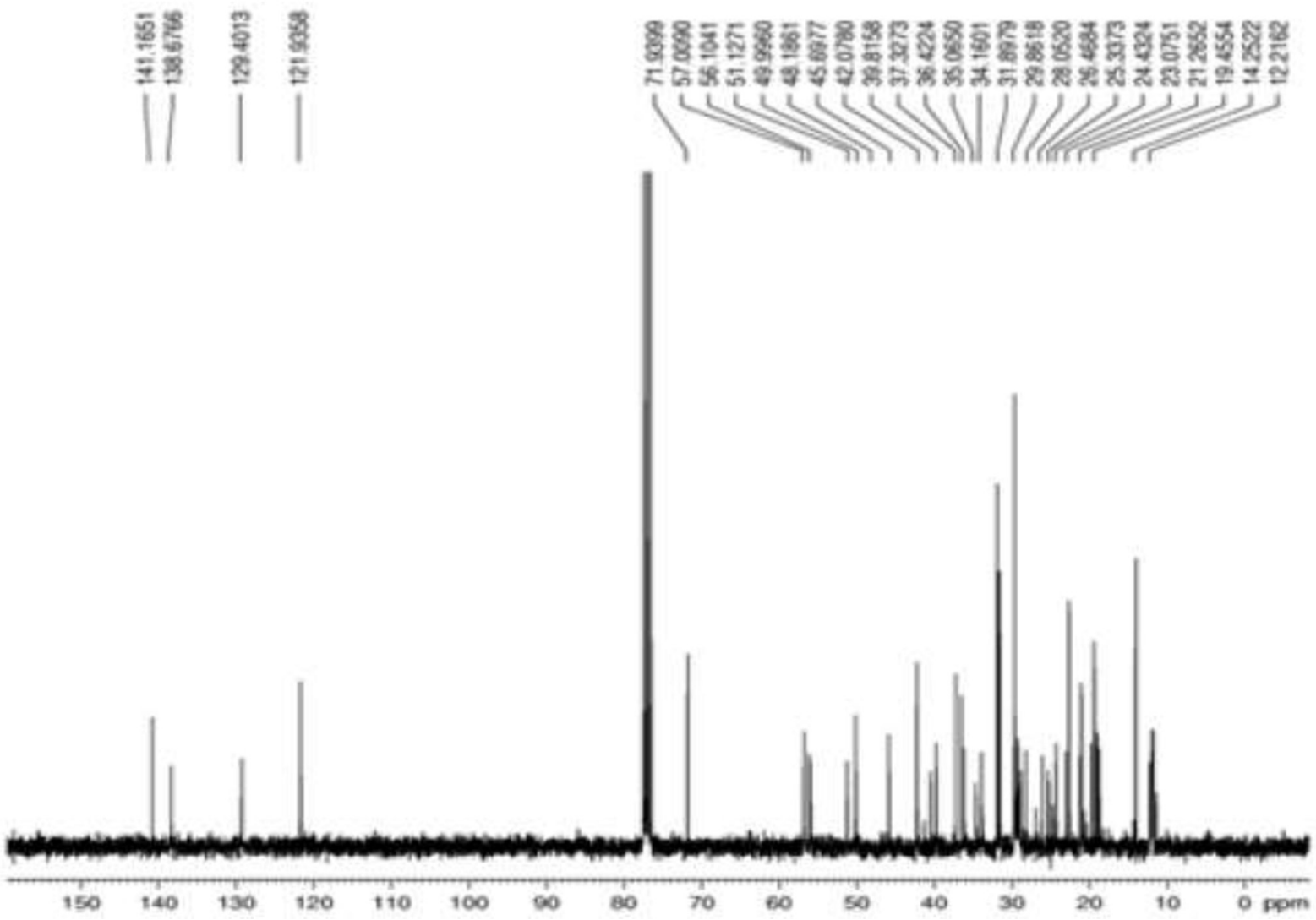

3.2: ^{13}C NMR spectrum of compound 30

4.0: Spectra for compound **31**; 5-hydroxy-7,8-(2'',2''-dimethylchromene)-flavanone

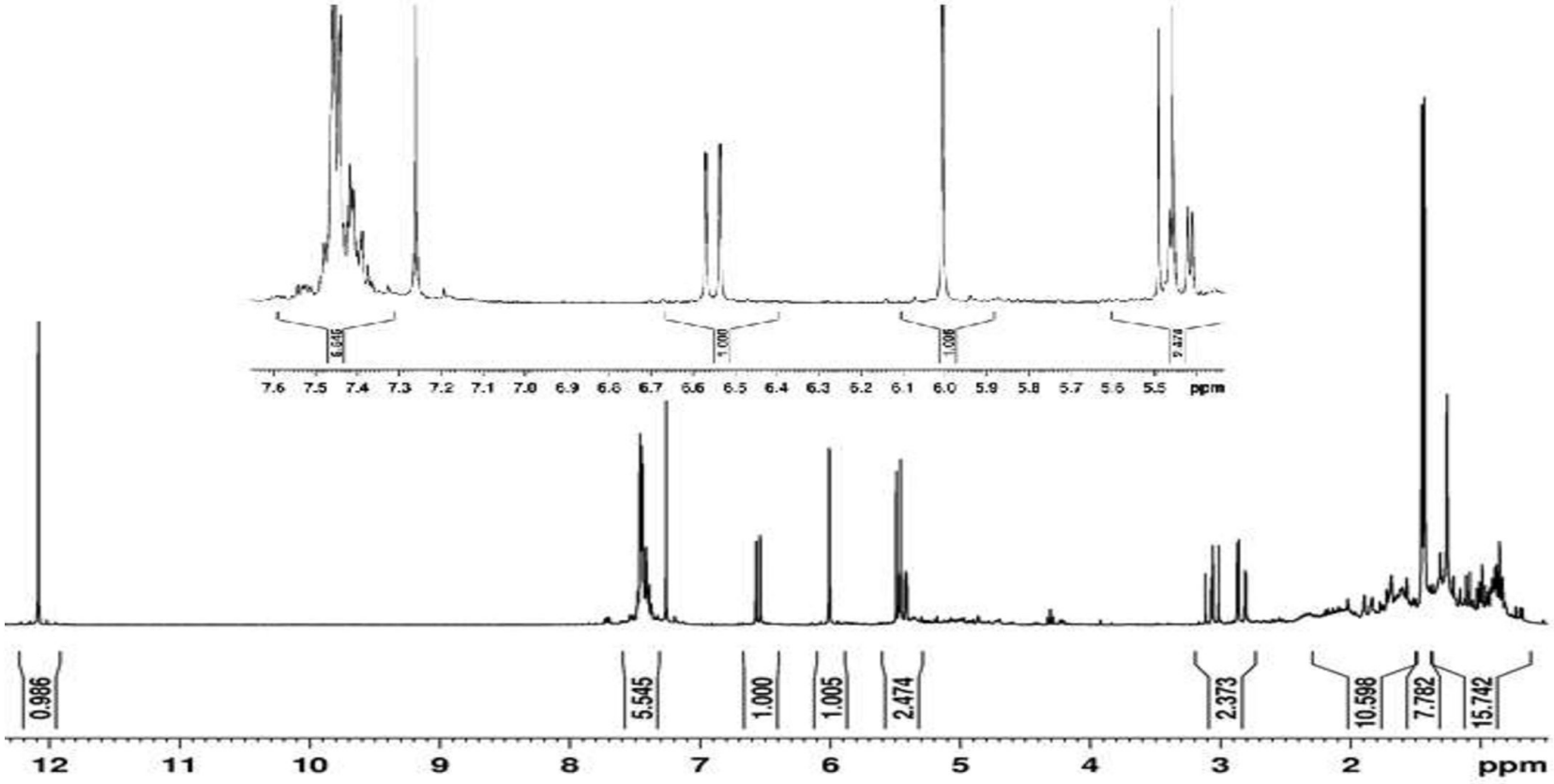

4.1: ^{1}H NMR spectrum of compound 31

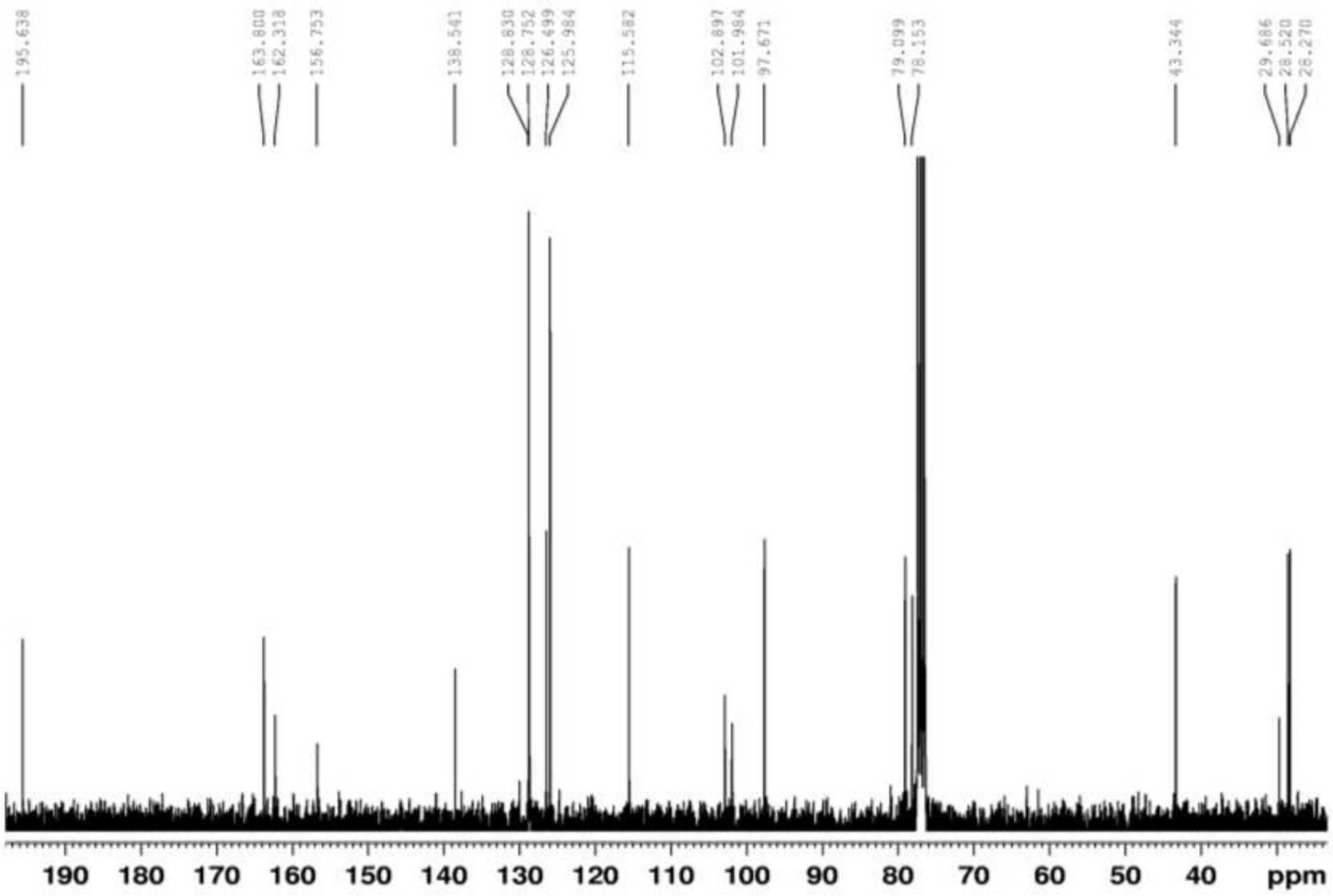

4.2: ^{13}C NMR spectrum of compound 31

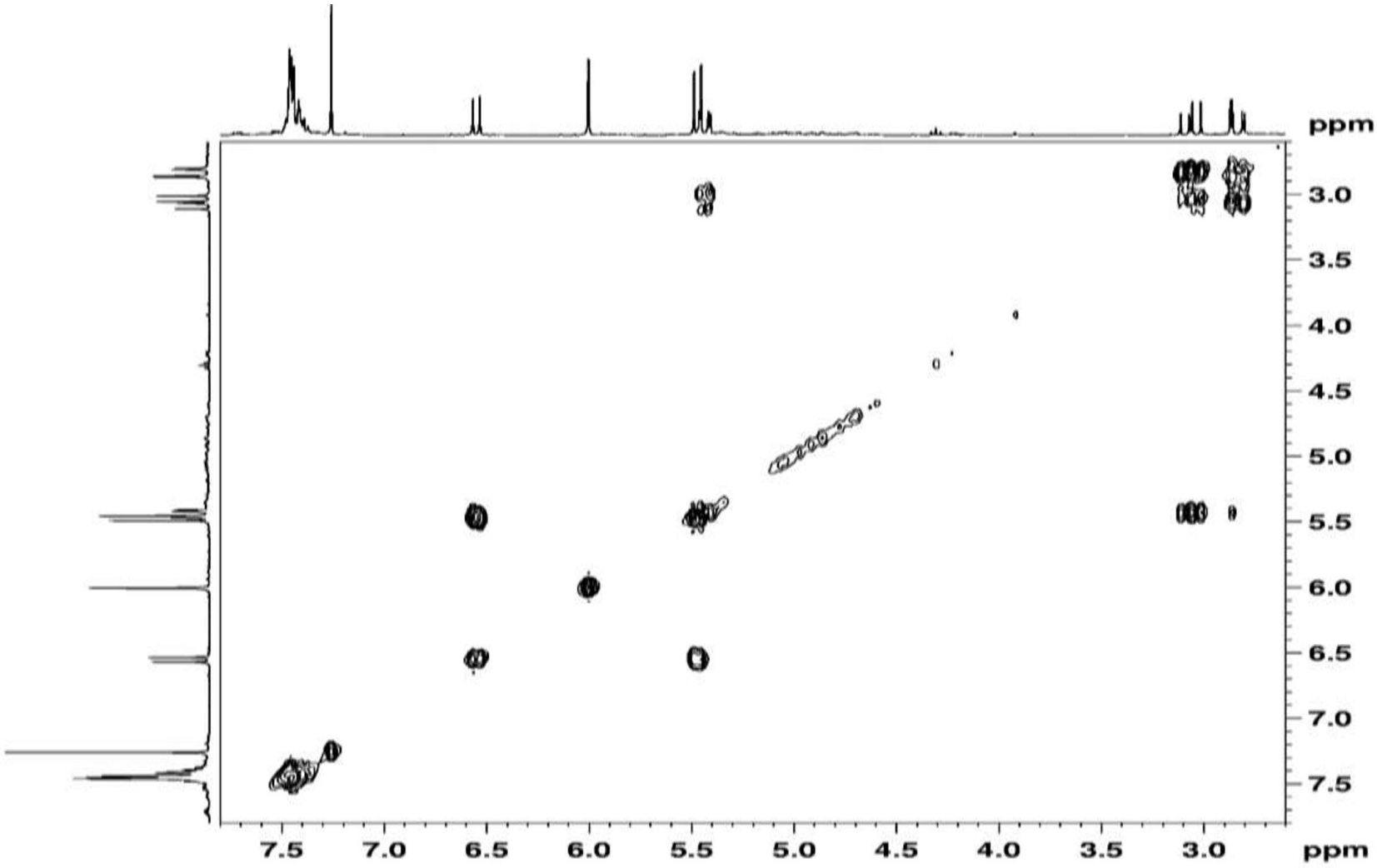

4.3: COSY spectrum of compound 31

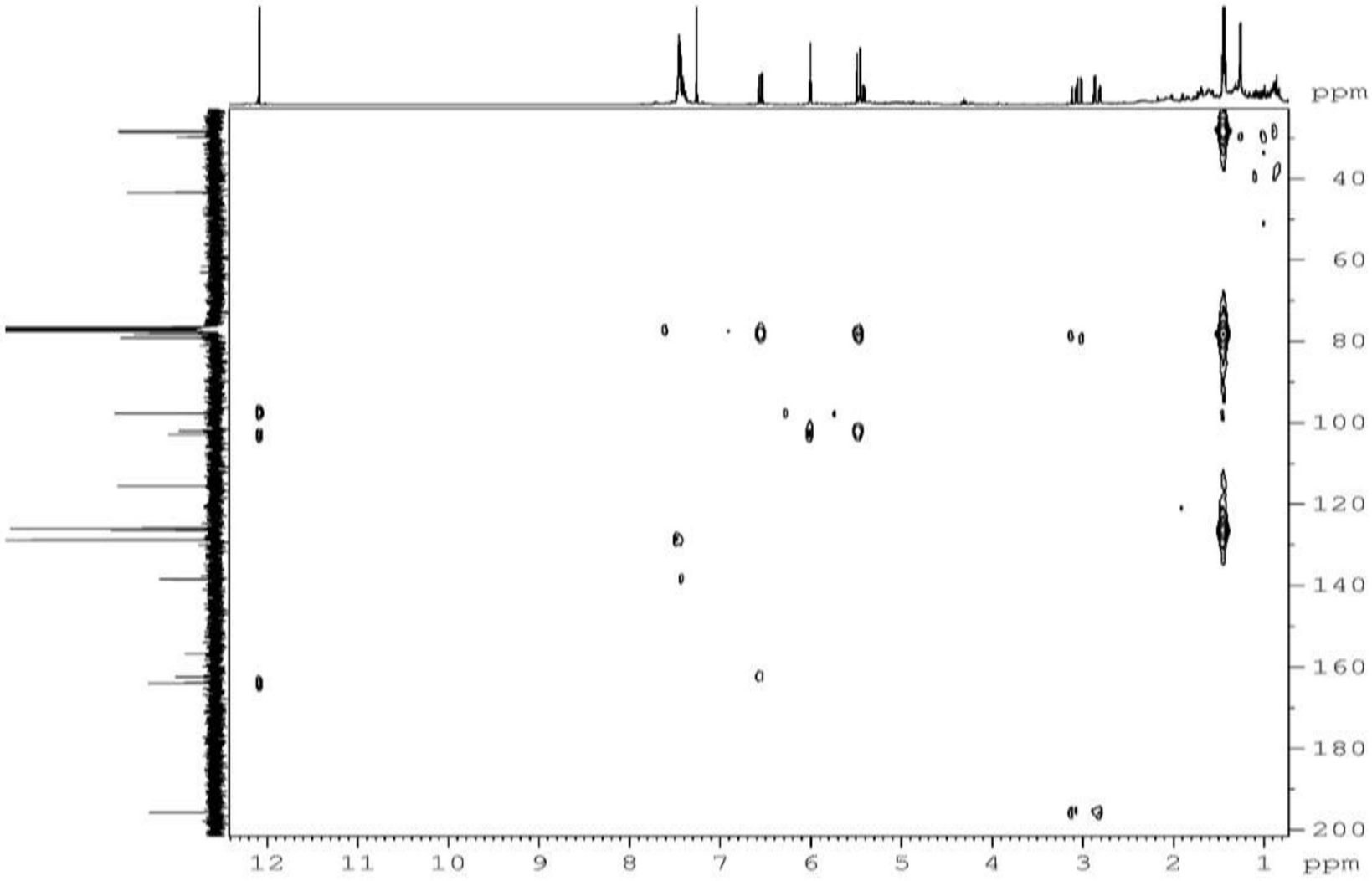

4.4: HMBC spectrum of compound 31

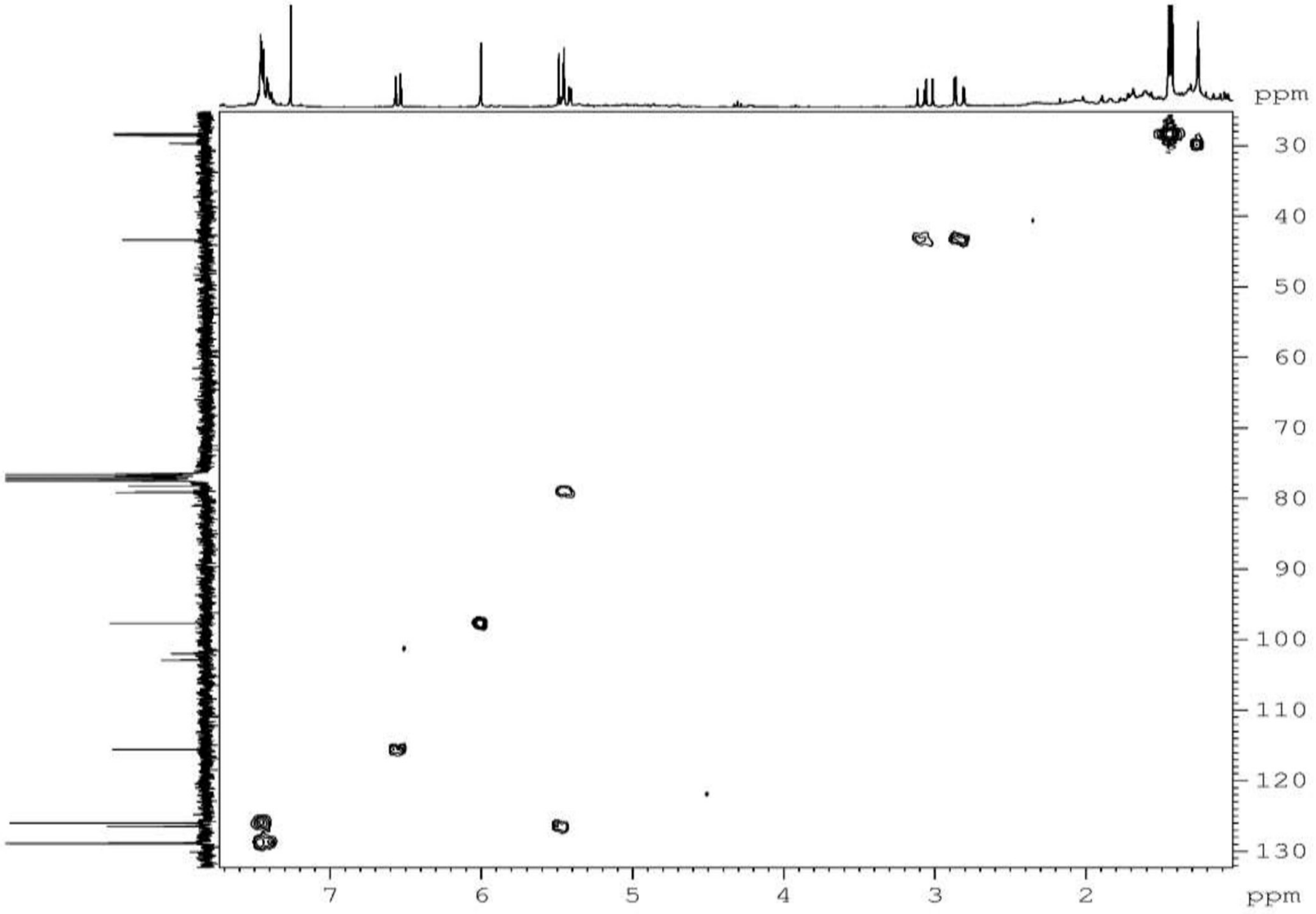

4.5: HSQC spectrum of compound 31

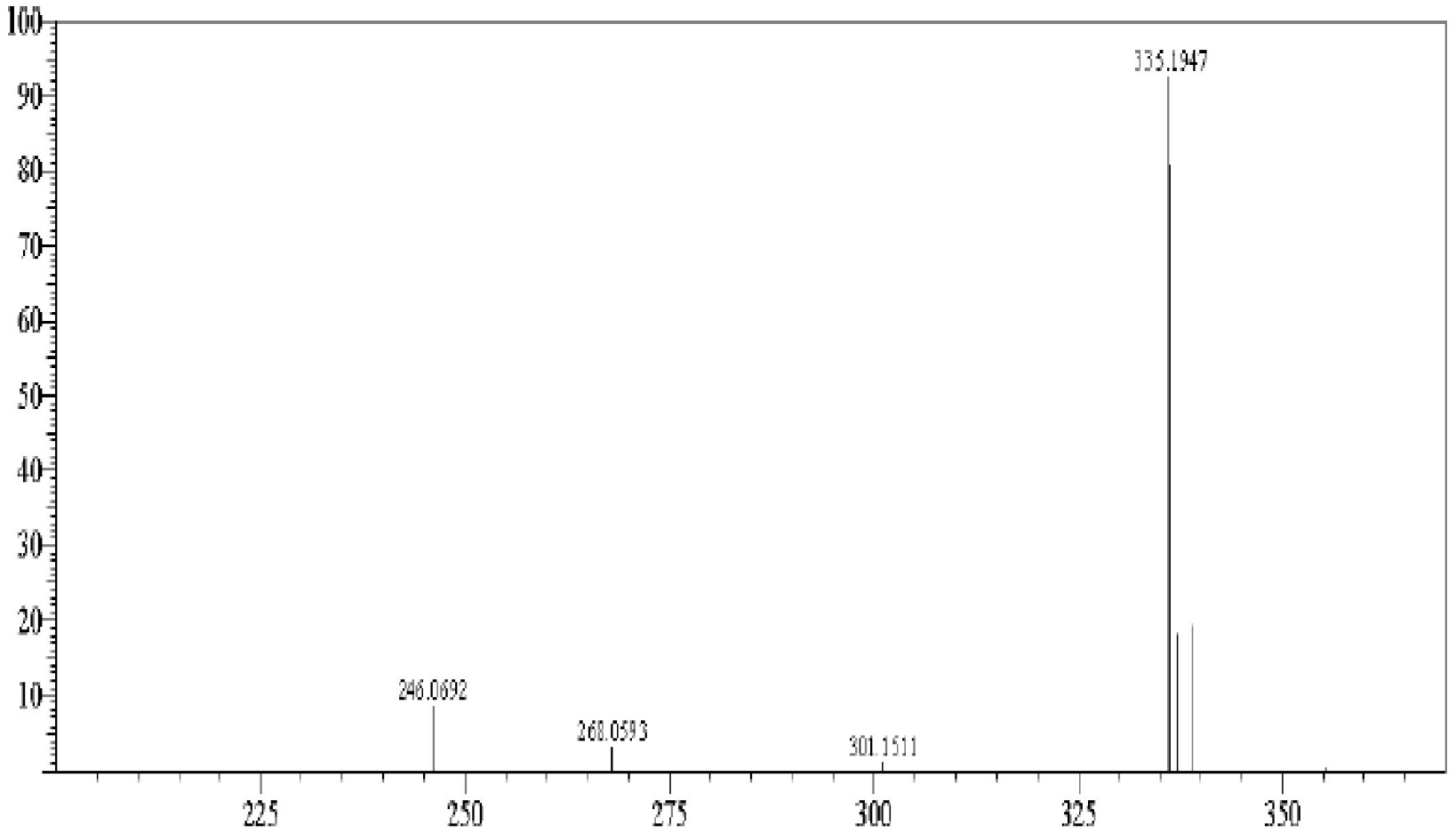

4.6: EIMS spectrum of compound **31**

5.0: Spectra of compound **32**; 5-methoxy-7,8-(2'',2''-dimethylchromene)-flavanone

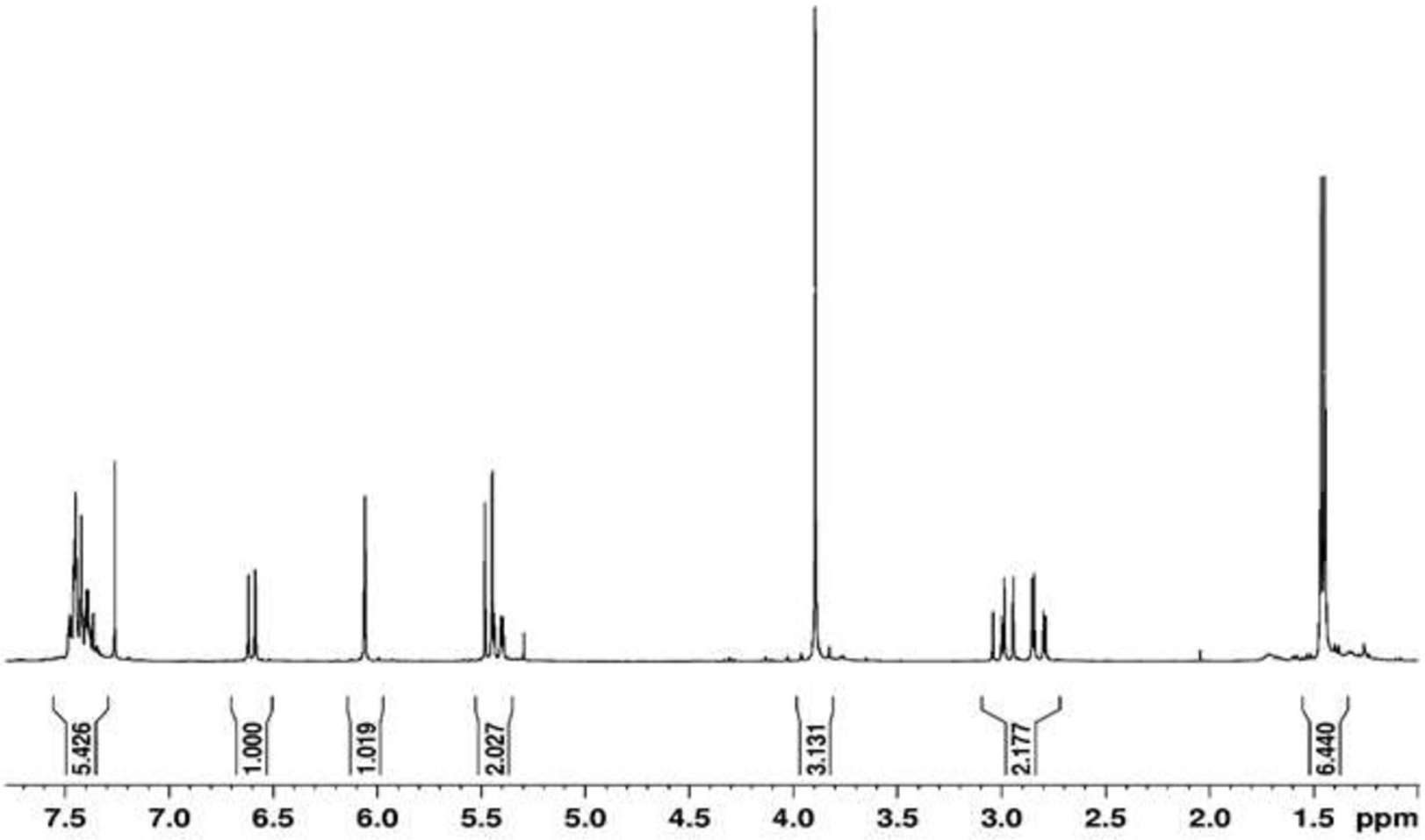

5.1: ^{1}H NMR spectrum of compound 32

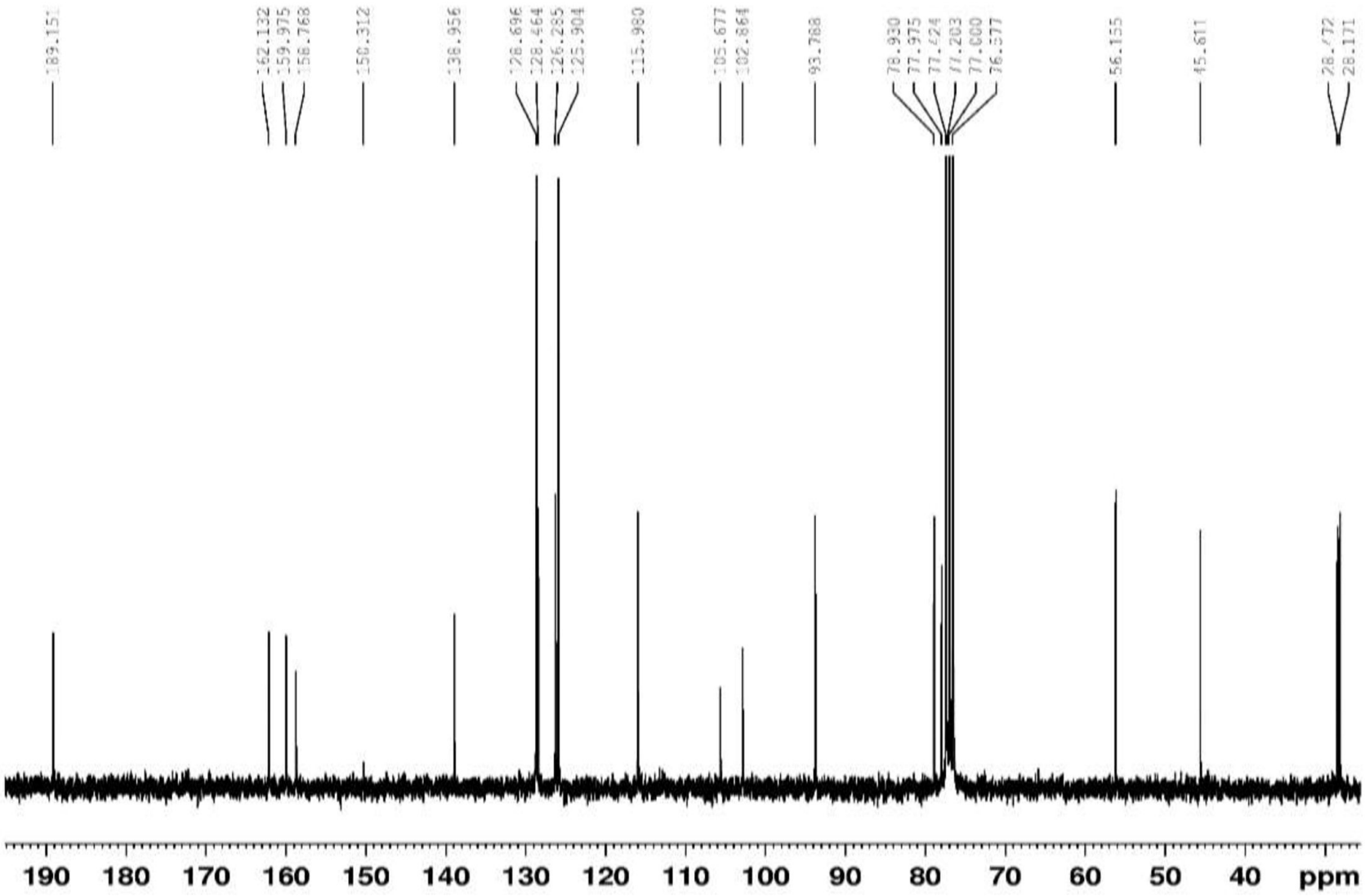

5.2: ^{13}C NMR spectrum of compound 32

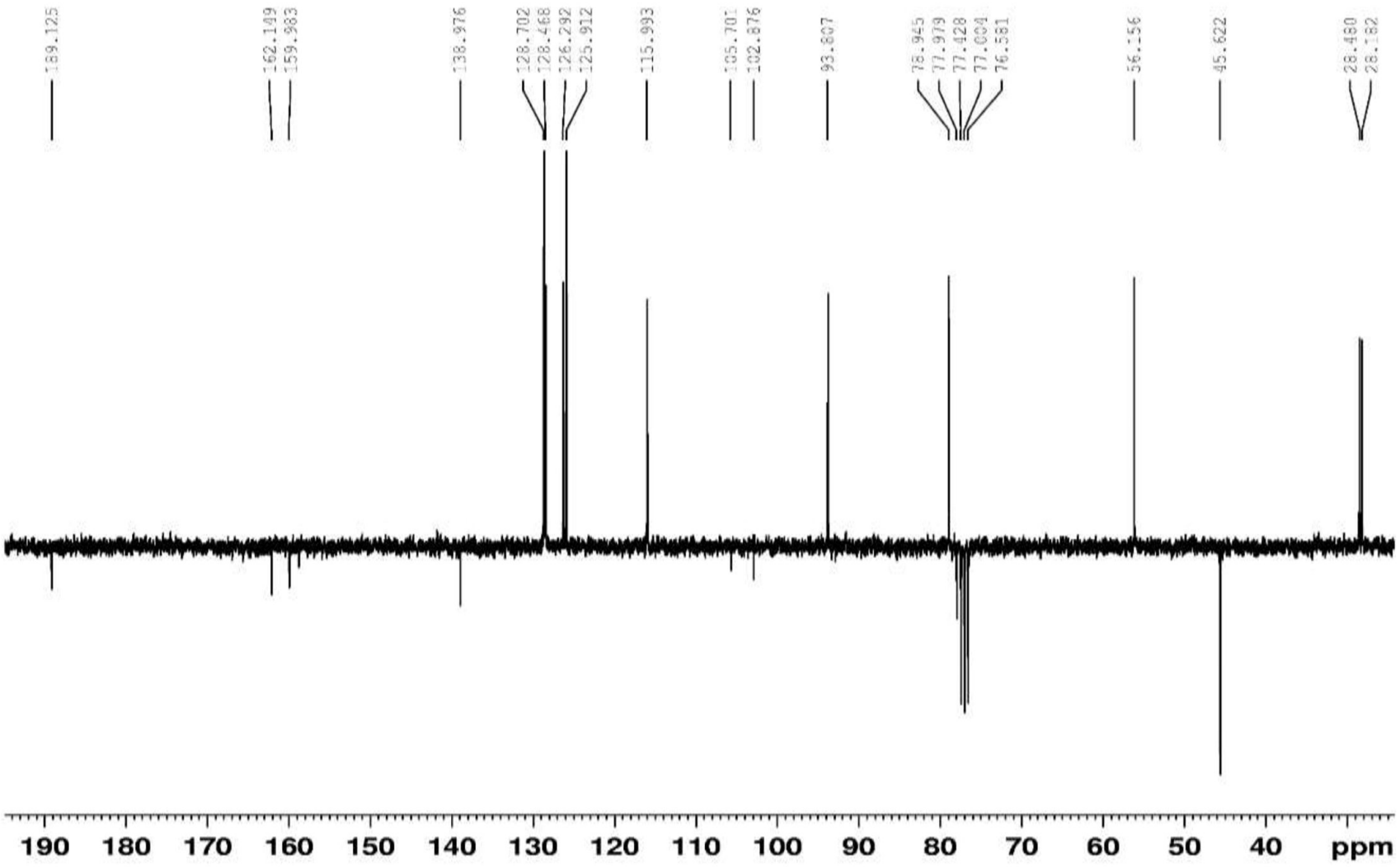

5.3: DEPT 135 spectrum of compound 32

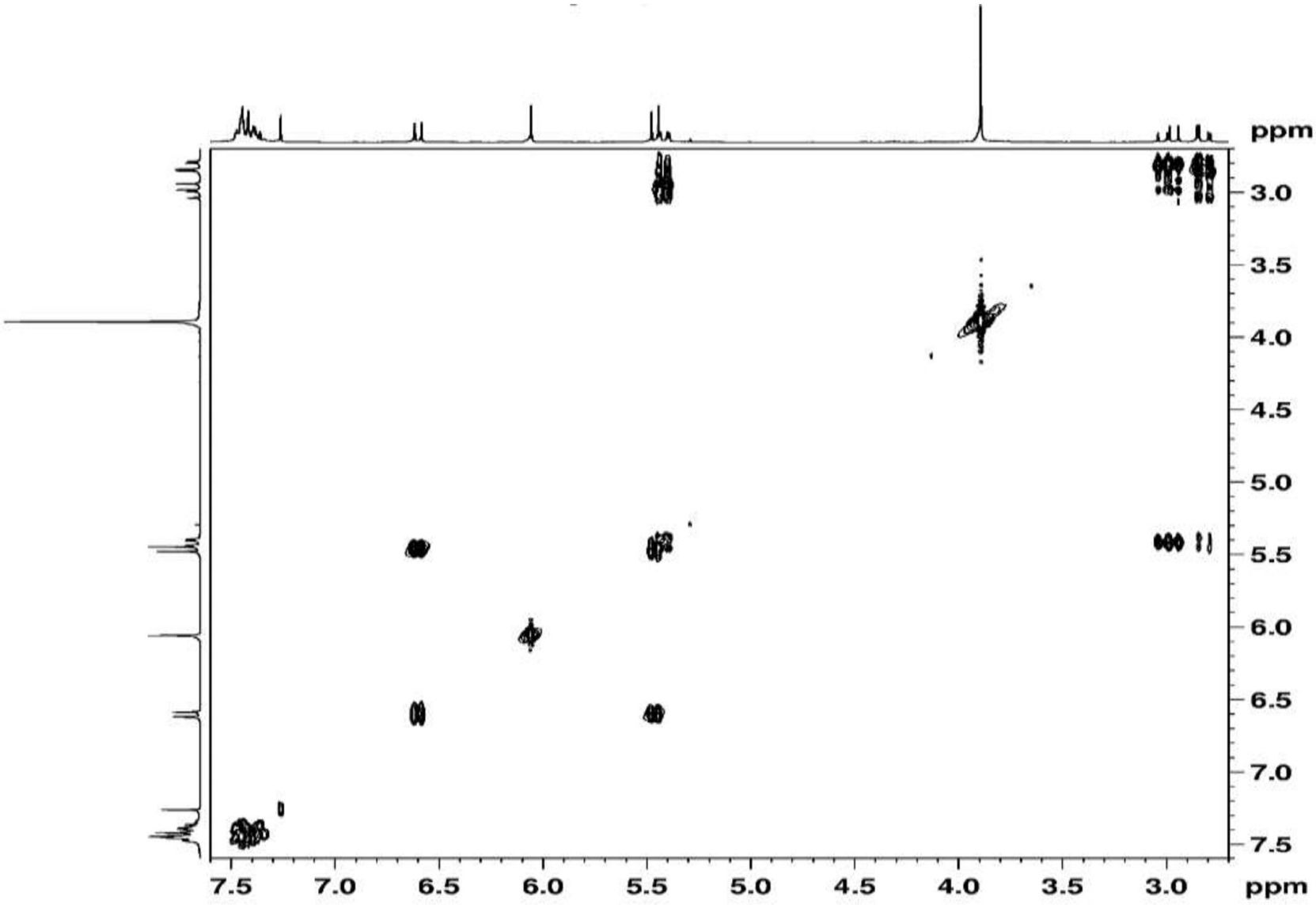

5.4: COSY spectrum of compound 32

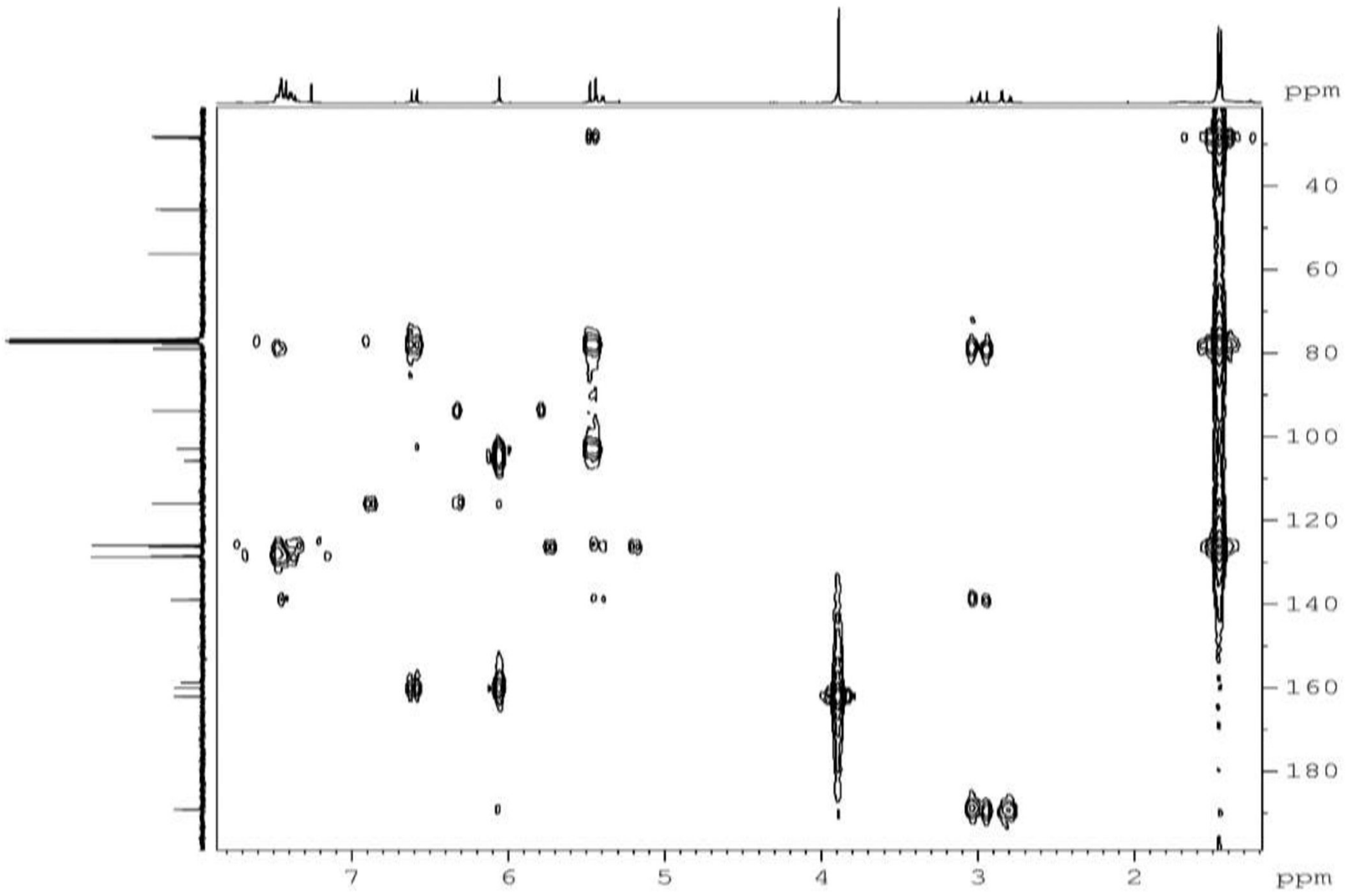

5.5: HMBC spectrum of compound 32

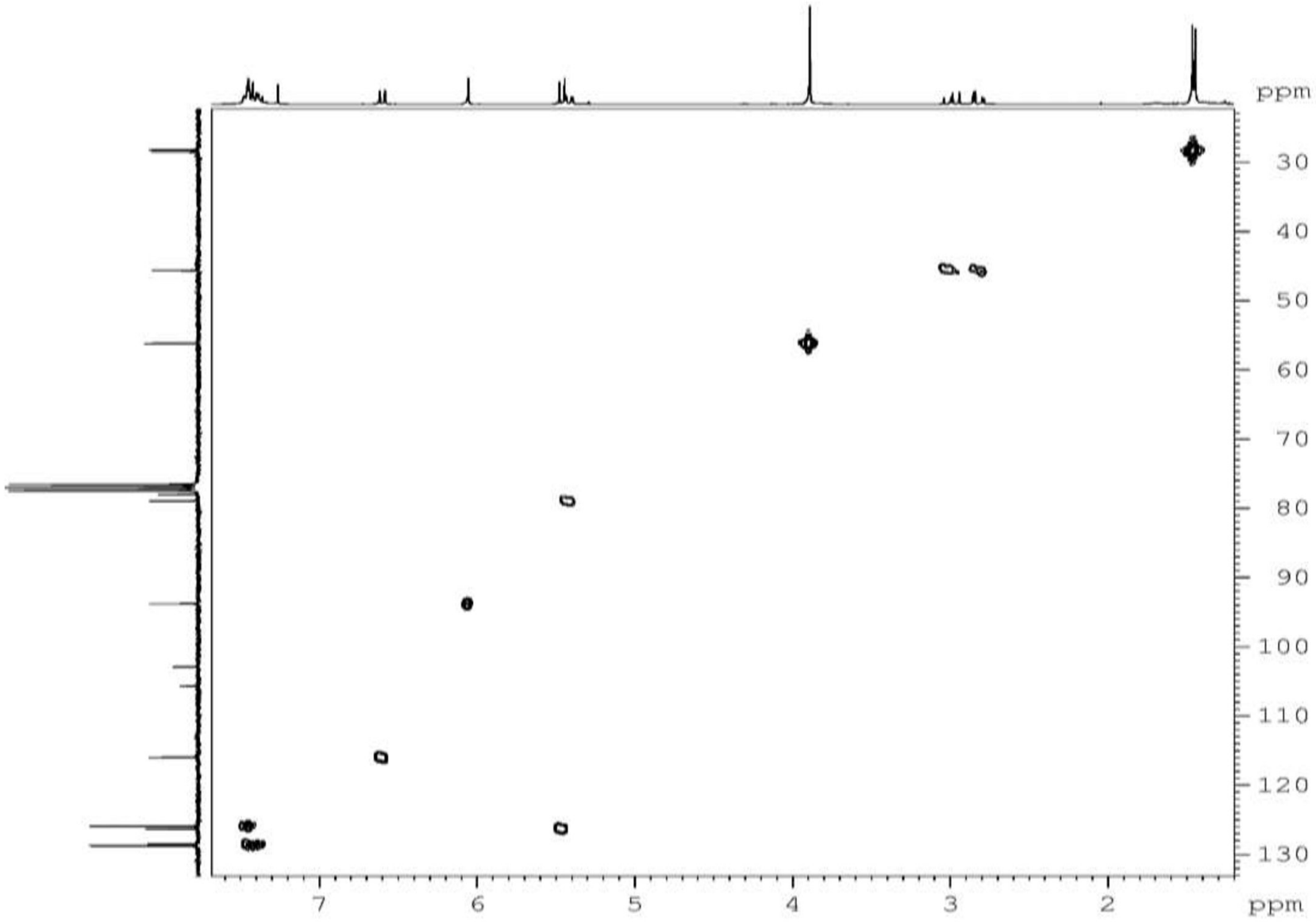

5.6: HSQC spectrum of compound 32

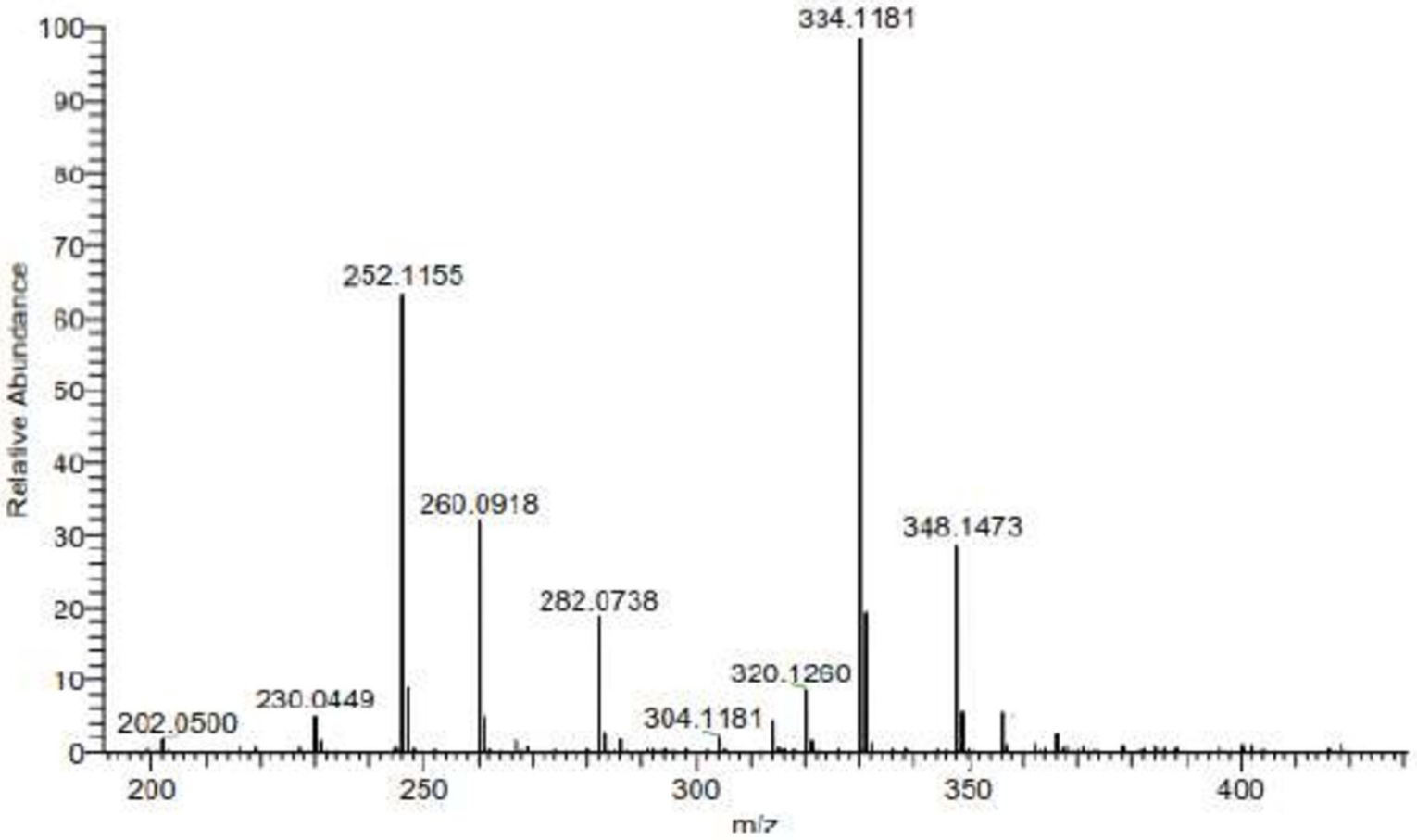

5.7: EIMS spectrum of compound **32**

6.0: Spectra for compound **33**; 3-*O*-[β-glucopyranosyl-(1''→2')-*O*-β-xylopyranosyl]-β-stigmasterol

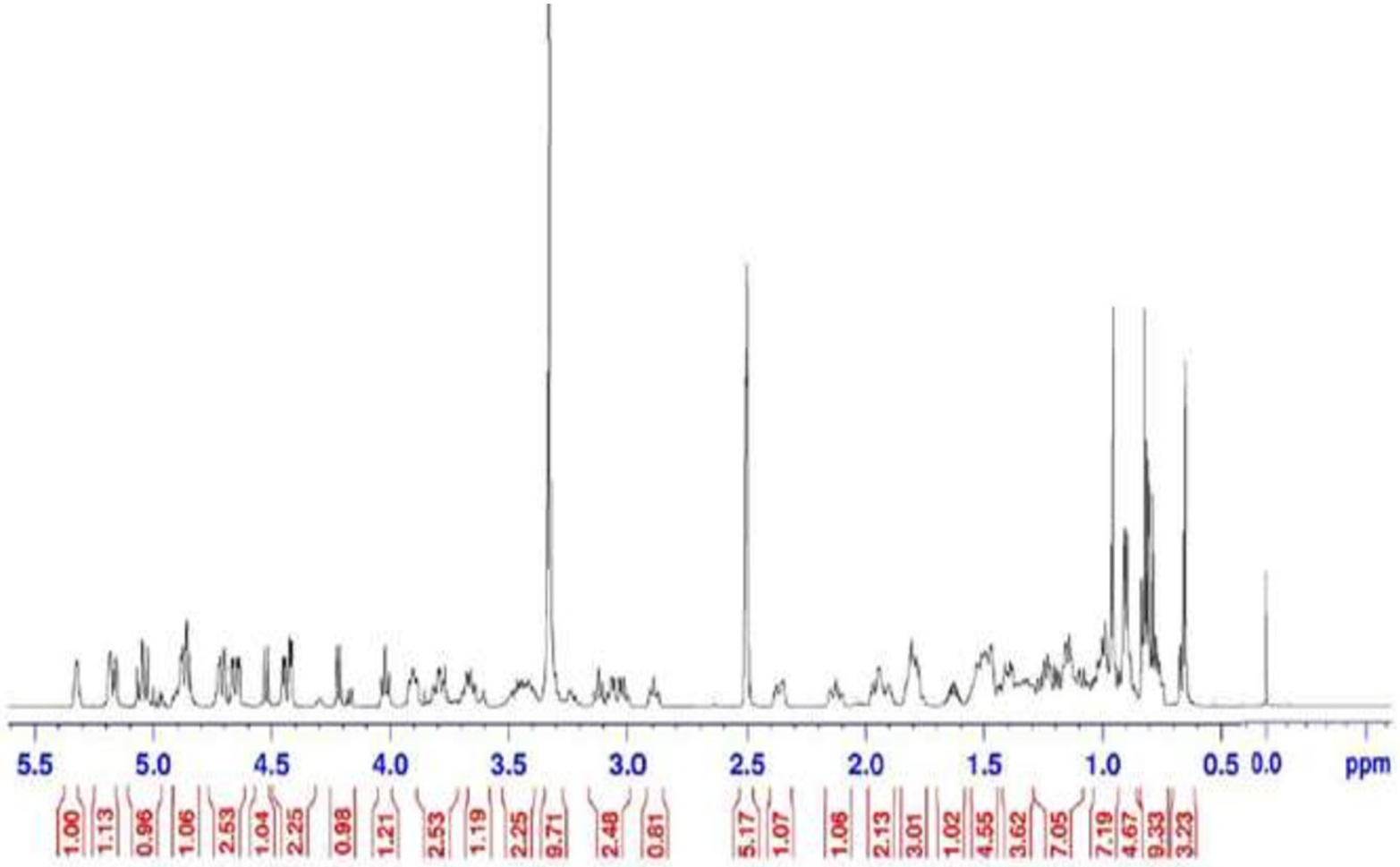

6.1: ^{1}H NMR spectrum of compound 33

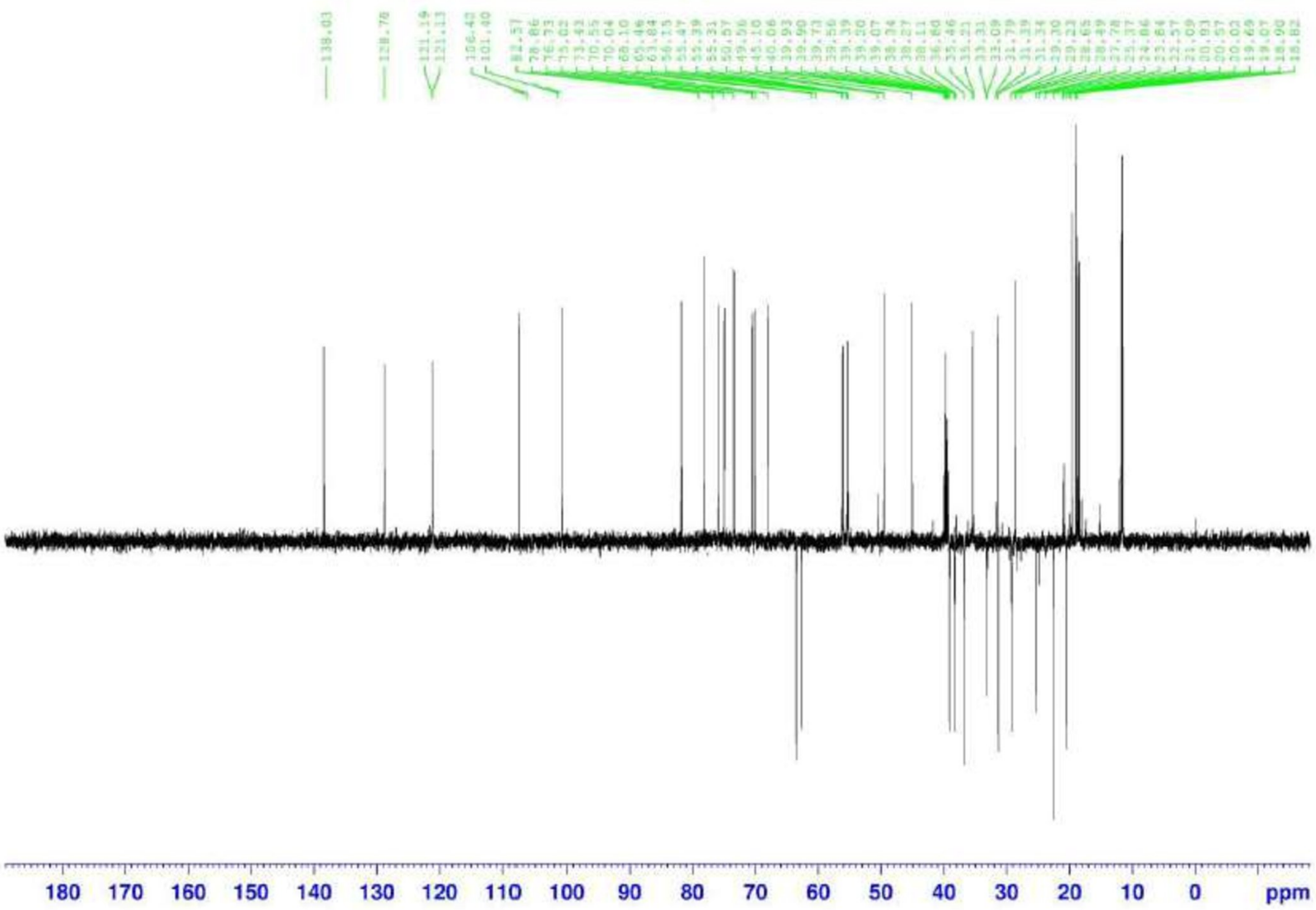

6.2: DEPT 135 spectrum of compound 33

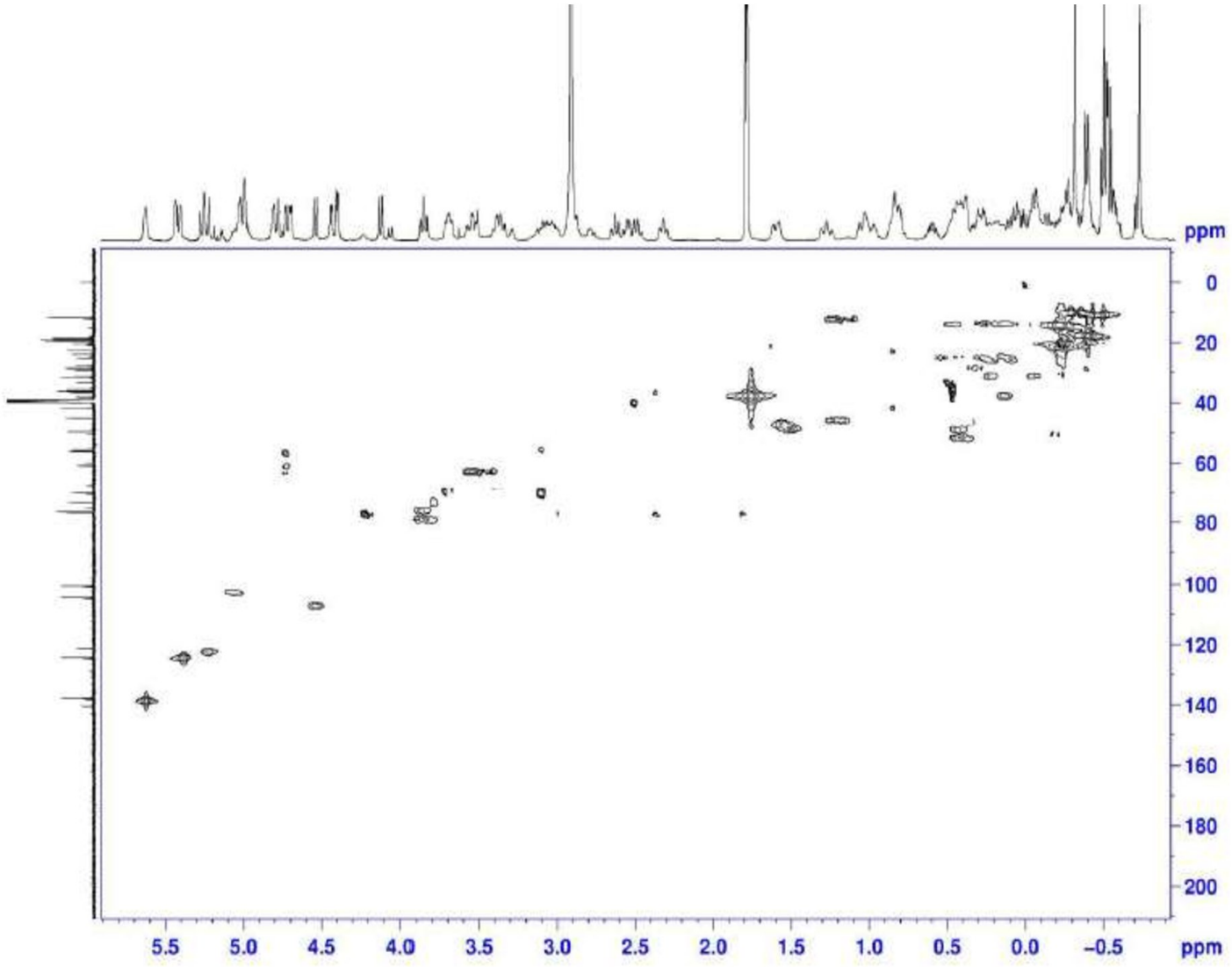

6.3: HSQC spectrum of compound 33

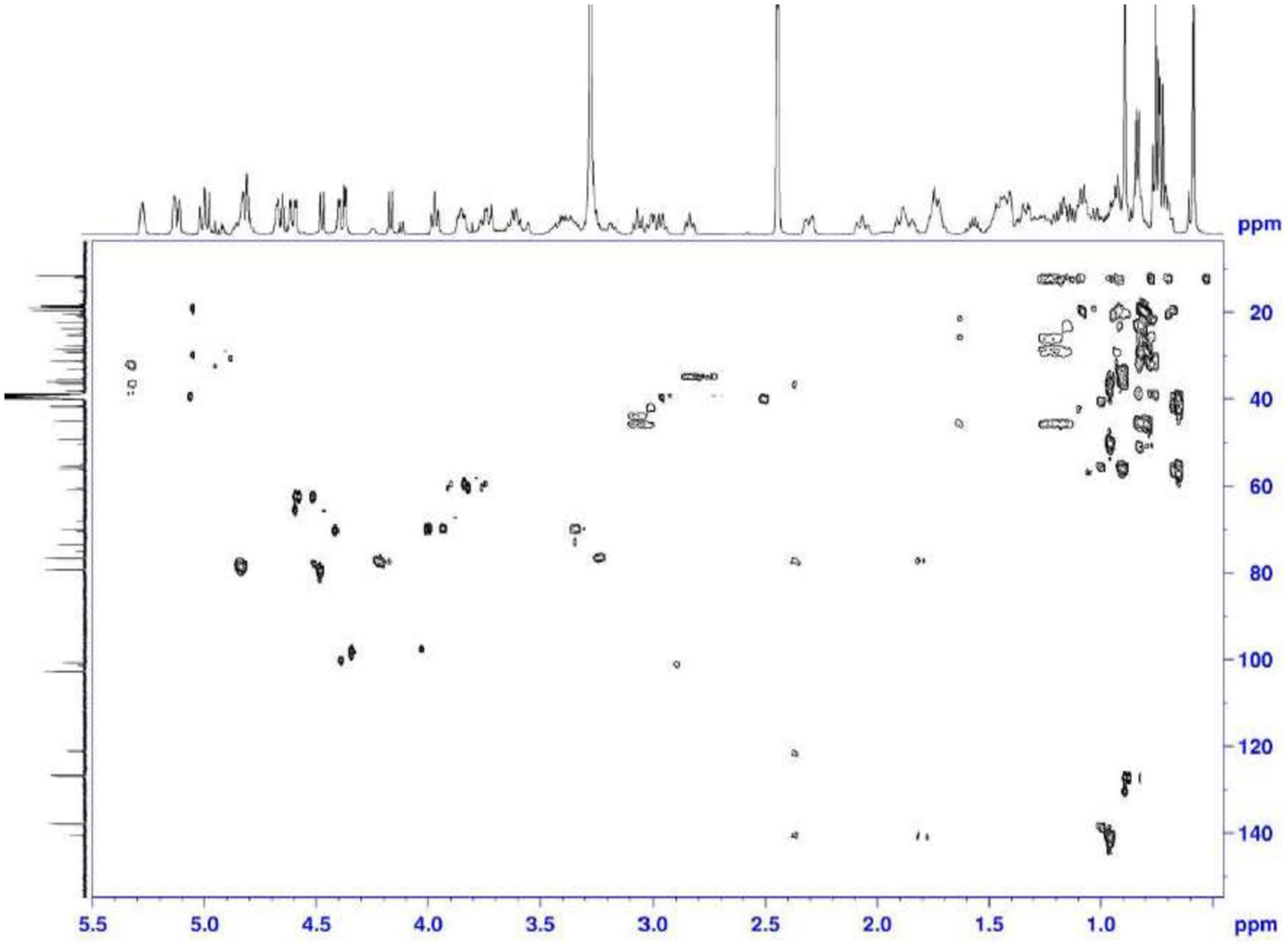

6.4: HMBC spectrum of compound 33

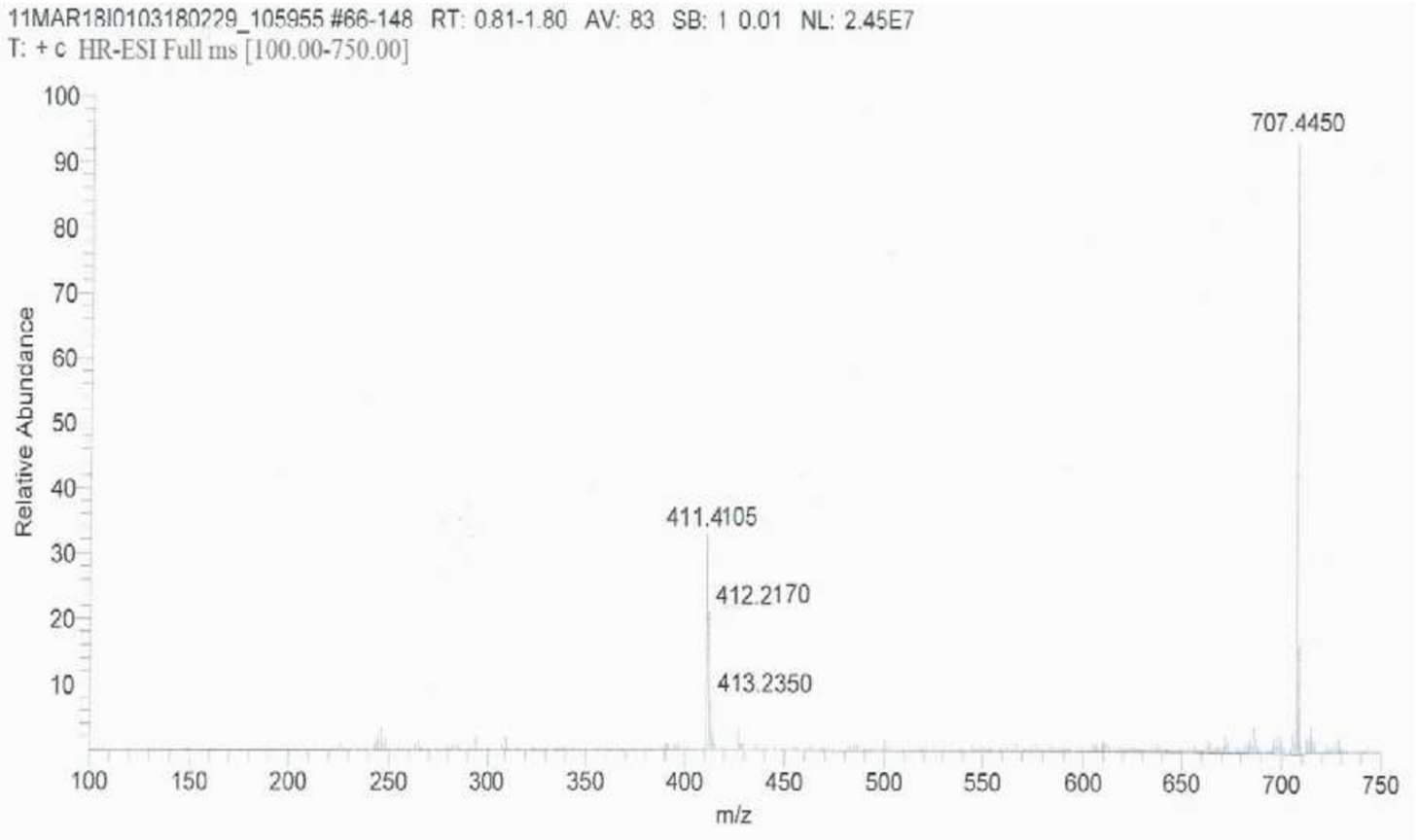

6.5: ESIMS spectrum of compound of compound 33